

2014

Boron Removal by Nanofiltration and Reverse Osmosis Membranes

Kha Le Tu

University of Wollongong

UNIVERSITY OF WOLLONGONG

COPYRIGHT WARNING

You may print or download ONE copy of this document for the purpose of your own research or study. The University does not authorise you to copy, communicate or otherwise make available electronically to any other person any copyright material contained on this site. You are reminded of the following:

Copyright owners are entitled to take legal action against persons who infringe their copyright. A reproduction of material that is protected by copyright may be a copyright infringement. A court may impose penalties and award damages in relation to offences and infringements relating to copyright material. Higher penalties may apply, and higher damages may be awarded, for offences and infringements involving the conversion of material into digital or electronic form.

**UNIVERSITY OF
WOLLONGONG**



**Faculty of Engineering and Information Science
School of Civil, Mining, and Environmental Engineering**

Boron removal by nanofiltration and reverse osmosis membranes

Kha Le Tu

**This thesis is presented as part of the requirements for the
award of the Degree of Doctor of Philosophy
of the
University of Wollongong**

August 2014

CERTIFICATE OF ORIGINALITY

I, Kha Tu, declare that this thesis, submitted in fulfilment of the requirements for the award Doctor of Philosophy, in the School of Civil, Mining, and Environmental Engineering, University of Wollongong, is wholly my own work unless otherwise referenced or acknowledged. The document has not been submitted for qualifications at any other academic institution.

Kha Tu

August 2014

ABSTRACT

This dissertation aims to enrich the literature on boron rejection by nanofiltration (NF) and reverse osmosis (RO) membranes. A novel method to improve boron rejection by NF/RO membranes, which is based on the complexation reactions between boron and poly-alcohols (polyols), was investigated. The impacts of chemical cleaning and chemical preservation on the boron rejection efficiency of RO membranes were examined. In addition, the dissertation assessed the feasibility of utilising boron rejection data as a surrogate for the rejection of N-nitrosodimethylamine (NDMA) – an emerging pollutant which attracts major concerns in contemporary water reclamation applications. Filtration experiments were conducted using a laboratory-scale cross-flow membrane filtration system. Experimental results were elaborated based on the recognised transport mechanisms of boron through NF/RO membranes and also on the characterised membrane surface properties.

In the presence of polyols, significant boron rejection improvement was obtained and the extent of the impact was directly related to the stability constant of the boron–polyol complex. Polyols could complex with boron in either the boric acid or borate anion forms; however the complexation between polyol and boric acid appeared to be incomplete. With and without the presence of polyols, boron rejection was strongly pH dependent. The increase in boron rejection due to polyol addition was higher for the NF membrane compared to the RO membrane. A boron:polyol molar ratio of 1:1 appeared to be adequate. The presence of polyols did not cause any observable membrane fouling. Results reported here suggest that the addition of polyols could allow NF membranes to be effectively used for boron removal.

Experimental results of this study showed that chemical cleaning can significantly change the hydrophobicity and water permeability of the RO membrane; however, its impacts on the rejections of boron and sodium were marginal. Although the presence of surfactant or chelating agent could cause decreases in the rejections, solution pH was found to be the key factor responsible for the loss of membrane separation and surface properties. The impacts of solution pH on the water permeability could be reversed by applying a subsequent cleaning with the opposite pH condition.

Nevertheless, the impacts of solution pH on boron and sodium rejections were irreversible in most cases.

Chemical preservation could change the membrane surface properties, and consequently water permeability and solute rejection efficiency of the membrane were negatively impacted. The impacts of preservation on boron rejection and sodium rejection were similar in magnitude and more significant than those on water permeability. The results indicated that the impact of chemical preservation on the membrane depends on both the preserving chemicals used and the solution pH value. More importantly, the undesirable impacts of chemical preservation could be minimised by appropriate selection of the preservatives and by preserving the membrane in a reducing condition. A near-neutral pH (i.e., pH 7) is necessary to avoid any significantly negative impacts on membrane performance due to chemical preservation using either formaldehyde or sodium metabisulfite. The study results suggested that the previously recommended minimum pH value of 3 of the preservative solution may be inadequate.

A strong linear correlation ($R^2 = 0.95$) between the rejections of boron and N-nitrosodimethylamine (NDMA) by six different reverse osmosis (RO) membranes was obtained, suggesting that boron can be used as a surrogate for NDMA rejection. This proposal is based on the premise that the rejection of both boric acid and NDMA is governed by steric hindrance and that they have similar molecular dimensions. The concept proposed here is shown to be valid at pH 8 or below where boron exists as the neutral boric acid species and NDMA is also a neutral solute. Observed changes in the rejections of these two species, as a function of permeate fluxes and feed solution temperatures, were also almost identical. Boron rejection increased from 21 to 79% and the correlation coefficient of the linear regression between boron and NDMA rejections was 0.99 as the permeate flux increased from 5 to 60 $\text{L}\cdot\text{m}^{-2}\cdot\text{h}^{-1}$. Similarly, a linear correlation between boron and NDMA rejections was observed as the feed solution temperature increased from 10 to 40 °C. This linear correlation was also validated in a tertiary treated effluent matrix.

ACKNOWLEDGEMENTS

What a fabulous journey, and today is the day to make it count! Doing a PhD has never been an easy job. However, I was lucky enough to have amazing companions who I would like to thank from the deepest part of my soul. Without the support of these people my PhD journey would be a lot rougher or even impossible.

My foremost and very special thanks go to my research supervisor Associate Professor Long Nghiem. He gave me enormous support from the initial time of preparing the research proposal to the day when my thesis was bound and submitted. I thank him for providing me with the best facilities and arrangements which guaranteed my experimental works went as smoothly as possible. Long also gave me precious advice in writing the journal papers and answering tough questions from the reviewers. The results of this assistance and guidance are not only a complete PhD thesis but also a Research Fellowship offer from Monash University coming to me even before the thesis submission. These daydreamed outcomes would not have come true without Long's support.

I would like to send a big thank you to my co-supervisor Professor Allan Chivas who offered and facilitated my access to his state-of-the-art ICP-MS instrument. My research work might have been an impossible task without his support. I am also grateful to Allan for his meticulous and professional editing of my writing. Allan's staff Helen, Lily, and David are thanked for their arrangement and technical support with the ICP-MS analysis.

I am grateful to our laboratory technicians Frank, Linda and Taka for maintaining an effective and safe laboratory in which my experiments run smoothly.

A very special appreciation goes to my dear wife Chipxinh. Every day she brought me enjoyable meals, entertaining laughter, and heaps of extra time for doing my research. She is a very special wife who can help and nicely helped the husband even with research work. Her skills in data recording and sample labelling are fantastic.

Mom and Dad, thank you for believing in me and encouraging me at all times.

TABLE OF CONTENTS

ABSTRACT	i
ACKNOWLEDGEMENTS	iii
TABLE OF CONTENTS	iv
LIST OF FIGURES	ix
LIST OF TABLES	xv
LIST OF ABBREVIATIONS	xvi
NOMENCLATURES	xvii
CHAPTER 1: INTRODUCTION	1
1.1 Background	1
1.2 Research scope and opportunities	3
1.3 Research objectives and expected outcomes.....	3
1.4 Thesis outline	4
CHAPTER 2: LITERATURE REVIEW	6
2.1 Boron in the environment	6
2.1.1 Health and ecological impact of boron	7
2.1.2 Regulations and guidelines for boron content in waters	8
2.1.3 Chemistry of boron	9
2.1.4 Analytical methods for boron.....	12
2.1.5 Boron determination by ICP-MS	14
2.2 Factors governing boron rejection by NF/RO membranes	16
2.2.1 Feedwater pH	16
2.2.2 Feedwater ionic strength	17
2.2.3 Operating pressure	18
2.2.4 Feedwater temperature	19

2.2.5	Membrane configurations for improving boron rejection.....	19
2.3	Modelling boron transport in NF/RO membranes	22
2.3.1	Solution-Diffusion Model	22
2.3.2	Irreversible Thermodynamic Model	24
2.3.3	Pore models	27
2.3.4	Charge-based models	29
2.3.5	Combined models	30
2.4	Chemical contact during membrane lifetime and its implication on the membrane integrity	31
2.4.1	Membrane cleaning chemicals.....	31
2.4.2	Oxidising chemicals	34
2.4.3	Membrane preserving chemicals.....	36
2.5	Methods for membrane characterisation.....	38
2.5.1	Surface morphology	38
2.5.2	Electro-kinetics	38
2.5.3	Hydrophobicity	39
2.5.4	Chemical structure	40
2.6	NDMA in water and monitoring issues	40
2.7	Conclusions	41
CHAPTER 3: ENHANCED BORON REJECTION BY COMPLEXATION WITH POLYOLS.....		44
3.1	Introduction.....	44
3.2	Materials and methods	45
3.2.1	Chemical and reagents	45
3.2.2	Selected membranes.....	46
3.2.3	Cross-flow membrane filtration system.....	47

3.2.4	Experimental protocol.....	47
3.2.5	Analytical methods.....	48
3.3	Results and discussions.....	49
3.3.1	Boric acid – polyol complexation.....	49
3.3.2	The rejection of boron and polyols.....	50
3.3.3	The effects of polyol addition.....	51
3.4	Conclusions.....	57
CHAPTER 4: EFFECTS OF CHEMICAL CLEANING ON BORON REJECTION		
.....		58
4.1	Introduction.....	58
4.2	Materials and methods.....	58
4.2.1	Membrane and chemicals.....	58
4.2.2	Cross-flow membrane filtration system and experimental protocol.....	59
4.2.3	Simulation of membrane cleaning.....	60
4.2.4	Membrane characterisation methods.....	60
4.2.5	Chemical analytical methods.....	61
4.3	Results and discussion.....	62
4.3.1	Charge density.....	62
4.3.2	Hydrophobicity and surface bonding.....	64
4.3.3	Water permeability.....	67
4.3.4	The rejection of boron and sodium.....	70
4.4	Conclusions.....	77
CHAPTER 5: EFFECTS OF MEMBRANE PRESERVATION ON BORON REJECTION		
.....		79
5.1	Introduction.....	79
5.2	Materials and methods.....	79

5.2.1	Membranes and chemicals	79
5.2.2	Cross-flow membrane filtration system	80
5.2.3	Membrane preservation protocol	80
5.2.4	Membrane characterisation methods.....	81
5.2.5	Analytical methods.....	81
5.3	Result and discussion	82
5.3.1	Charge density.....	82
5.3.2	Hydrophobicity	84
5.3.3	Chemical composition.....	85
5.3.4	The rejection of boron and sodium by virgin RO membranes.....	88
5.3.5	Changes in the membrane performance.....	90
5.4	Conclusion	95
CHAPTER 6: BORON AS A SURROGATE FOR NDMA REJECTION		97
6.1	Introduction	97
6.2	Materials and methods	98
6.2.1	Chemicals and reagents.....	98
6.2.2	Membranes	98
6.2.3	NF/RO filtration system and experimental protocol.....	99
6.2.4	Chemical analytical methods	100
6.3	Result and discussion	100
6.3.1	Correlation between boron and NDMA rejection by RO membranes .	100
6.3.2	Effects of operating conditions on boron and NDMA rejection	103
6.4	Conclusion	108
CHAPTER 7: CONCLUSIONS AND RECOMMENDATIONS		109
REFERENCES.....		113

THESIS-RELATED PUBLICATIONS.....	129
APPENDIX.....	130

LIST OF FIGURES

Figure 1. Outline of the structure of this dissertation.....	5
Figure 2. The dissociation of boric acid in diluted solution.....	10
Figure 3. Impacts of the feedwater pH on boron rejection by different NF/RO membranes [86].....	17
Figure 4. Single-pass membrane configuration in SWRO desalination.....	20
Figure 5. Double-pass membrane configuration in SWRO desalination	21
Figure 6. Schematic of the process used in the Ashkelon seawater desalination plant	22
Figure 7. Typical chemical structure of polyamide membranes [149]	35
Figure 8. Proposed changes in the membrane polymeric structure under chlorine attack.	36
Figure 9. Schematic diagram of the NF/RO filtration system used in this study.....	47
Figure 10. Changes in pH and conductivity as a result of complexation between 10 mM boric acid and 2 M glycerol, mannitol or sorbitol.	50
Figure 11. The rejection of boron and polyols by the (a) NF90 and (b) ESPA2 membranes. Feedwater contains 10 mM NaCl, 1 mM CaCl ₂ , 1mM NaHCO ₃ , either 0.43 mM B(OH) ₃ or 0.43 mM polyol. Feedwater temperature 20 °C, permeate flux 42 LMH, cross-flow velocity 42 cm.s ⁻¹ . The error bars show the standard deviations of two repetitive experiments.....	51
Figure 12. The rejection of sodium and calcium by the NF90 membrane in polyol-free and polyol-present conditions. The feedwater contains 0.43 mM B(OH) ₃ , 2.15 mM polyol (corresponding to a boron:polyol molar ratio of 1:5). Other constituents include 10 mM NaCl, 1 mM CaCl ₂ and 1 mM NaHCO ₃ . Feedwater temperature 20 °C, permeate flux 42 LMH, cross-flow velocity 42 cm.s ⁻¹	52
Figure 13. Membrane fouling propensity of the NF/RO filtration experiments. Feedwater contains 0.43 mM B(OH) ₃ , either 0.43 mM or 2.15 mM polyol, 10	

mM NaCl, 1 mM CaCl₂ and 1 mM NaHCO₃. Feed temperature 20 °C, cross-flow velocity 42 cm.s⁻¹..... 53

Figure 14. Boron rejection by the (a) NF90 and (b) ESPA2 membrane with feedwater containing different boron:polyol molar ratios. The feedwater contains 0.43 mM B(OH)₃, 10 mM NaCl, 1 mM CaCl₂ and 1 mM NaHCO₃. Feed temperature 20 °C, permeate flux 42 LMH, cross-flow velocity 42 cm.s⁻¹. The error bars show the standard deviations of two repetitive experiments..... 55

Figure 15. Boron rejection by the NF90 membrane with feedwater containing different boron:sorbitol molar ratios. The feed solution contains 0.093 mM B(OH)₃, 10 mM NaCl, 1 mM CaCl₂ and 1 mM NaHCO₃. Feed temperature 20 °C, permeate flux 42 LMH, cross-flow velocity 42 cm.s⁻¹. The error bars show the standard deviations of two repetitive experiments..... 57

Figure 16. Changes in zeta potential of the ESPA2 membrane as a consequence of single and sequential chemical cleaning. The measurements were conducted at room temperature (ca. 25 °C) in a 1 mM KCl solution..... 64

Figure 17: Changes in contact angle values of the ESPA2 membrane as a consequence of single and sequential chemical cleaning. A positive value indicates an increase in the hydrophobicity, and vice versa. The measurements were conducted at room temperature (ca. 25 °C) with Milli-Q water used as a reference solvent. The error bars show the standard deviation of five replicated measurements..... 66

Figure 18. FTIR absorption spectra of virgin and chemically cleaned ESPA2 membranes at 2 cm⁻¹ resolution. 67

Figure 19. Relative change in the water permeability of ESPA2 membranes as a consequence of single and sequential chemical cleaning. The water permeability was measured with Milli-Q water from 5 to 30 bar with 5 bar increments and at 20 °C; cross-flow velocity 42 cm.s⁻¹..... 69

Figure 20. Changes in boron and sodium rejections by the ESPA2 membrane as a consequence of acidic (citric acid, CA) or caustic (NaOH) cleaning. Unless otherwise stated, the testing conditions are: pH 8, feedwater contains 0.43 mM

B(OH)₃, 10 mM NaCl, 1 mM NaHCO₃, and 1 mM CaCl₂; temperature 20 °C, permeate flux 20 LMH, cross-flow velocity 42 cm.s⁻¹. 72

Figure 21. Changes in boron and sodium rejections by the ESPA2 membrane after membrane cleaning with SDS solution (pH 11) and SDS solution followed by citric acid solution (pH 3). Unless otherwise stated, the testing conditions are: pH 8, feedwater contains 0.43 mM B(OH)₃, 10 mM NaCl, 1 mM NaHCO₃, and 1 mM CaCl₂; temperature 20 °C, permeate flux 20 LMH, cross-flow velocity 42 cm.s⁻¹. 73

Figure 22. Changes in boron and sodium rejections by the ESPA2 membrane after membrane cleaning with EDTA solution (pH 11) and EDTA solution followed by citric acid solution (pH 3). Unless otherwise stated, the testing conditions are: pH 8, feedwater contains 0.43 mM B(OH)₃, 10 mM NaCl, 1 mM NaHCO₃, and 1 mM CaCl₂; temperature 20 °C, permeate flux 20 LMH, cross-flow velocity 42 cm.s⁻¹. 74

Figure 23. Changes in boron and sodium rejections by the ESPA2 membrane after membrane cleaning with EDTA+SDS solution (pH 11) and EDTA+SDS solution followed by citric acid solution (pH 3). Unless otherwise stated, the testing conditions are: pH 8, feedwater contains 0.43 mM B(OH)₃, 10 mM NaCl, 1 mM NaHCO₃, and 1 mM CaCl₂; temperature 20 °C, permeate flux 20 LMH, cross-flow velocity 42 cm.s⁻¹. 75

Figure 24. Changes in boron and sodium rejections by the ESPA2 membrane after membrane cleaning with MC11 solution (pH 11) and MC11 solution followed by citric acid solution (pH 3). Unless otherwise stated, the testing conditions are: pH 8, feedwater contains 0.43 mM B(OH)₃, 10 mM NaCl, 1 mM NaHCO₃, and 1 mM CaCl₂; temperature 20 °C, permeate flux 20 LMH, cross-flow velocity 42 cm.s⁻¹. 76

Figure 25. Changes in boron and sodium rejections by the ESPA2 membrane after membrane cleaning with MC3 solution (pH 3) and MC3 solution followed by sodium hydroxide solution (pH 11). Unless otherwise stated, the testing conditions are: pH 8, feedwater contains 0.43 mM B(OH)₃, 10 mM NaCl, 1 mM

NaHCO₃, and 1 mM CaCl₂; temperature 20 °C, permeate flux 20 LMH, cross-flow velocity 42 cm.s⁻¹..... 77

Figure 26. Zeta potential of virgin and preserved ESPA2 and SWC5 membranes. Measurements conducted at room temperature (ca. 25 °C) in a 1 mM KCl solution. Abbreviations: S7 for SMBS at pH 7, S3 for SMBS at pH 3, F7 for formaldehyde at pH 7, F3 for formaldehyde at pH 3, D7 for DBNPA at pH 7. 84

Figure 27. Contact angle values of virgin and preserved ESPA2 and SWC5 membranes. Measurements conducted at room temperature (approximately 25 °C), Milli-Q water used as reference solvent. The error bars show the standard deviation of five replicate measurements. Abbreviations: S7 for SMBS at pH 7, S3 for SMBS at pH 3, F7 for formaldehyde at pH 7, F3 for formaldehyde at pH 3, D7 for DBNPA at pH 7..... 85

Figure 28. FTIR absorption spectra of virgin and preserved ESPA2 and SWC5 membranes obtained at 2 cm⁻¹ resolution. Abbreviation: F3 for formaldehyde at pH 3, F7 for formaldehyde at pH 7, S3 for SMBS at pH 3, S7 for SMBS at pH 7, D7 for DBNPA at pH 7..... 87

Figure 29. The rejection of boron, sodium and conductivity by the virgin ESPA2 and SWC5 membranes at various operating conditions. Unless otherwise stated, the testing conditions are: pH 8, feedwater contains 0.43 mM B(OH)₃, 10 mM NaCl, 1 mM NaHCO₃, and 1 mM CaCl₂; temperature 20 °C, permeate flux 20 LMH, cross-flow velocity 42 cm.s⁻¹. The error bars indicate the standard deviation of seven replicate experiments. 89

Figure 30. Relative change in pure-water permeability and rejection of boron and sodium by ESPA2 and SWC5 membranes after exposure to preservatives. Standard test conditions: pH 8, feedwater contains 0.43 mM B(OH)₃, 10 mM NaCl, 1 mM NaHCO₃, and 1 mM CaCl₂; temperature 20 °C, permeate flux 20 LMH, cross-flow velocity 42 cm.s⁻¹. The error bars show the standard deviation of two replicate experiments. Abbreviations: S7 for SMBS at pH 7, S3 for SMBS at pH 3, F7 for formaldehyde at pH 7, F3 for formaldehyde at pH 3, D7 for DBNPA at pH 7..... 91

- Figure 31.** Redox potential of the preserving solutions. Abbreviations: S7 for SMBS at pH 7, S3 for SMBS at pH 3, F7 for formaldehyde at pH 7, F3 for formaldehyde at pH 3, D7 for DBNPA at pH 7..... 92
- Figure 32.** Relative change in boron rejection by the ESPA2 membrane at different testing fluxes, temperatures, and pH values. Standard test conditions: pH 8, feedwater contains 0.43 mM B(OH)₃, 10 mM NaCl, 1 mM NaHCO₃, and 1 mM CaCl₂; temperature 20 °C, permeate flux 20 LMH, cross-flow velocity 42 cm.s⁻¹. Abbreviations: S7 for SMBS at pH 7, S3 for SMBS at pH 3, F7 for formaldehyde at pH 7, F3 for formaldehyde at pH 3, D7 for DBNPA at pH 7. 94
- Figure 33.** Relative change in boron rejection by the SWC5 membrane at different testing fluxes, temperatures, and pH values. Standard test conditions: pH 8, feedwater contains 0.43 mM B(OH)₃, 10 mM NaCl, 1 mM NaHCO₃, and 1 mM CaCl₂; temperature 20 °C, permeate flux 20 LMH, cross-flow velocity 42 cm.s⁻¹. Abbreviations: S7 for SMBS at pH 7, S3 for SMBS at pH 3, F7 for formaldehyde at pH 7, F3 for formaldehyde at pH 3, D7 for DBNPA at pH 7. 95
- Figure 34.** The correlation between the rejections of boron and NDMA by different membranes at pH 8. Feedwater contains 250 ng.L⁻¹ NDMA, 5.75 mg.L⁻¹ B(OH)₃, 20 mmol.L⁻¹ NaCl, 1 mmol.L⁻¹ NaHCO₃, and 1 mmol.L⁻¹ CaCl₂; temperature 20 °C, permeate flux 20 LMH, cross-flow velocity 42 cm.s⁻¹..... 102
- Figure 35.** The speciation of boric acid and NDMA in de-ionised water matrix, temperature 25 °C, pressure 1 atm. 103
- Figure 36.** (a) The rejection of boron and NDMA as functions of permeate flux at different pH values; and (b) the correlation between boron and NDMA rejections at various permeate fluxes at pH 8. The TFC-HR membrane was used; feedwater contains 250 ng.L⁻¹ NDMA, 5.75 mg.L⁻¹ B(OH)₃, 20 mmol.L⁻¹ NaCl, 1 mmol.L⁻¹ NaHCO₃, and 1 mmol.L⁻¹ CaCl₂; temperature 20 °C, cross-flow velocity 42 cm.s⁻¹..... 105
- Figure 37.** (a) The rejection of boron and NDMA as functions of temperature at different pH values; and (b) the correlation between boron and NDMA rejections at various temperatures at pH 8. The TFC-HR membrane was used; feedwater contains 250 ng.L⁻¹ NDMA, 5.75 mg.L⁻¹ B(OH)₃, 20 mmol.L⁻¹ NaCl,

1 mmol.L⁻¹ NaHCO₃, and 1 mmol.L⁻¹ CaCl₂; permeate flux 20 LMH, cross-flow velocity 42 cm.s⁻¹. 106

Figure 38. (a) The rejection of boron and NDMA as functions of temperature; and (b) the correlation between boron and NDMA rejections at various temperatures. The TFC-HR membrane was used. Tertiary treated effluent dosed with 250 ng.L⁻¹ NDMA was used as feed solution. Permeate flux 20 LMH, cross-flow velocity 42 cm.s⁻¹. 107

LIST OF TABLES

Table 1. Regulation and guideline values for boron in drinking water from several institutions and countries [28, 36-42]	9
Table 2. Methods available for boron determination [39, 53, 59, 62, 63].....	13
Table 3. Manufacturer-recommended cleaning chemicals for RO membranes [137, 138]	32
Table 4. Solutions recommended by membrane manufacturers for membrane storage [162-164].....	37
Table 5. Properties of the polyols used in this study [46, 48-50].....	46
Table 6. Properties of the membranes used in this study	46
Table 7. Solutions used for membrane cleaning simulation in this study.....	59
Table 8. Water permeability and salt rejection of the selected RO membranes.....	99
Table 9. Properties of boric acid and NDMA.....	102

LIST OF ABBREVIATIONS

Abbreviation	Full form	Abbreviation	Full form
AAS	Atomic Absorption Spectrophotometry	NF	Nanofiltration
AES	Atomic Emission Spectroscopy	NOAEL	No-observed-adverse-effect-level
AFM	Atomic Force Microscopy	OES	Optical Emission Spectroscopy
BWRO	Brackish water reverse osmosis	PhACs	Pharmaceutically Active Compounds
CTAB	Cetyltrimethyl ammonium bromide	RO	Reverse Osmosis
DTAB	Dodecyltrimethyl ammonium bromide	SDS	Sodium Dodecylsulfate
EDS	Energy Dispersive X-ray Spectroscopy	SEM	Scanning Electron Microscopy
EDTA	Ethylene-Diamine Tetra-acetic Acid	SMBS	Sodium Meta Bi-Sulfite (Na ₂ S ₂ O ₅)
EU	European Union	SPE	Solid Phase Extraction
FTIR	Fourier Transform Infrared	SWRO	Seawater reverse osmosis
GC	Gas Chromatography	TDS	Total Dissolved Solids
IC	Ion Chromatography	TEM	Transmission electron microscopy
ICP	Inductively Coupled Plasma	TTAB	Tetradecyltrimethyl ammonium
LMH	L.m ⁻² .h ⁻¹	WHO	World Health Organisation
MS	Mass Spectrometry	XPS	X-ray Photoelectron Spectrometry
NDMA	N-nitrosodimethyl amine		

NOMENCLATURES

J_w Water flux	J_s Solute flux
P_w Pure water permeability coefficient	P_s Solute permeability coefficient
ΔP Hydraulic pressure difference	$\Delta \pi$ Osmotic pressure difference
C_M Solute concentration at the membrane surface in feed side	C_P Solute concentration at the membrane surface in permeate side
R or R_o Apparent rejection	R_r Real rejection
C_B Solute concentration in the bulk feed solution	k Mass transfer coefficient
D Diffusion coefficient	δ Thickness of boundary layer or pore length
σ Reflection coefficient	C Superficial concentration
\bar{C} Average solute concentration in feed and permeate	K Efficiency of spacer
T Absolute temperature	Sc Schmidt number
μ Dynamic viscosity	ρ Density
Pe Peclet number	h_b Thickness of feed channel
ΔL Characteristic length of spacer	K_D Distribution coefficient
D_{sp} Diffusivity	γ Electron surface tension
F Faraday constant	

CHAPTER 1: INTRODUCTION

1.1 Background

Freshwater scarcity has been recognised as one of the most vexing challenges in sustaining improved living standards and population growth. Although water covers 75% of the Earth's surface, the majority (95%) is salty water in the oceans and inland seas, only 0.8% is freshwater [1]. On a global scale, this 0.8% freshwater availability is shared by agricultural (70%), industrial (22%) and domestic use (8%) [2]. In addition, water is not evenly distributed around the globe. Nine countries possess 60% of the world's available freshwater supply: Brazil, Russia, China, Canada, Indonesia, USA, India, Colombia and the Democratic Republic of Congo [3]. Although these include some of the most populated countries, the remaining 40% freshwater is insufficient for the rest of the world.

Some conventional freshwater sources such as rivers, lakes, and groundwater have been over-exploited and misused. Consequently, these resources are either declining or becoming saline. Worldwide efforts have been devoted towards the development of unconventional water resources such as seawater and reclaimed wastewater. Seawater is not only abundant but also accessible to most countries in the world. To produce potable water from seawater, desalination processes are needed to remove salts and other impurities. Thermal distillation, which has been used on ships and remote islands for hundreds of years, has been successfully applied to produce municipal potable water during 1930s and is still a commonly employed desalination process. However, reverse osmosis (RO) membrane technology has attained substantial development since its arrival in the 1960s to become a major competitor to the thermal process in the desalination market. Significant developments in membrane materials and technologies in the past few decades have greatly improved the cost effectiveness and performance capability of membrane processes. Thermal distillation, on the other hand, is negatively affected by the rise of fossil fuel price and therefore has become less attractive. Consequently, thermal distillation is restricted mostly to the Middle East region where fossil fuel is still affordable. In fact, RO membranes nowadays account for about half of the current worldwide desalination capacity [4-6]. RO and other membrane systems are responsible for

almost 96% of the USA online desalination capacity and 100% of the municipal desalination capacity [7]. All of the more than 100 desalination projects being implemented in Europe use RO technology [6]. Since 2003, in Australia, more than 30 new RO plants have been constructed and commissioned for either seawater desalination or water recycling [8, 9]. In addition, the widespread use of small-to medium-scale RO systems has been seen for brackish water desalination for mine sites [10], remote communities [11], military outposts [12] and a range of industrial applications such as coal seam gas produced water treatment, cooling water demineralisation [13], and wine-making [14].

Another solution to the problem of freshwater scarcity is water reclamation. In recent years, water reclamation for different applications has been rapidly growing around the world. Some major water reclamation schemes are the Western Corridor Recycled Water Project (Queensland, Australia), NEWater (Singapore), Goreangab Water Reclamation Plant (Namibia), Scottsdale Water Campus (Arizona, U.S.), and Hampton Advanced Water Treatment (London, England). Most of these water schemes recycle municipal and industrial wastewater to use for irrigation, industry, indirect or direct drinking water supply. Wastewater reclamation has several advantages making it a preferable option over seawater desalination, including lower salinity (so lower energy required to desalt the water), climate-independence, and the adjacency between the water source and consumption.

The emerging trend of using unconventional water sources for drinking water supply and agricultural irrigation has raised the concern of water quality. The utilisation of seawater and recycled wastewater for drinking (direct or indirect) and irrigation requires some impurities such as boron and N-nitrosodimethylamine (NDMA) to be removed from those waters. Boron naturally exists in seawater at a concentration of approximately 4.6 mg.L^{-1} . On the other hand, water used for the irrigation of boron-sensitive crops must satisfy a boron level of less than 0.5 mg.L^{-1} . Elevated boron levels are also found in municipal wastewater because of the use of boron-rich household chemicals such as bleach and detergent. Although state-of-the-art RO membranes can reject more than 99% of sodium chloride (which is the dominant salt in seawater), they have a much lower rejection of low-molecular-weight solutes. In fact, the requirement for adequate boron rejection has been considered as one of the

major challenges to the application of membrane technology in water and wastewater treatment [15, 16]. The problem of low boron rejection efficiency of typical RO membranes resulted in membrane manufacturers such as Toray and Hydranautics recently developing seawater reverse osmosis (SWRO) and brackish water reverse osmosis (BWRO) membranes specific for boron rejection improvement.

1.2 Research scope and opportunities

To produce freshwater satisfying stringent regulations for low boron content, RO desalination plants usually utilise multi-pass membrane configurations associated with pH elevation. This method substantially increases the capital and operational cost, and therefore reduces the economic efficiency of the process. As a result, innovations to improve boron rejection efficiency of RO membranes are in high demand.

In addition, the membrane gradually loses its integrity over an operational period due to interactions with various chemicals (i.e. pre-treatment, cleaning, and preservative agents). Consequently, the membrane performance is expected to deteriorate. However, the performance of membranes under aged condition has not been well understood, to date.

There exist major difficulties to effectively monitor the NDMA level in water reclamation plants due to the limitation in analytical techniques available for this compound. Quantitative analysis of this compound at regulated concentrations requires sophisticated facilities and proficient expertise which are not commonly available. It is therefore desired that a more readily monitored parameter can be used as a surrogate for NDMA fate in RO water reclamation plants.

1.3 Research objectives and expected outcomes

The objectives of this study include:

- To investigate the technical and practical feasibility of a novel technique to improve boron rejection efficiency by RO and nanofiltration (NF) membranes. This method involves the addition of a poly-alcohol (polyol) to the feedwater to make complexes with boron existing in the water. The boron-polyol complex is not only larger than boric acid but also negatively

charged. These conformational changes are expected to result in boron rejection enhancement due to the increase in both steric hindrance and charged repulsion mechanisms. The result of this study may provide a potential technical option for improving boron rejection in RO water and wastewater treatment installations.

- To evaluate the impacts of chemical cleaning and chemical preservation on the membrane performance, particularly on the water permeability and the rejection of boron and sodium. The membrane performance was examined at various permeate fluxes, temperatures, and pH conditions. Impacts of chemicals on the membrane performance were elucidated based on a variety of characterised membrane properties. The result of this study can help to predict the membrane performance in aged conditions and also provide a technical guideline for improving the current process of chemical cleaning and chemical preservation.
- To evaluate the feasibility of using boron rejection as a surrogate for NDMA rejection in RO water reclamation application. Since NDMA and boron have comparable molecular properties at $\text{pH} < 9.2$, there are possibilities that these two compounds are rejected by RO membranes at a comparable magnitude. In this study, the rejection of boron and NDMA was examined at various operating conditions and with different membranes used. The initial experimental results conducted with laboratory-synthetic feedwater were further examined using a real tertiary-treated wastewater sample.

1.4 Thesis outline

The structure of this dissertation is schematically described in Figure 1. The dissertation includes seven Chapters. Chapter 1 provides an introduction to the research topic, research questions and objectives of this study. Chapter 2 delivers a comprehensive review on the state-of-the-art literature of boron rejection by NF/RO membranes together with related concerns. At the end of Chapter 2, key knowledge gaps in this area are presented. Such research gaps are then addressed by four studies that form the core of this dissertation, including Chapters 3, 4, 5 and 6. In Chapter 3, different aspects of the method to improve boron rejection by polyol addition were

experimentally examined and discussed. Chapters 4 and 5 present the experimental results of the impacts of chemical cleaning and chemical preservation, respectively, on the membrane performance. In Chapter 6, the feasibility of using boron as a surrogate for NDMA rejection is experimentally examined and discussed. Chapter 7 produces overall conclusions for the whole dissertation and recommendations for future studies on the topic.

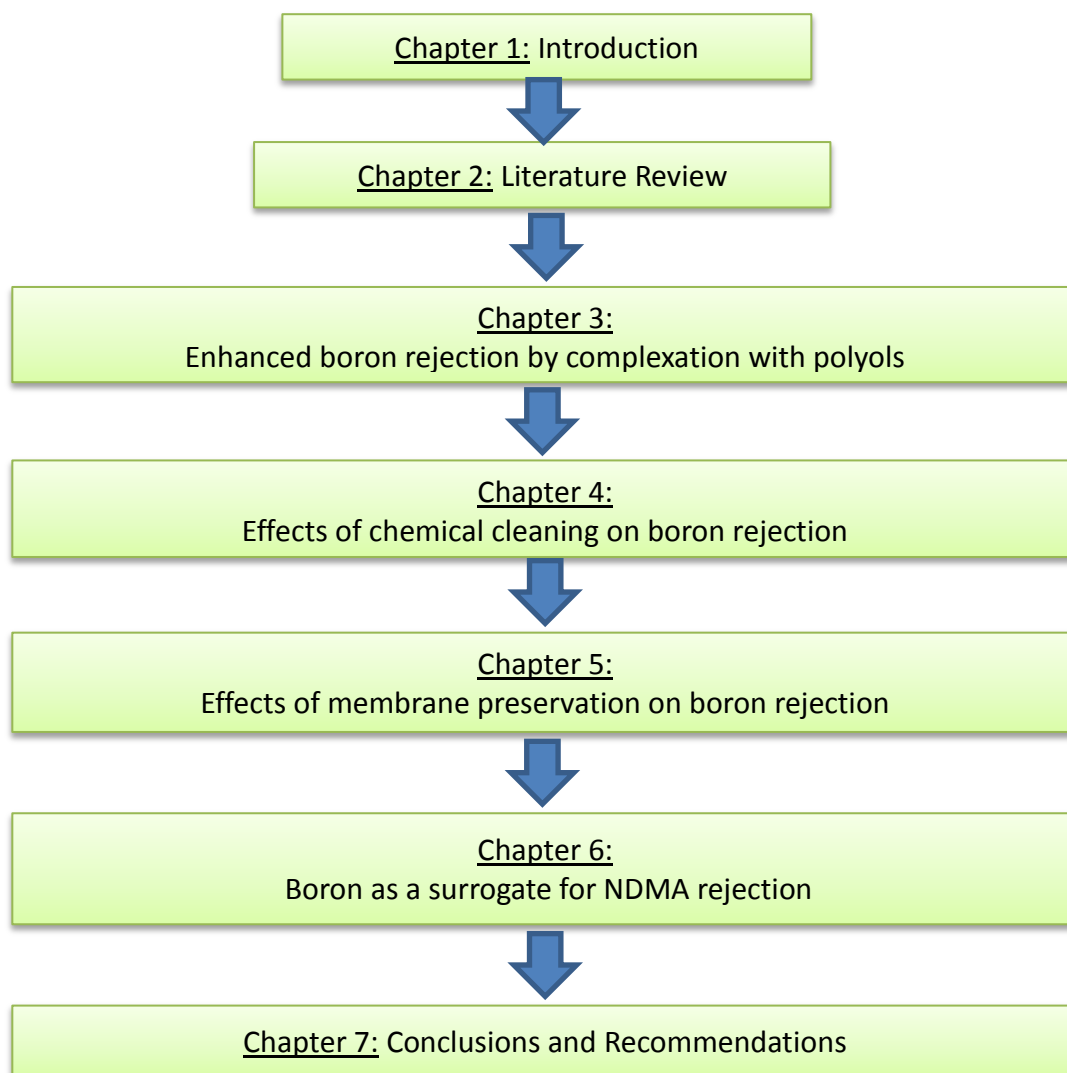


Figure 1. Outline of the structure of this dissertation

CHAPTER 2: LITERATURE REVIEW

2.1 Boron in the environment

Boron is a naturally occurring element, primarily found in the form of boric acid $[B(OH)_3]$ and borate salts $[B(OH)_4^-]$. Boron is present in natural reservoirs of the hydrological cycle, such as surface water, groundwater, and ice. Boron levels in surface water are generally lower than 0.5 mg.L^{-1} , but the level in seawater is significantly higher than groundwater and other surface water sources [17, 18]. The average boron concentration in seawater is approximately 4.6 mg.L^{-1} , and can range between 0.52 mg.L^{-1} in the Baltic Sea to 9.57 mg.L^{-1} in the Mediterranean Sea [19]. The average concentration of boron in surface freshwaters is usually less than 0.1 mg.L^{-1} with levels of up to 0.5 mg.L^{-1} close to wastewater effluent discharge [19, 20]. Concentrations up to 6.5 mg.L^{-1} have been reported in some groundwater supplies, but these high concentrations are associated with seawater intrusion or boron-rich geological formations. Naturally occurring boron is present in groundwater primarily as a result of leaching from rocks and soils containing borates and borosilicate minerals. The amount of boron in freshwaters depends on such factors as the geochemical nature of the drainage area and proximity to marine coastal regions [21].

Human activities also contribute to high boron levels in the aquatic environment. Fertilisers, herbicides, and industrial wastes are among the sources of soil boron-contamination. Industrial wastewater and municipal sewages usually contain a relatively high level of boron from detergents, soaps, and personal care products [19, 22, 23]. Condensed water from the hydro-thermal power plants in Turkey and Russia has been reported to contain $40\text{-}70 \text{ mg.L}^{-1}$ boron [24]. According to Dyer and Caprara [25], about 50% of the boron in wastewater effluent comes from detergents. Calculations by the German Government Environment Agency attribute 50% of the boron in wastewater to the use of detergent products [21]. This boron source easily reaches the natural water sources since boron is not substantially adsorbed in sewage and cannot be biodegraded or removed during sewage treatment processes [26]. Indeed, Neal and Robson [27] supposed that high levels of boron concentrations

were found mostly in rivers which are associated with urban and industrial drainage relative to those from rural areas.

2.1.1 Health and ecological impact of boron

Scientific data to date on particular effects of boron on human health are insufficient and mostly inferred from experimental animal data [28]. Although boron is a micro nutrient in the human diet, toxicity can occur when the boron intake reaches the tolerance limit which is different for different species. Short- and long-term oral exposures to boric acid or borax in laboratory animals have demonstrated that the male reproductive zone is a consistent target of toxicity. Testicular lesions have been observed in rats, mice and dogs administered boric acid or borax in food or drinking-water [21, 29, 30]. The no-observe-adverse-effect-level (NOAEL) for female and male rat reproductive toxicity is 23.76 and 17.28 mg.[kg bodyweight]⁻¹.day⁻¹, respectively [28]. For humans, the World Health Organisation (WHO) have proposed a NOAEL of 0.22 mg[kg bodyweight]⁻¹.d⁻¹ [31].

The toxic effects of boron on aquatic organisms are governed by several factors, including: form and concentration of boron, type and characteristics of the organism, period and type of exposure to boron (acute or chronic). For instance, Birge and Black [32] reported that embryonic stages in fish and amphibians were more sensitive to boron compounds than the early post-hatched stages. Butterwick et al. [21] found that environmental factors such as reconstituted water showed greater toxicity to trout embryo larval stages than if they were exposed to boron in natural water.

The range between deficiency and toxicity levels of boron in plants is narrow. The optimum boron content in soil solution for plant growth ranges from 2.2 to 4.5 mg.L⁻¹ and deficiency or toxicity of boron appears when the boron level falls or rises beyond this range [29]. Toxicity levels do not usually occur on agricultural lands unless boron compounds have been added in excessive quantities, such as with fertiliser materials, irrigation water sewage sludge or coal ash [33]. Irrigation water contaminated with boron is one of the main causes of boron toxicity in plants, especially in arid regions with high evapo-transpiration [29]. Precipitation, climate, and salinity of the irrigation water also play a role in the boron toxicity in plants.

Boron toxicity has been reported to limit crop yields in Australia, North Africa, and West Asia where alkaline and saline soils are present together with a low rainfall and limited leaching. Boron toxicity in plants is characterised by stunted growth, leaf malformation, browning and yellowing, chlorosis, necrosis, increased sensitivity to mildew, wilting and inhibition of pollen germination and pollen tube growth.

2.1.2 Regulations and guidelines for boron content in waters

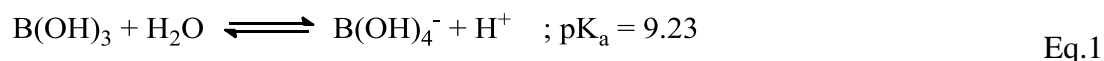
The regulations and guidelines for boron content, as for other contaminants, are mostly driven by: (1) scientific data about its impacts on human and ecological health; (2) social and natural characteristics of regions; (3) the capability of treatment technologies to remove the contaminant. It is exceptionally complicated with boron because herein all the listed factors are deeply involved and affect each other. As discussed in Section 2.1.1, the toxicity level of boron to human is not adequately known, although the scientific data for plants are recognised. Nevertheless, because humans are supposed to have a higher tolerance level to boron than many agricultural crops, most existing boron limit guidelines are based on the tolerance of crops that are grown in the region. For instance, Israel has a very stringent boron limit in their drinking water guidelines (Table 1) because such water is eventually used for irrigating crops, including citrus - an extremely boron-sensitive plant [34]. Natural characteristics, especially geological condition strongly affect the regulation by local government on boron limit, and also render the compliance more intricate. Cyprus, as an example, possesses a long history of policy action to deal with boron; however, has difficulty to comply with the European Union's (EU) Drinking Water Directive (Table 1) because of the exceptionally high natural boron in the groundwater. The capability of technology to remove boron also plays an important role in determining the regulated/guideline value. The WHO's Guidelines for Drinking Water Quality published in 1998 increased the recommended boron level to 0.5 mg.L^{-1} from the value of 0.3 mg.L^{-1} established in 1993 because the existing removal technology was unable to reduce the boron level to 0.3 mg.L^{-1} [22]. Again, in the 4th Edition of these guidelines, the regulated boron level was increased to 2.4 mg.L^{-1} due to the lack of boron toxicity data on human [35].

Table 1. Regulation and guideline values for boron in drinking water from several institutions and countries [28, 36-42]

Institution/country	Boron regulated value [mg.L ⁻¹]	Institution/country	Boron regulated value [mg.L ⁻¹]
WHO	2.4	Japan	1.5
EU	1.0	New Zealand	1.4
Canada	5.0	Singapore	1.0
South Korea	1.0	Saudi Arabia	1.5
Israel	0.3		

2.1.3 Chemistry of boron

Boron in the aquatic environment is present mainly in the form of boric acid [B(OH)₃]. Boric acid is a waxy solid and is soluble in water (55 g.L⁻¹ solubility at 25 °C). Being the only non-metallic element in group 13 of the periodic table, the chemistry of boron and its compound boric acid is unique. Boric acid behaves as a very weak Lewis acid according to the hydrolysis:



The dissociation curve of boric acid is shown in Figure 2. Boric acid is principally present at pH below 9.23, whereas at higher pH borate ions are dominantly present. Boric acid is poorly hydrated and so possesses a small molecular size, whose Stokes radius is estimated to be about 0.155 nm (which is only double that of the water molecule) [43]. Having three hydroxyl groups, boric acid can form up to six hydrogen bonds with water leading to a strong association with water.

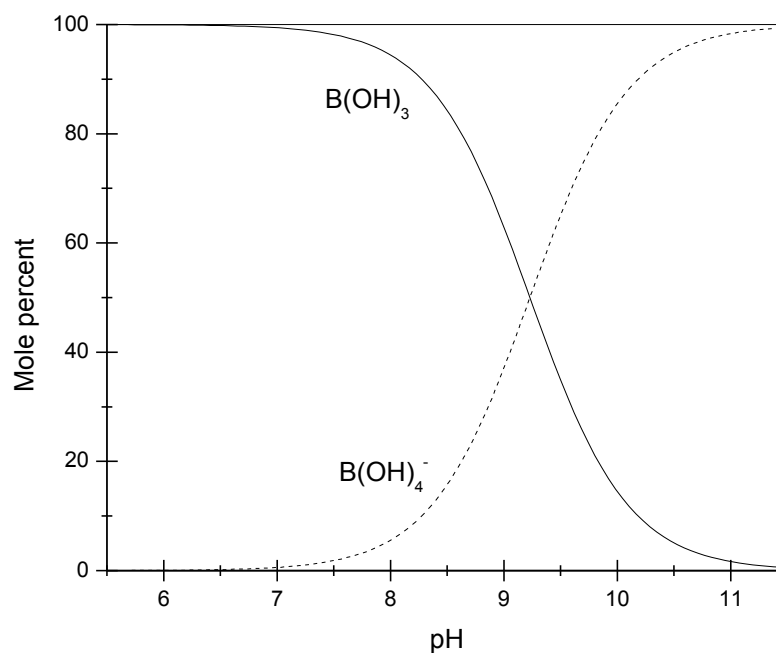
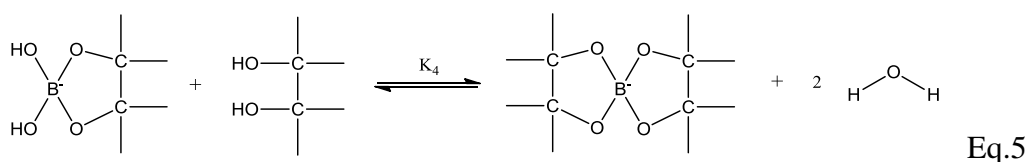
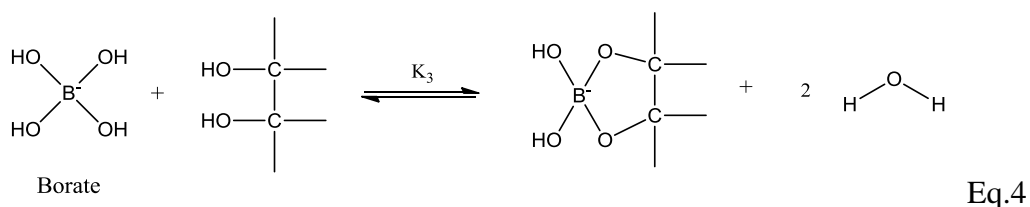
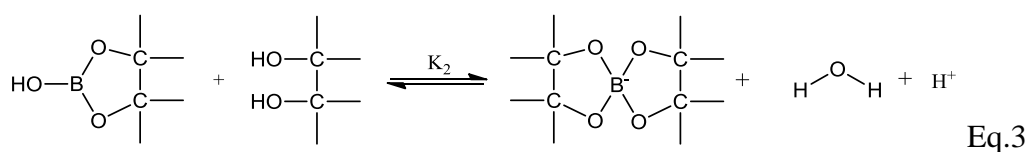
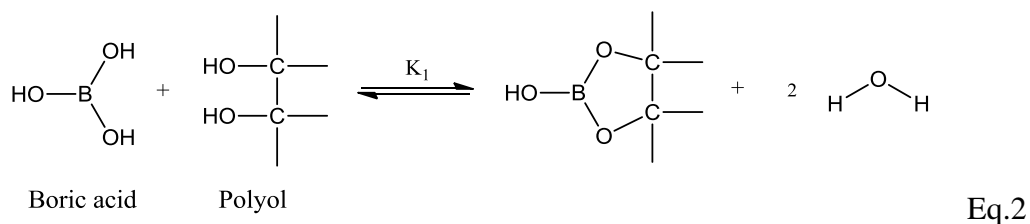


Figure 2. The dissociation of boric acid in diluted solution

Being a weak Lewis acid, the pK_a of boric acid shifts according to the surrounding conditions such as temperature, pressure, and the ionic strength of its solution. For example, the pK_a of boric acid is decreased from 9.23 to 8.60 when the solution salinity increases from 0 to 40,000 mg.L^{-1} [44]. An increase in the solution temperature from 10 to 50 $^{\circ}\text{C}$ will decrease the pK_a by 0.3 unit [45]. At relatively low concentrations ($\leq 0.02 \text{ mol.L}^{-1}$ or 22 mg.L^{-1} as B), only the mononuclear species B(OH)_3 and B(OH)_4^- are present. However, at higher concentrations with high pH, especially above pH 10, poly-nuclear ions such as $[\text{B}_3\text{O}_3(\text{OH})_5]_2^-$ and $[\text{B}_4\text{O}_5(\text{OH})_4]_2^-$ would be formed [46]. Given that boron concentration in seawater and other natural water sources hardly exceeds 10 mg.L^{-1} (Section 2.1), it is expected that only mononuclear species of boron exist in such natural waters.

It is well-known that boric acid and borate ions can react with multiple hydroxyl compounds (polyols) to produce complexes. The complexation, which increases the acidity of boric acid, has been utilised for many years as the basis of boric acid quantitative analysis that cannot be done by direct titration [47]. The complexation of boron with polyols involves two distinct mechanisms: boric acid with polyol (Eq.2 & Eq.3) and borate ion with polyol (Eq.4 & Eq.5). The contribution of each mechanism in the overall complexation depends on the solution pH where either boric acid or borate ion is dominantly present. The stability constants of borate complexes (K_3 and

K_4) have been investigated [48-50], whereas those of boric complexes (K_1 and K_2) are not available in the literature.



The complexation of boric acid/borate ions with polyols involves complicated equilibria in which one boron atom can associate with one or two polyol molecules forming different types of complexes. The stability of the complexation products greatly depends on the type of diol used and the solution pH. If the diol used involves the OH groups oriented in such a way that they accurately match the structural parameters required by a tetrahedral coordinate, a stable complex will be formed. The esters formed with cis-diols on a furanoid ring have been found to be most stable, but these structures are rare in nature and limited to apiose and rebose [46].

2.1.4 Analytical methods for boron

Many quantitatively analytical methods have been tested for boron quantitative determination. The method of preference depends on the required analytical range and sensitivity, the matrix of the boron-containing water, and also the availability of analytical instruments. Methods typically considered for boron determination include spectrophotometric, ionometric, and atomic spectrometric methods.

Several spectrophotometric methods rely on the colorimetric reactions of boron with some specific reagents such as curcumin, carmine, azomethine-H, and methylene blue. The spectrophotometric methods are well suited for field analysis. However, these methods generally suffer from numerous interferences such as Al, Cu, Fe, Zn, and Mo [51] which limit their application to simple matrices only. The spectrophotometric methods are also known for their lack of sensitivity and precision, which makes it difficult to determine boron at low levels. Among the typically used reagents, azomethine-H is faster, simpler, comparatively sensitive and has fewer interferences, and is therefore probably the most commonly used spectrophotometric method for boron determination [52].

Ionometric methods, represented by ion chromatography (IC), are emerging techniques for determining boron in environmental applications. IC offers low cost, high sensitivity, with the ability to monitor on-line, which makes it suitable for seawater desalination applications [15]. In the IC method, boron is usually extracted from the sample matrix, treated with HF and the resulting tetrafluoroborate ion BF_4^- is measured potentiometrically with a suitable BF_4^- ion selective electrode [53]. IC was initially employed to determine BF_4^- concentrations. To determine the total boron concentration, boron-containing samples must be quantitatively converted to BF_4^- beforehand [54]. Although an IC method that does not require boron extraction from the sample has also been reported [55], it is crucial to either remove the matrix or match the calibration matrix with that of the sample because the IC method is highly dependent on the sample matrix [56].

Atomic spectrometric methods, including atomic emission spectroscopy (AES) (also known as optical emission spectroscopy (OES)) and atomic absorption spectrophotometry (AAS) involve the introduction of liquid samples into a flame

where elements of the sample are atomised. The AES/AAS determination of boron usually requires the separation and pre-concentration of boron from the sample matrix for the best results [57]. These methods generally have poor sensitivity, serious memory effect, and numerous interferences [58]. Nevertheless, when a plasma flame is used as the ionisation source, the techniques become exceptionally advantageous. There are several types of plasma, but most commercial plasma-source instruments use an argon inductively-coupled plasma (ICP). The ICP was combined with various detection techniques such as AES (ICP-AES) (also known as ICP-OES), and mass spectrometry (ICP-MS) to provide excellent sensitivity and detection capacity. The reported detection limit for boron by ICP-MS was ten times lower than that of the IC and hundreds of times lower than spectrophotometric methods (

Table 2). ICP-MS is usually the method of choice over ICP-AES, IC and spectrophotometric methods for boron determination. The advantages of ICP-MS over other methods are higher sensitivity, lower detection limit, less interferences and simultaneous measurement of ^{10}B to ^{11}B isotopic ratio. The detection limit for boron was reported as $0.15 \mu\text{g.L}^{-1}$ in saline waters [59], $1 \mu\text{g.L}^{-1}$ in human serum [60], and $3 \mu\text{g.L}^{-1}$ in biological material [61]. A brief description of the ICP-MS method is given below.

Table 2. Methods available for boron determination [39, 53, 59, 62, 63].

Methods	Limit of quantification, $\mu\text{g.L}^{-1}$
ICP-MS	0.15
ICP-AES	5 - 6
IC	50
Azomethine-H	10 - 20
Curcumine	100 - 200
Carmine	1000 - 2000

Limitations of these analytical techniques are primarily associated with the complex sample matrix, and spectral and isobaric interferences. Consequently, the choice of method depends on the sample type and the degree of complexity acceptable for sample preparation. Spectrophotometry is preferred as its simple functioning, but it suffers from low sensitivity and severe matrix interference compared to other

methods. Although AES and AAS revolutionised the quantitative analysis of many elements, their application for boron suffers from serious interferences.

2.1.5 Boron determination by ICP-MS

The liquid sample is introduced into the ICP as aerosol, produced by passing the liquid sample through a pneumatic nebuliser. Larger aerosol droplets are removed from the gas stream by a spray chamber, and the remaining smaller droplets are swept into a quartz torch where an argon plasma is formed under high power (up to 1600 W) and high frequency electric current (27.12 MHz). The very high temperature of the plasma (up to 10,000 K) renders the aerosol droplets desolvated, atomised, and ionised. The positively charged ions that are produced in the plasma are extracted into the vacuum system via a sample cone and a skimmer cone. Electrostatic lenses keep the ions focused in a compact ion beam as they pass through the vacuum system to the final chamber, where a MS and ion detector are housed. The detector counts and stores the total signal for each isotope as a mass/charge ratio (m/z).

Typically used calibration methods for ICP-MS are external calibration with an internal standard, standard addition and isotope dilution. The first method is most widely used because of its simplicity and labour efficiency [56]. Other methods are generally utilised to deal with difficult sample matrices or to improve precision. For the choice of internal standard element, beryllium is recommended for boron determination because beryllium is the closest mass number to boron and also rarely found in nature [61, 64]. It is also noted that beryllium may cause a strong matrix effect in some cases [65]. Gregoire [59] compared three calibration methods including external calibration with internal standard, standard addition and isotope dilution on freshwater and brine water samples. The author concluded that the isotope dilution calibration method provides the best recovery and is the calibration method of choice. The advantage of the isotope dilution calibration method comes from the fact that isotopic variations in natural waters are common, and thus errors can only be avoided if the isotopic composition of the sample is known in advance [59].

No corrections for isobaric interferences or spectroscopic interferences were necessary as no other isotopes of any other element occur at mass 10 or 11. With the exception of ^{12}C overlap, no molecular ions originating from water, plasma or atmospheric gases were found to interfere with either of the boron isotopes [59]. However, as a light element with relatively low ionisation in the argon plasma (approximately 58% at 7,500 K), boron is expected to have serious non-spectroscopic interferences from the sample matrix.

The presence of associated elements in solution may render the determination of boron complicated. Excessive dissolved solids cause loss of analytical sensitivity and a matrix-induced mass discrimination effect, resulting in analytical error. When the sensitivity of the technique is insufficient or interferences are overwhelming, then purification, flow injection, and pre-concentration of the samples can be used to enhance the boron detection limits [66]. The use of cation exchange is effective in removing dissolved salts and permitted the accurate determination of boron by ICP-MS [59]. Pre-concentration of boron requires additional sample handling and therefore enhances possibility of contamination, losses, incomplete yields, and isotopic fractionation [66]. In the determination of boron at trace levels, contamination from borosilicate glassware including containers and sample introduction system can be severe, and so the use of this material must be avoided [59, 67].

A memory effect can result from boron's tendency to volatilise as boric acid from the sample solution layer covering the spray chamber's inside surface, whereas the cones, ion lenses, quadrupole and other components seem not to contribute to the boron memory effect [68]. Al-Ammar et al. [68, 69] reported the injection of 10–20 mL.min⁻¹ of ammonia gas into the spray chamber during boron determination would eliminate the memory effect of a 1 µg.mL⁻¹ B solution within a 2-min washing time. Ammonia gas injection also reduces the boron blank by a factor of four and enhances the sensitivity by 33–90%.

Variation in the ratio of the two naturally occurring boron isotopes in geological materials is commonly known. Depending on the source and the nature of the material, the natural variation of the $^{11}\text{B}:^{10}\text{B}$ ratio in rocks and minerals can range from 3.8 to 4.2. The boron isotope ratio of natural waters can exhibit the same range

of variability, as waters in contact with rocks, soils and sediments commonly adopt the isotopic signature of the contact material [70].

The ICP technique generates signals as a function of flow rate rather than the weight introduced to the nebuliser. This would cause major difficulties if the samples, blanks, and standards are somewhat varied in flow rate, viscosity, total dissolved solids, and compositions [66]. Another potential problem is the incomplete dissolution of solids in the samples which produces particles or precipitates. During the aspiration of the solution into the plasma, these particles can enhance or depress the boron signal, or even block the nebuliser [66]. Therefore, samples should be carefully prepared by filtering and acidifying before being introduced to the plasma.

2.2 Factors governing boron rejection by NF/RO membranes

2.2.1 Feedwater pH

The effect of solution pH on boron rejection by NF/RO membranes has been thoroughly investigated by numerous studies which consistently found that pH is the most imperative factor affecting boron rejection by NF/RO membranes [37, 71-83]. The pH of feedwater affects boron rejection by NF/RO membranes through its impact on the existence of different boron species (boric acid and borate ion) in the solution. The effect of solution pH on the dissociation of boric acid has been thoroughly elucidated in Section 2.1.3. Increases in the borate fraction directly result in increases in the rejection of overall boron since the borate molecule is not only larger in size than the boric acid molecule but also negatively charged which facilitates the rejection by both steric hindrance and charged repulsion.

Feedwater pH also governs boron rejection by affecting the charge density of the membranes. Most commercial polyamide NF/RO membranes are negatively charged in the natural pH range, and will become more negative as the solution pH increases [84, 85]. The increased negative charge enhances the charged repulsion between borate ions and membrane surface, and thus improves overall boron rejection. Tu et al. [86] reported that the boron rejection by NF270, NF90 and BW30 membranes enhance most rapidly in the pH range of 8-10 (Figure 3) which is in good agreement with the progression of borate ion in the solution. The authors also reported that the impact of solution pH to increase boron rejection is most significant at NF

membranes rather than RO membranes [86] because charged repulsion mechanism plays a more important role in boron rejection by NF membranes than by RO membranes.

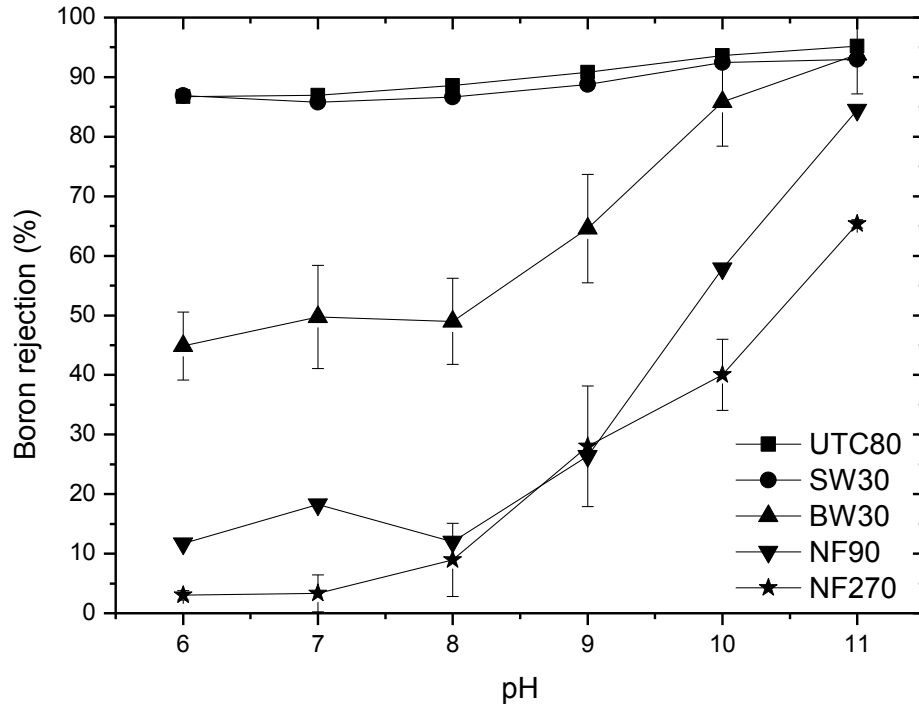


Figure 3. Impacts of the feedwater pH on boron rejection by different NF/RO membranes [86].

2.2.2 Feedwater ionic strength

The effect of the ionic strength or salinity of the feedwater on boron rejection is still controversial. A few studies report that an increase in the ionic strength leads to an increase in boron rejection [86], whereas others report the opposite [73, 87]. Both tendencies can be theoretically possible, and the effects of ionic strength on boron rejection could be dependent on the membrane used and feedwater pH. A range of ionic strength used in different studies may also contribute to the discrepant results. Indeed, changes in the solution ionic strength affect the membrane surface charge and the dissociation of boric acid which subsequently causes different impacts on boron rejection.

To the membrane, a high feedwater ionic strength can compress the electrical double-layer on the membrane surface and therefore leave more space for ion

transport through the membrane, consequently leading to a lower rejection of borate ions [88, 89]. This phenomenon is expected not to affect the transport of neutrally charged solutes such as boric acid molecules. Consequently, the impact of the ionic strength on boron rejection is probably exhibited only at high pH conditions where borate ions are dominantly present [86].

On the other hand, a high feedwater ionic strength would decrease the apparent pK_a of boric acid (Section 2.1.3), and thus result in an increase in boron rejection at a certain feedwater pH. Tu et al. [86] reported that the impacts of ionic strength on boron rejection would be stronger at the pH range close to the apparent pK_a of boric acid (pK_a 9.23). In addition, since the charged repulsion mechanism is more important in NF than RO membranes [86], the impacts of ionic strength on boron rejection would be more substantial in NF than RO membranes.

2.2.3 Operating pressure

It was consistently reported that boron rejection by NF/RO membranes is strongly affected by the operating pressure or permeate flux [74, 78, 79, 90]. Koseoglu et al. [91] reported that boron rejection by the SW30 membrane increased from 88% to 92% as the applied pressure increased from 41 to 48 bar. Similarly, Cengeloglu et al. [74] found boron rejection by the BW30 membrane increased from 74% to 84% as the applied pressure increased from 16 to 35 bar. This impact has been explained using an irreversible thermodynamic principle which will be elucidated in the latter sections of this thesis. Basically, irreversible thermodynamics describe that increased operating pressure would increase the water flux but not the boron flux transporting through the membrane, and thus lead to lower boron concentration in the permeate or higher boron rejection of the system. It is also noteworthy that an increase in water flux due to increasing applied pressure would lead to an increase in concentration polarisation which may consequently increase the solute flux [92]. Nevertheless, the increased boron flux due to this mechanism seems to be dominated by the increased water flux at higher pressures, and an improved boron rejection is the result.

2.2.4 Feedwater temperature

Along with solution pH and operating pressure, temperature of the feedwater has been found to significantly affect the rejection of boron by NF/RO membranes. The effect of feedwater temperature on boron rejection is a multifaceted interaction between the impacts of temperature on (1) pK_a of boric acid; (2) membrane pore size; and (3) mass transfer coefficient and permeability of boron. It was established that increasing temperature would decrease the pK_a of boric acid (Section 2.1.3) and so a higher boron rejection is expected. A theoretical study of Sharma et al. [93] reported a thermal expansion of the polymer constituting the membrane active layer at elevated temperatures, which subsequently resulted in a decrease in solute rejection. Hyung and Kim in a comprehensive mechanistic study [94] revealed that both mass transfer coefficient (k_B) and permeability constant (P_B) of boron were enhanced at increasing feedwater temperature. An increase in the k_B would decrease the concentration polarisation effect and therefore likely increase boron rejection, whereas an increase in the P_B could result in a lower boron rejection. The final result of the above complex interaction has been given by experimental data, that boron rejection would be decreased at increasing feedwater temperature [73, 92]. Hung et al. [73] reported a boron rejection decrease from 85% to 75% as feedwater temperature increased from 17 °C to 35 °C. This result implied that the impact of feedwater temperature on boron rejection is mostly governed by changes in the membrane pore size and P_B , rather than changes in the pK_a and k_B .

2.2.5 Membrane configurations for improving boron rejection

Although boron rejection by many commercial SWRO membranes can reach 88-91% under laboratory standard test conditions [6], these membranes would obtain approximately 15% lower boron rejection when being applied to full-scale desalination plants because of the higher water-recovery required [5, 76]. Consequently, a single-pass membrane configuration is suitable only in cases where the required overall boron rejection is less than 80%. Although this rejection efficiency can be improved by increasing the feedwater pH, this alkaline condition can produce severe membrane scaling caused by the precipitation of divalent cations such as Ca^{2+} and Mg^{2+} which are commonly present in seawater and other natural

waters. In seawater desalination plants, a typical single-pass process would operate at a recovery between 40-50%, permeate flux between 12-15 L.m⁻².h⁻¹ (LMH), temperature between 18-26 °C, and pH between 6.0-8.2 [92, 95]. Under these conditions, a single-pass SWRO membrane unit generally produces permeate with salinity within the potable limits (i.e. less than 500 mg.L⁻¹ TDS). However, boron concentration in the permeate is likely to be higher than 0.5 mg.L⁻¹ which is above the regulated limit for some applications (Section 2.1.2). Variations in the seawater temperature and membrane integrity can also largely contribute to decrease boron rejection efficiency of membrane installations [76, 82, 92, 96, 97].

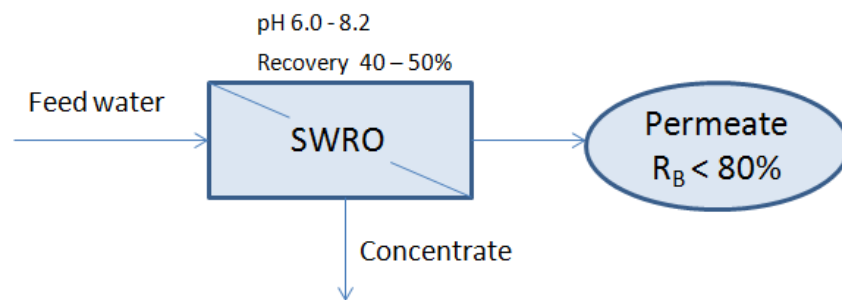


Figure 4. Single-pass membrane configuration in SWRO desalination

Stringent regulations/guidelines for boron levels in permeate water render the single-pass RO configuration insufficient, and multi-pass configurations are usually required. Double-pass RO is probably the most commonly employed configuration for RO seawater desalination plants. The process typically consists of a primary SWRO unit operating at a recovery of 40 to 50% followed by a low pressure BWRO unit operating at a recovery of 85 to 90% (Figure 5). Since most of the total dissolved solids (TDS) have been rejected in the first pass, the second pass is allowed to run at such high recovery without the risk of membrane scaling and therefore the number of elements required for the second pass is minimised. In order to effectively remove boron by the BWRO membrane, permeate of the first pass is usually alkalised up to pH 10 by dosing NaOH. Although the levels of Ca²⁺, Mg²⁺ and alkalinity have been substantially reduced after the first pass, the residual constituents may form scales under high pH condition and therefore anti-scalant must be added to the feed of the BWRO. With the attempt to decrease the foot-print of the BWRO pass, part of the SWRO permeate at the feed end where boron and salinity level is lower could be

bypassed directly to the final water product. Depending on the overall performance of the system, the bypass fraction can be adjusted to satisfy the final water quality. As an example, the 50,000 m³.d⁻¹ plant at Larnaca, Cyprus, constructed in 2001 with a partial two-pass configuration, produced final water containing 0.8-1.2 mg.L⁻¹ boron from a seawater containing 4.5-6.5 mg.L⁻¹ boron [92].

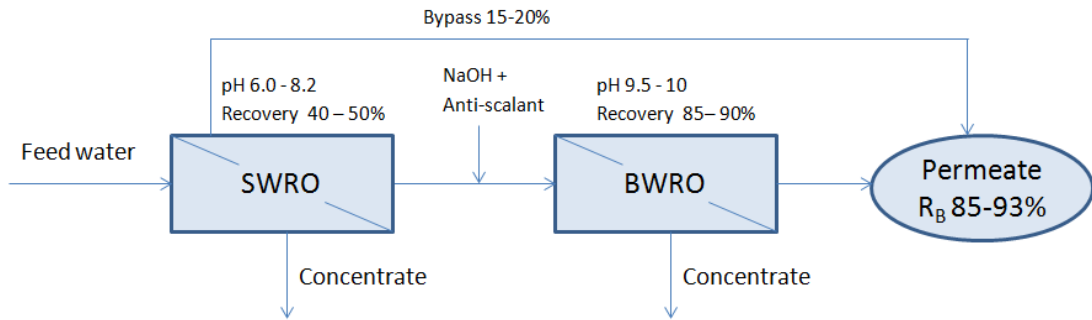


Figure 5. Double-pass membrane configuration in SWRO desalination

A disadvantage of the multi-pass RO process compared to the single-pass process is its lower overall recovery which consequently increases the product price [92]. More membrane passes are employed result in more water is discharged as concentrate. To overcome this obstacle, the concentrate can be fed to another membrane unit, and then a multi-stage membrane process is formed. Representatives of this process can be listed such as the RO desalination plants in Eilat [76, 98] and Ashkelon [77] (Figure 6), Israel. The Ashkelon seawater desalination plant is the world largest its type to date, and also a representative for advances in RO plant design. The plant employs four RO units in series to treat seawater from an open-water intake in the Mediterranean Sea, leading to a boron level in the final water less than 0.3 mg.L⁻¹ with an overall recovery > 95% [77].

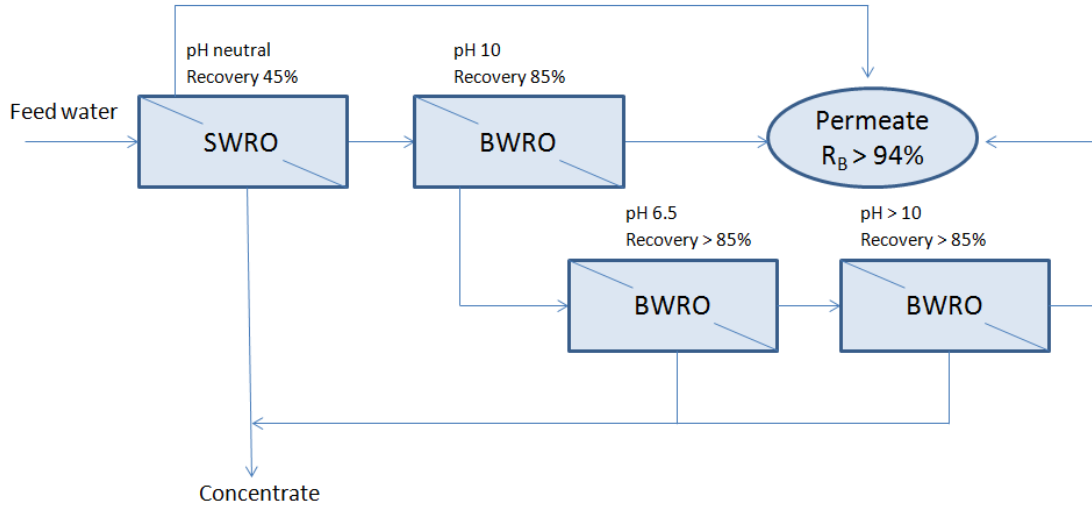


Figure 6. Schematic of the process used in the Ashkelon seawater desalination plant

2.3 Modelling boron transport in NF/RO membranes

2.3.1 Solution-Diffusion Model

The solution-diffusion model is probably the earliest and simplest model to be considered for describing boron transport in RO membranes. The solution-diffusion model describes the transport of water and solute in NF/RO membranes as three succeeding stages: sorption, diffusion, and desorption. The separation process occurs as the consequence of different rates of these three stages of each permeant to a membrane material [99]. The solution-diffusion model was built on the basis of assumptions: (1) the fluids on either side of the membrane are in equilibrium with the membrane material at the interface, which implies that the rates of adsorption and desorption stages are much higher than of diffusion [99]; (2) the membrane surface is homogeneous and nonporous; (3) there is no coupling between solute and water because they have different chemical gradients across the membrane; (4) the solute flux is independent on hydraulic pressure but concentration gradient; (5) the diffusion coefficient of water is constant across the membrane due to membrane swelling. These assumptions lead to the principal transport equations of water and solute [100]:

$$J_w = P_w(\Delta P - \Delta \pi) \quad \text{Eq.6}$$

$$J_s = P_s(C_M - C_P) \quad \text{Eq.7}$$

Where J_w is the volumetric water flux [$\text{m}^3 \cdot \text{m}^{-2} \cdot \text{s}^{-1}$]; J_s is the gravimetric solute flux [$\text{kg} \cdot \text{m}^{-2} \cdot \text{s}^{-1}$]; P_w is the pure water permeability coefficient [$\text{m}^2 \cdot \text{s} \cdot \text{kg}^{-1}$]; P_s is the solute permeability coefficient [$\text{m} \cdot \text{s}^{-1}$] (P_w and P_s are determined by experiments); ΔP and $\Delta \pi$ are the applied pressure difference and osmotic pressure difference between two sides of the membrane [$\text{kg} \cdot \text{m}^{-1} \cdot \text{s}^{-2}$], respectively; C_M and C_P are the solute concentrations at the membrane surface in feed and permeate side [$\text{kg} \cdot \text{m}^{-3}$], respectively.

The apparent rejection of solute is expressed as:

$$R_o = \frac{J_s}{J_s + J_w} \quad \text{Eq.8}$$

Whereas the real rejection is expressed as:

$$R_r = \frac{J_w}{J_w + P_s} \quad \text{Eq.9}$$

Due to concentration polarisation phenomenon, the concentration of solute at the membrane surface (C_M) can be different from that in the bulk solution (C_B). The expression representing the transport of solutes in the concentration polarisation layer can be derived from thin-film theory:

$$\frac{C_M - C_P}{C_B - C_P} = \exp \frac{J_w}{k} \quad \text{Eq.10}$$

Where $k = \frac{D}{\delta}$ is the mass transfer coefficient of solute [$\text{m} \cdot \text{s}^{-1}$], δ is the thickness of the boundary layer [m].

The mathematical expressions indicate that solute flux is controlled by the diffusion (Eq.6), whereas the water flux is driven by convection transport (Eq.7). Although this model has been widely used to describe the transport of typical salts (i.e. sodium chloride) and organic compounds through membranes [83, 101], the number of studies employing the solution-diffusion model for estimating boron rejection are somewhat limited [73, 83]. Some studies [81, 83] considered a single boron permeability coefficient for both boric and borate species, whereas others [73] suggested permeability coefficients of boric and borate species are considerably

different and so two distinct permeability values for the two species should be employed.

The application of the solution-diffusion model is limited to the low flux membranes only (i.e. RO) where the convection transport is restricted [102]. This model would also cause major inaccuracy due to the imperfection of the membrane active layer and solute-solvent interactions. To tackle such drawbacks, extended forms of the solution-diffusion model have been proposed. An example is the solution-diffusion-imperfection model which includes the pore-flow transport addition to the diffusion of water and solute [103].

2.3.2 Irreversible Thermodynamic Model

The irreversible thermodynamic model is probably the most widely used model to simulate transport of solutes through NF/RO membranes. This model assumes that the membrane is not far from equilibrium and so fluxes can be described by phenomenological relationships [104, 105]. One of the early models was that derived by Kedem and Katchalsky [106] which expressed the water flux and solute flux across the membrane as:

$$J_w = -P_w(\Delta P - \sigma\Delta\pi) \quad \text{Eq.11}$$

$$J_s = -P_s\Delta C + (1 - \sigma)J_w\bar{C} \quad \text{Eq.12}$$

Where, σ is the reflection coefficient which represents the extent of boron-water coupling or the imperfection of the membrane surface; C is the superficial boron concentration [$\text{kg}\cdot\text{m}^{-3}$] which is in equilibrium with the concentration of solute in the membrane phase; \bar{C} is the average value of solute concentrations in the feed and permeate side [$\text{kg}\cdot\text{m}^{-3}$].

Although based on different theoretical foundations, the irreversible thermodynamic model can be considered as an extended form of the solution-diffusion model. In the irreversible thermodynamic model, impacts of osmotic pressure on the water permeability are corrected by σ which represents the theoretical separation efficiency of a semi-permeable membrane (Eq.11). The use of σ results in an important additional transport mechanism of solute through membranes – convection, apart

from the diffusion mechanism (Eq.12). σ approaches zero for a completely open membrane and unity for a very dense membrane where there is little or no coupling of solute and water [94]. In the latter case, the solute transport by convection is negligible. For the transport of typical salts through RO membranes, $\sigma = 1$ is usually assumed due to almost-complete salt rejection of RO membranes. Nevertheless, for boron, σ was found to be significantly smaller than 1 and also distinctive for boric acid and borate species. Using SWRO membranes, the reflection coefficient was estimated between 0.975-0.981 for boric acid, whereas it was > 0.996 for borate [94, 107]. For BWRO membranes, the reflection coefficient of boric acid was found as low as 0.45 [108]. This result implies that the transport of boric acid through BWRO membranes is governed by not only diffusion but also by convection.

Integration of Eq.12 gives the expression of solution rejection, known as the Spiegler-Kedem [109] equation:

$$R = \frac{\sigma(1-F)}{1-\sigma F} = \frac{C_M - C_P}{C_M} \quad \text{Eq.13}$$

$$\text{Where, } F = \exp\left(-\frac{J_w(1-\sigma)}{P_s}\right)$$

Combining Eq.13 and Eq.10, the overall rejection of the solute through the membrane can be expressed as:

$$\frac{R}{1-R} = \frac{C_B - C_P}{C_P} = \frac{\sigma \left[1 - \exp\left(-\frac{J_v(1-\sigma)}{P_s}\right) \right]}{(1-\sigma) \exp\left(-\frac{J_v}{k}\right)} \quad \text{Eq.14}$$

Eq.14 has been employed by many studies to describe the transport of solutes through RO membranes [107, 110, 111]. In order to predict the separation performance from this model, it is necessary to determine the unknown parameters such as k , P_s and σ . This can be done by a linearisation of Eq.14 with assumptions of no coupling ($\sigma = 1$, or very high rejection) and infinite mass transfer ($k = \infty$, or ideally dilute solution) [112]. It can be seen that these assumptions are inappropriate for solutes like boron which have moderate rejection by RO membranes, and for concentrated feed

solution like seawater having considerable concentration polarisation. Alternatively, Eq.14 can be solved by a non-linearisation combined with experiments. Experiments can be conducted to determine R , J_w , and k ; then a non-linearisation of Eq.14 can estimate σ and P_s [111, 113, 114]. The accuracy of this method depends on the numerical algorithm used, particular solution property, and the experimentally obtained k .

The above estimation protocol has been widely employed to simulate the rejection of boron in both laboratory- [81, 83], pilot- [108], and full-scale [107, 115] membrane modules. Hyung and Kim [94] conducted a fundamental study to predict boron rejection on a laboratory-scale RO system as a function permeate flux, feedwater temperature and pH. The authors considered different transport coefficients for boric acid and borate which were experimentally estimated at various fluxes, temperatures and pH values. This model has been further developed for modelling boron rejection in pilot- and full-scale studies. Mane et al. [107] found that boron rejection in a single spiral-wound membrane module is mainly governed by feed pressure, temperature and pH condition. Nevertheless, when the model was applied for a series of six or eight spiral-wound membrane modules, the overall system recovery is another important factor which needs to be considered to achieve the targeted overall boron rejection [107]. Because the hydraulic condition in a spiral-wound membrane module is very different from in a spread-sheet membrane module, the mathematical estimation of mass transfer coefficient in such condition was proposed as [116, 117]:

$$k = 0.753 \left(\frac{K}{2-K} \right)^{0.5} \left(\frac{D}{h_b} \right) Sc^{-1/6} \left(\frac{Pe \times h_b}{\Delta L} \right)^{0.5} \quad \text{Eq.15}$$

$$D = 6.725 \times 10^{-6} \exp \left(0.1546 \times 10^{-3} C - \frac{2513}{T} \right) \quad \text{Eq.16}$$

$$\mu = 1.234 \times 10^{-6} \exp \left(0.00212 C + \frac{1965}{T} \right) \quad \text{Eq.17}$$

Where, K is the efficiency of spacer [dimensionless]; T is the absolute temperature [K]; Sc is the Schmidt number = $\mu/\rho D$ [dimensionless]; μ is the dynamic viscosity [Pa.s]; ρ is the density [kg.m^{-3}]; Pe is the Peclet number = $2h_b U_b/D$ [dimensionless]; h_b is the thickness of feed channel [m]; ΔL is the characteristic length of spacer [m].

Park et al. [115] took a further step to simulate boron rejection in full-scale membrane configuration with the consideration of membrane fouling. The authors took into account the decrease in k (mass transfer coefficient) of a fouled membrane, whereas they considered the hydraulic resistance of the fouling layer was negligible compared to the resistance of the SWRO membrane. The simulation resulted in three principles to improve boron rejection: (1) minimise membrane fouling, (2) employ a boron-specific RO membrane, and (3) increase pH in the second membrane pass. The latest is concluded to be the most suitable method to control boron rejection in full-scale RO desalination plants [115].

A major disadvantage of the irreversible thermodynamic model is that it treats the membrane as a "black box" by neglecting the porosity of the membrane, and so provides no insight into the transport mechanisms of the membrane. Consequently, irreversible thermodynamic models are not very useful for optimising separations based on the membrane structure and physiochemical properties.

2.3.3 Pore models

An early form of the pore model is the pore-flow model proposed by Okada and Matsuura [118]. The pore-flow model was mostly applied for porous membranes and neutral solutes. The model is based on three assumptions: (1) fluids on either side of the membrane are in equilibrium with the membrane at the interface; (2) the solute and solvent activity gradients across the membrane are zero and the chemical potential gradient across the membrane can be expressed as a pressure gradient; (3) straight cylindrical pores exist across the thickness of the membrane. The pore-flow model considers only axial solute concentration gradient, and excludes the pore shape and tortuosity. The water flux (J_w) and solute flux (J_s) are expressed as:

$$J_w = \frac{A}{\delta} (p_f - p_p) \quad \text{Eq.18}$$

$$J_s = \frac{B}{\delta} (p_f^2 - p_p^2) \quad \text{Eq.19}$$

Where, A and B are the transport parameters of the solvent and solute, respectively; p_f and p_p are the pressure in the feed and permeate side, respectively; δ is the pore length [m].

The pore-flow model was later modified by Matsuura and Sourirajan [119] to form the so called “surface force-pore-flow model”. The modified model provides more accurate predicted results because it relates membrane performance with both membrane structure (pore size and length) and membrane-solute interactions [120]. Nevertheless, this model was later found to employ an inconsistent form of material balance and potential function in the pore with the cylindrical pore geometry [121].

A model based on membrane surface phenomenon was proposed by Sourirajan [122] and called the “preferential sorption-capillary flow model”. In contrast to the solution diffusion model, this model considers the membrane as a micro-porous structure. This model assumes that the mechanism of separation is determined by both surface phenomena and fluid transport through pores in the RO membrane [122]. The model also assumes that the membrane has a preferential sorption for the solvent or preferential repulsion for the solutes of the feed solution. Solvent transport occurs through the membrane capillary pores as a result of hydraulic pressure. The water flux and solute flux are described as:

$$N_w = A\{\Delta P - [\pi(X_F) - \pi(X_P)]\} \quad \text{Eq.20}$$

$$N_s = \frac{D_{sp} K_D C_T}{\delta} (X_F - X_P) \quad \text{Eq.21}$$

Where, A is the pure water permeability of the membrane; $\pi(X)$ is the osmotic pressure of the feed or permeate side with solute mole fraction X; K_D is the distribution coefficient of the solute from the feed into the membrane pore; D_{sp} is the diffusivity of the solute in the membrane pore. Solute rejection is expressed as:

$$\frac{1}{R} = 1 + \frac{D_{sp} K_D C_T}{\delta} \frac{1}{A\{\Delta P - [\pi(X_F) - \pi(X_P)]\}} \quad \text{Eq.22}$$

The pore models have not been applied for boron transport through NF/RO membranes because for a long time it was believed that NF/RO membranes are non-porous. Nevertheless, recent studies [123] found that convection plays an important role in boron transport through NF/RO membranes, thus NF/RO membranes should be considered as a porous structure. This finding proposes a potential for using pore models for the prediction of boron rejection by NF/RO membranes.

2.3.4 Charge-based models

Some models were specifically developed to describe the transport of charged solutes in semi-permeable membranes. A model based on Donnan Equilibrium suggested that as a charged membrane is placed in an electrolyte solution, ion equilibrium will exist between the membrane and solution so as to maintain the electro-neutrality. The counter-ion of the solution, which is opposite in charge to the fixed membrane charge (typically carboxylic or sulfonic groups), is present in the membrane at a higher concentration than that of the co-ion (same charge as the fixed membrane charge) because of electrostatic attraction and repulsion effects. A potential gradient existing on the interface, which is called Donnan potential, prevents the diffusive exchange of the counter-ion and co-ion between the solution and membrane phase. When a pressure driving force is applied to force feedwater through the charged membrane, the effect of Donnan potential is to repel the co-ion from the membrane. Because an electro-neutrality must be maintained in the solution phase, the counter-ion is also rejected, resulting in ionic solute rejection [124, 125]. The rejection of charged solute as described by the model is given by [125]:

$$R = 1 - K = 1 - \frac{c_{im}}{c_{Fi}} = 1 - \left[\left(\frac{nC_{Fi}}{C_m^*} \right)^n \left(\frac{\gamma}{\gamma_m} \right)^{m+n} \right]^{1/m} \quad \text{Eq.23}$$

The expression of the model implies that the solute rejection is a function of membrane charge capacity C_m^* , ion feed concentration C_{Fi} , and ion charge (m, n). However, this model does not take into account solute diffusion and convection which are crucial in NF/RO transportation.

Dresner and Johnson [126] extended the Nernst-Planck model and expressed as:

$$j_i = -D_{i,p} \frac{dc_i}{dx} - \frac{z_i c_i D_{i,p}}{RT} F \frac{d\phi}{dx} + K_{i,c} c_i J_v \quad \text{Eq.24}$$

On the right side of Eq.24, the three expressions from left to right represent the transport by diffusion, electro-migration and convection, respectively. In order to cover three such crucial transport mechanisms, this model assumes that: (1) the solution is ideal; (2) the charge capacity is uniform in any point within the separation

zone in the membrane; (3) all ions exist in the membrane are transportable; and (4) Donnan equilibrium occurs in the interface between membrane and outer solution.

In order to include both steric and charged effects, Wang et al. [127] proposed the electrostatic and steric-hindrance model which takes into account both electrostatic and steric effects to describe the transport of charged solutes through NF membranes. The assumptions of this model are: (1) the membrane consists of a bunch of capillaries with pore radius r_p , ratio of membrane surface porosity to membrane thickness $A_k/\Delta x$, and surface charge density q_w ; (2) the organic electrolyte is distributed completely into ions; (3) steric hindrance effect is only considered for large ions; (4) the ion flux and pure water velocity phenomena in membrane capillary is respectively represented by the extended Nernst-Planck equation and Hagen-Poiseuille; and (5) for a ternary system, which is water/inorganic electrolyte/organic electrolytes, the contribution of organic solution toward the radial and axial electrical potential distribution is assumed negligible.

These charge-based models have not been commonly employed for simulating boron transport because boron exists mainly in the form of neutrally charged boric acid in typical pH conditions ($\text{pH} < 9.2$) (Section 2.1.3). Nevertheless, these models can be used in combination with other models for a comprehensive description of boron transport including boric acid and borate species, especially simulating the boron rejection at high pH conditions.

2.3.5 Combined models

A recent work conducted by Keiza et al. [123] incorporated the irreversible thermodynamic, pore flow, and Extended Nernst-Planck models for a complete description of boron transport through a flat-sheet BWRO membrane. Boron rejection was considered as the total rejection of neutral boric acid and borate ion, and various transport mechanisms including diffusion, convection, steric-hindrance, and charged repulsion were taken into account [123]. Although this work provided a comprehensive mechanistic explanation of boron transport in RO membranes, the complicated algorithms used in the simulation may inhibit its application in spiral-wound membrane modules due to the complex hydraulic condition.

Nir and Lahav [128] simulated the transport of boric acid through SWRO membranes by combining the solution-diffusion model with thin-film theory and chemical equilibrium. Advantages of this model include the involvement of solution pH and a wide application range. However, the algorithm is relatively complicated and further validations are required.

2.4 Chemical contact during membrane lifetime and its implication on the membrane integrity

During its functioning lifetime, NF/RO membranes can come in contact with a wide range of chemicals used in different water and wastewater treatment applications. Many of these are used for the pretreatment of the feedwater to produce the most suitable water quality feeding to the membrane, and thus guarantee the best system performance and a longest possible membrane lifespan. Conventional pretreatment method with coagulation-flocculation using ferric and aluminum species followed by chlorination-dechlorination has been successfully applied to most water and wastewater treatment plants for decades. However, an excessive dose of these chemicals was proved to be detrimental to polyamide membranes. Remaining ferric and aluminum ions were found to be good catalysts for the oxidation of polyamide membranes by residual chlorine, leading to serious damages or shorter membrane lifetime [129-131].

2.4.1 Membrane cleaning chemicals

Chemical cleaning is an inevitable process in all membrane applications. Chemicals typically used for membrane cleaning can be categorised as acidic (i.e. HCl, citric acid), caustic (i.e. NaOH, KOH), surfactant (i.e. sodium dodecylsulfate (SDS)), metal chelating agent (i.e. ethylenediaminetetraacetic acid (EDTA)), and disinfectant (i.e. NaOCl, H₂O₂). Depending on the nature of the fouling layer, chemicals used for cleaning can be either acidic or caustic solution with some additives such as surfactants and/or metal chelating agents. Generally, a low pH is recommended for dealing with inorganic salt foulants, whereas high pH is used coupling with surfactants for silica, biofilm and organic foulants. A temperature of 35-40 °C is recommended for most of the cleaning processes. As fouling layers are usually cocktails of different types of foulant and each foulant is best removed by a specific

cleaning chemical, a complete cleaning process usually involves the use of various cleaning agents either simultaneously or consecutively (Table 3). The use of SDS or EDTA in caustic condition was recommended to improve cleaning efficiency [132, 133]. In addition, the combination of these two chemicals in caustic solution would be more efficient to mitigate membrane fouling than when each chemical is individually used [134] (Table 3). The frequency of the cleaning could range from a routine daily processes such as in whey processing to long-term annual processes such as in desalination plants according to the frequency and extent of fouling events [135]. However, the application of chemical cleaning should be limited to a minimum frequency since repeated chemical cleaning may affect the membrane performance and lifetime [136]. In fact, some studies reported that chemical cleaning can cause significant impacts on the membrane surface properties and thus affect the separation efficiency of the membrane.

Table 3. Manufacturer-recommended cleaning chemicals for RO membranes [137, 138]

Foulant type	FilmTec BW30, LE, TW30, SW30		Hydranautics polyamide membranes	
	Preferred	Alternative	Preferred	Alternative
CaCO ₃	0.2% (wt) HCl, 25 °C, pH 1-2	1% (wt) Na ₂ S ₂ O ₄ , 25 °C, pH 5	0.5% (V) HCl, 35 °C, pH 2.5	2% (wt) citric acid, 40 °C, pH adjustment not required
CaSO ₄ , BaSO ₄	0.2% (wt) HCl, 25 °C, pH 1-2	---	0.5% (V) HCl, 35 °C, pH 2.5	0.83% (wt) Na-EDTA, 40 °C, pH 10
Metal Oxides (Fe, Mn, Zn, Cu, Al)	1% (wt) Na ₂ S ₂ O ₄ , 25 °C, pH 5	0.5% (wt) H ₃ PO ₄ , 25 °C, pH 1-2	1% (wt) Na ₂ S ₂ O ₄ , 35 °C, pH adjustment not required	2% (wt) citric acid, 40 °C, pH adjustment not required
Inorganic colloid	0.1% (wt) NaOH + 0.025% (wt) SDS, pH 12, 35 °C	---	0.5% (V) HCl, 35 °C, pH 2.5	2% (wt) citric acid, 40 °C, pH adjustment not required
Silica	0.1% (wt) NaOH +	0.1% (wt) NaOH + 1%	---	---

	0.025% (wt) SDS, pH 12, 35 °C	(wt) Na ₄ EDTA, pH 12, < 35 °C		
Biofilm	0.1% (wt) NaOH + 0.025% (wt) SDS, pH 12, 35 °C	0.1% (wt) NaOH + 1% (wt) Na ₄ EDTA, pH 12, < 35 °C	0.1% (wt) NaOH + 0.03% (wt) SDS, pH 11.5, 30 °C	0.83% (wt) Na-EDTA, 40 °C, pH 10
Natural organic matter	0.1% (wt) NaOH + 0.025% (wt) SDS, pH 12, 35 °C	0.1% (wt) NaOH + 1% (wt) Na ₄ EDTA, pH 12, < 35 °C	0.1% (wt) NaOH + 0.03% (wt) SDS, pH 11.5, 30 °C	0.83% (wt) Na-EDTA, 40 °C, pH 10

Al-Amoudi [139] reported that the nominal pore size of a NF membrane would be increased by more than 12% when the membrane was soaked in either a caustic SDS solution or a mixture of tri-sodium phosphate, sodium tri-polyphosphate, and EDTA in 18 h. The enlargement of the membrane pores resulted in an increase in water and solute permeability (i.e. rejection decreased). In contrast, the membrane pore size was not affected by acidic cleaning (with HCl) [139]. Nevertheless, Simon et al. [140] observed that the NF membrane pores could be enlarged by both strongly acidic (pH 1.5) and caustic (pH 12) solutions. The authors [140] argued that both strongly acidic and caustic conditions caused an internal charged repulsion effect amongst charged groups in the membrane polymer matrix, leading to the expansion of the membrane structure. Some studies reported a decrease in salt rejection of membranes after caustic cleaning, however, such rejection loss can be recovered by applying an acidic cleaning subsequently [133, 141]. Chemical cleaning was also found to be able to alter the membrane surface charge density and hydrophobicity. However, the impacts of such changes on the membrane separation appeared to be inconclusive and membrane-dependent [140, 142-145]. In fact, Simon et al. [146] reported that impacts of cleaning chemicals on the membrane performance depend on the thickness of the membrane active layer. Membranes with a thinner active layer would be more delicate to the impacts of cleaning chemicals. A study of Fujioka et al. [143] reported that chemical cleaning of RO membranes would affect the rejection of small and neutrally charged solutes such as NDMA at a higher magnitude than the rejection of hydrated salts such as sodium chloride. This result

has raised the concern of inadequate rejection of other small and neutrally charged pollutants such as boron by aged membranes.

2.4.2 Oxidising chemicals

Although polyamide RO membranes are well known for being vulnerable to oxidising agents such as hypochlorite (OCl^-) and hydrogen peroxide (H_2O_2), the use of these chemical is inevitable in most of water treatment processes including membranes. These oxidants have been standard chemicals used for the disinfection of feedwater for decades. Although a dechlorination step is always implemented before the RO membranes, the risk of residual chlorine reaching the membrane is still high. This residual chlorine would become more detrimental to the membrane once catalysed by residual coagulants (i.e. Fe^{3+} or Al^{3+}) [129-131].

It is well established that the chlorine sensitivity of membranes is greatly dependent on the chemical structure of the membrane [147]. Polyamide membranes are chlorine susceptible because their polymeric structure usually contains a large number of amide nitrogen and aromatic rings (Figure 7), which are considered vulnerable to chlorine substitution. The degree to which polyamide membranes are attacked depends on the particular acids and amines employed in the formation of the polyamide [147]. The reduced performance of chlorinated membranes is usually attributed to the deterioration and cleavage of cross-linkages within the polymeric structure which changes the selectivity of membranes. In addition, Soice et al. [148] proposed that the major cause of reduced performance caused by chlorination is not due to polymer chain cleavage but physical separation of the polyamide skin layer from the polysulfone support layer. Two general mechanisms were proposed to elucidate the impact of chlorination on the membrane polymer structure. The first involves polymer deformation, which leads to the deterioration of the salt rejection barrier. The second concept involves the amide bond cleavage resulting in complete or partial depolymerisation.

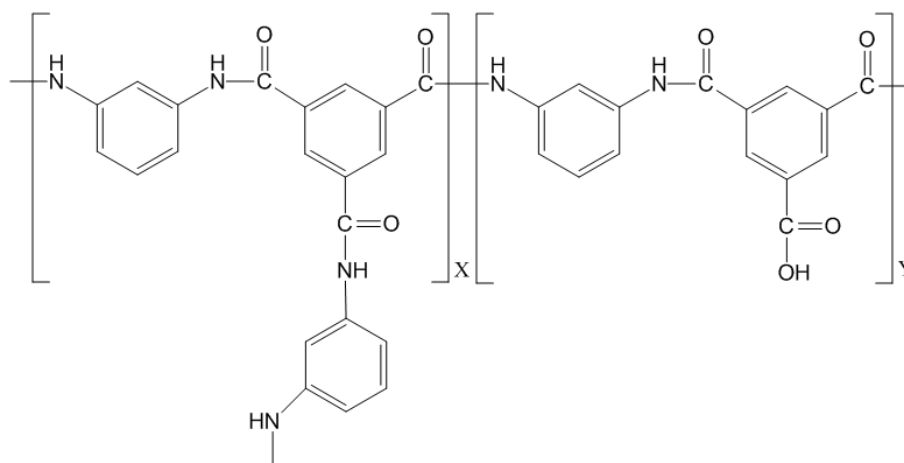


Figure 7. Typical chemical structure of polyamide membranes [149]

The deformation of the linear polyamide was proposed by Glater and Zachariah [150] who suggested a transition of hydrogen bonding from inter to intramolecular within a linear polymer chain, which causes chain deformation followed by alteration in gross polymer properties. According to the authors [150], this process involves three rigorous steps: (1) aromatic ring chlorination; (2) disruption of intermolecular cross linkages and conversion to intramolecular hydrogen bonding; and (3) subsequent chain structure deformation. The chlorination of the aromatic rings was proposed to initiate by a reversible N-chlorination and subsequently an irreversible ring-chlorination [151, 152]. This process is usually called the Orton Rearrangement, which is demonstrated in Figure 8. Amide nitrogen is vulnerable to chlorine attack because of electron withdrawing effects of the carbonyl group [153]. The resulting N-chloro amide then experiences an intermolecular rearrangement forming various aromatic substitution products [151]. Nevertheless, the aromatic chlorination can also take place directly since the aromatic rings bonding to the N-H group are susceptible to electrophilic substitution by chlorine [153]. In an interesting study to investigate the impact of chlorination conditions, Antony et al. [154] reported that the applied pressure seemed to encourage the rearrangement of N-chlorination to ring-chlorination. Several studies reported the weakness and breakage of N-H hydrogen bonding due to chlorination [149, 155-157]. The role of the strength and density of the cross-links within the polymer chain toward chlorine resistance is still controversial. Koo et al. [158] claim that only membranes weakly cross-linked by hydrogen bonds are affected by the polymer deformation mechanism. Chlorination of

strongly cross-linked membranes preferably occurs by complete or partial depolymerisation [158]. On the other hand, the X-ray Photoelectron Spectrometry (XPS) and Fourier Transform Infrared Spectrometry (FTIR) analytical analysis conducted by Kwon et al. [156] showed that there is no difference in the chlorine attack on polyamide membranes of higher or lower cross-linking density.

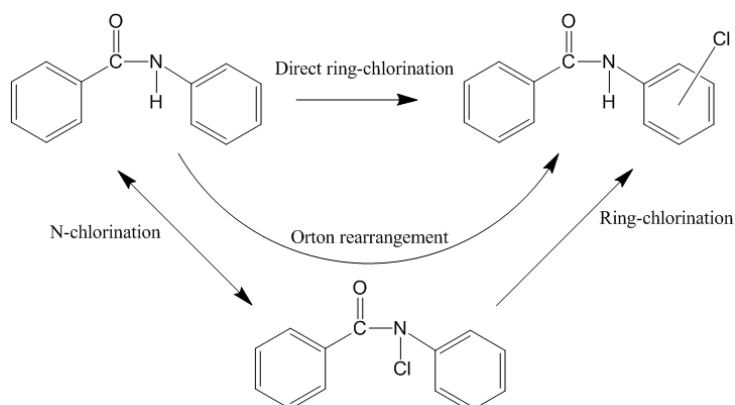


Figure 8. Proposed changes in the membrane polymeric structure under chlorine attack.

Whereas the polymer deformation mechanism has been supported and studied by a wide range of research, the amide bond cleavage mechanism has not been adequately studied. According to Avlonitis et al. [159], there exists a structural transition from crystal to amorphous state where chemical attack occurs preferentially. This change is supposed to result from the reduction of intermolecular bonding in response to continued chlorine exposure. The amorphous regions are highly susceptible to chlorine, and finally cause polymer chain cleavage [159]. Three mechanisms, which are hydrolysis, oxidation and Hoffman degradation, have been suggested to explain the chemical route to the amide bond cleavage. However, none of these theories is adequate or completely persuasive, mostly because the amide bonds are relatively stable at usual feedwater pH [153].

2.4.3 Membrane preserving chemicals

Although RO membranes are designed for continuous operation, many small-scale RO systems are operated on an intermittent basis to match the variations in the supply source and production demand. Some large-scale RO seawater desalination and water recycling plants that are located in regions with extreme climate variability

can also be subjected to demand variation. For example, in Australia where the climatic pattern is characterised by intense droughts and flooding rains, several large-scale RO desalination plants, which were built to ensure a secured freshwater supply, have been recently mothballed for energy conservation. This is because seawater desalination is more expensive and energy intensive than the filtration of surface water, which has become abundant during the last few very wet years [160].

The widespread and diversified applications of RO have presented a new challenge to membrane technologists and practitioners. Once the RO plant operation is suspended for more than 48 hours, the membrane must be preserved in a chemical solution to prevent biological growth and material degradation [161]. Most membrane manufacturers provide only a brief guideline for chemical preservation (Table 4). Sodium metabisulfite (SMBS) at 0.05-1.5 % (wt/wt) is currently the most widely used preservative chemical for RO membranes [161]. Formaldehyde solution at 0.1-1% (wt/wt) has also been recommended as an alternative preservative solution due to its biocide property. However, because of its toxicity, the application of formaldehyde for membrane preservation is less common compared to SMBS [162]. In addition to SMBS and formaldehyde, in 2013, Hydranautics released a Technical Service Bulletin (TSB 110.11) considering the use of several other biocides including 2,2-Dibromo-3-nitrilopropionamide (DBNPA) and isothiazolin for chemical preservation [162]. Some commercially available pre-mixed solutions (Applied Membranes AM88, Applied Membranes AM225, PermaClean PC-55, PermaClean PC-56) have also been designed for RO membrane preservation although their exact ingredients are the proprietary information of the manufacturers. During membrane preservation, SMBS and formaldehyde can be oxidised resulting in a decrease in the preservative solution pH. Thus, several membrane manufacturers have specified that the pH of preservative solutions be regularly monitored and maintained at pH 3 or higher [161].

Table 4. Solutions recommended by membrane manufacturers for membrane storage [162-164]

	FilmTec	Hydranautics	Toray
Na ₂ S ₂ O ₅	1%	1%	0.05-0.1%
HCHO	Not available	0.1-1%	0.2-0.3%

2.5 Methods for membrane characterisation

2.5.1 Surface morphology

Surface morphology plays an important role in determining the fouling propensity of membranes and also the membrane separation performance. The most typically used methods to examine membrane surface morphology are Atomic Force Microscopy (AFM) and Scanning Electron Microscopy (SEM). The AFM technique is usually used to determine the surface roughness of cleaned and fouled membranes with nano-scale resolution. Rougher surfaces would be fouled more easily because the roughness increases surface area and produces more valleys which can accommodate more foulants [96, 165]. Song et al. [166] reported that significant difference between the surface morphologies of the virgin and fouled membranes could be recognised by AFM. Measurement of the mean pore distribution of porous membranes was also possible by AFM analysis, and the result obtained by AFM was claimed more accurate than SEM [167]. An excellent advantage of the AFM technique is its ability to image non-conducting materials without special sample preparation, which is essential for the SEM and transmission electron microscopy (TEM). SEM can be considered as a supplementary method to AFM, which is used to observed membrane surface morphology. SEM-imaging of porous membrane surfaces allows the determination of pore entrance shape and size. With suitable image processing software, all pores shown in the image can be characterised. However, this technique is limited by the resolution of the microscope used as well as by the quality of the membrane preparation [168, 169].

2.5.2 Electro-kinetics

Electro-kinetic properties of a membrane reveal the electrical characteristics of the membrane surface. Membrane electro-kinetic properties can be determined by streaming potential, sedimentation potential, electrophoresis or electro-osmosis. Amongst these techniques, streaming potential is probably the most suitable and extensively utilised for flat membrane surfaces [170]. Streaming potential involves the relative motion of charged surface and an electrolyte solution, with the results often expressed in term of membrane zeta potential (ζ), which is defined as the potential at the surface of shear [171]. By measuring streaming potential with

solutions of different pH, the membrane surface isoelectric point can be measured. The charge and resulting zeta potential of the membrane depend on the pH of the electrolyte because membrane functional groups protonate and deprotonate over the pH range.

The electrical charge of membrane surface is of critical importance because it determines the rejection efficiency of charged solutes, and also determines the fouling potential of the membrane. Although zeta potential measurement has been extensively applied on various membrane types, it was usually conducted on simple model electrolytes ($0.1-10 \text{ mmol.L}^{-1}$ KCl or NaCl) but not on practical water compositions [172]. This is a major drawback of the contemporary zeta potential measurement since potential results are strongly affected by the chemistry of the electrolyte. Higher ionic strength or the presence of multivalent cations would result in a more positive membrane potential [84, 172].

2.5.3 Hydrophobicity

The hydrophobicity indicates the wet-ability of the membrane surface. Dissociated groups on the membrane surface help it interact with the water molecules and make the surface more hydrophilic. Since the degree of dissociation of the functional groups depends on the solution chemistry such as pH and ionic strength, the hydrophobicity is also a function of these factors [173]. The hydrophobicity also has a major impact on the fouling propensity of membrane surface. A hydrophobic membrane surface would be prone to the adsorption of hydrophobic matter (i.e. colloids, organic molecules) due to the hydrophobic interaction, and therefore susceptible to membrane fouling [174]. A more hydrophobic membrane may also have higher selectivity against polar components [175, 176]. Hydrophobicity of a membrane surface is usually estimated through the contact angle measurement. A more hydrophobic membrane surface would have a higher contact angle, and vice versa. The contact angle of commercial polyamide RO membranes is mostly between $25-60^\circ$ [176, 177].

It is noteworthy that contact angle data should be used as a qualitative indicator only and caution should be taken when using this indicator. The contact angle value can be affected by various external factors such as sample pre-treatment, environmental

temperature and humidity, surface roughness and charged profile [178]. However, changes in the hydrophobicity may indicate some changes happened in the membrane integrity [176, 179].

2.5.4 Chemical structure

The chemical composition and nature of elements in the near surface region of the membrane are commonly determined by XPS and Energy Dispersive X-ray spectroscopy (EDS). Although these techniques can provide elemental analysis with similar accuracy, they have different efficient sampling depths which make them distinct in applications. Whereas XPS is most efficient for analysing the upper 1-5 nm of a surface [180], EDS gives information within 0.2-8 μm [181]. This distinction makes XPS preferable for the characterisation of fouling which may not be amenable by EDS. On the other hand, the FTIR technique was used to characterise functional groups and molecular structures on the membrane surface and the deposited foulants. Penetration depths of FTIR is approximately >300 nm depending on the surface material, the incident wave number and the incident angle [182]. Although less quantitative than XPS and EDS, FTIR provides significant qualitative details about the type of functional groups, making it a very useful method for investigating structures of membrane and foulant layers.

2.6 NDMA in water and monitoring issues

The presence of N-nitrosodimethylamine (NDMA) in recycled water and drinking water has recently emerged as a significant concern for human health [183]. NDMA can be formed when precursor-containing wastewater effluents are disinfected with chloramines or chlorine. NDMA is known to induce tumors at multiple sites in rodents exposed by various routes and has been classified as a probable human carcinogen [184, 185]. As a result, water authorities in Australia, the US, and several other countries have set a limit on NDMA concentration in drinking water and recycled water intended for potable water reuse of 10 ng.L^{-1} or below. NDMA concentrations in secondary treated effluents are commonly above this guideline value [183]. Thus, in many potable water reuse schemes, NDMA concentration is reduced by a sequence of reverse osmosis (RO) filtration and UV/advanced oxidation processes. NDMA rejection by RO membranes can be profoundly influenced by the

types of membrane used [183, 186] and operating conditions such as permeate flux and temperature [187]. This can present a major water quality compliance challenge for potable water reuse schemes and can have a significant impact on overall plant design and operation such as inclusion of UV/advanced oxidation processes in the treatment train [186]. Reliable chemical analysis at low part per trillion levels (ng.L^{-1}) is a further significant technical challenge for the control of NDMA. In fact, despite their significance in drinking water, reliable analytical methods for N-nitrosamines are only available at a few commercial and research laboratories around the world.

2.7 Conclusions

Boron removal by NF/RO membranes has been placed under the scientific spotlight for more than a decade and has attracted a large number of studies. The impacts of feedwater chemistry and operational conditions on boron rejection have been intensively investigated; consequently, various methods for optimising boron rejection have been suggested. Being able to change the form of boron existing in aqueous solutions, the pH condition appears to be the most important chemistry factor affecting boron rejection by NF/RO membranes. Consequently, the technique to increase pH up to pH 11 to improve boron removal has been commonly employed in RO seawater desalination plants. Further studies in boron rejection by NF/RO membranes are expected to continue using the solution pH as a fundamental factor in their methods. Among physical and operational parameters, temperature and permeate flux are major factors affecting boron rejection. The impacts of these parameters have been extensively studied and applied to optimise boron rejection in practical membrane installations. However, there are economic and engineering factors inhibiting the application of these methods. Consequently, many current membrane installations still have difficulty to produce permeate satisfying stringent regulated boron levels. Novel techniques to improve boron rejection by NF/RO membranes are of high demand.

A large amount of work has been dedicated to explain the mechanisms and to predict boron transport through NF/RO membranes. Models developed to date can be categorised as phenomenological-based and mechanistic-based models. Each group

has its own advantages and drawbacks. The phenomenological-based models, including solution-diffusion and irreversible thermodynamic models have simple algorithms which make them widely applied in various membrane configurations, from laboratory flat-sheet to industrial spiral-wound configuration. Boron rejection by fouled membranes was also simulated using the irreversible thermodynamic models. As a result, the simulation of boron rejection by RO membranes appears to be complete. Indeed, major RO membrane manufacturers provide commercial software packages to support the design of their membrane installations, such as ROSA of Dow-FilmTec, TorayDS/DS2 of Toray, and IMSDesign of Hydranautics. Eventually, from an industrial application point of view, there is little demand to improving models simulating boron transport through NF/RO membranes.

Nevertheless, the phenomenological-based models maintain an essential drawback. These models treat the membrane as a “black box”, so they do not provide any insight on the separation process and mechanisms. On the other hand, the mechanistic-based models, represented by the pore-flow and charged-based models, are able to explain the solute-membrane interactions, therefore they could help to design novel membranes with optimised boron rejection. Since boron is a special solute whose transport is affected by both steric-hindrance and charged repulsion depending on the solution chemistry (i.e. pH and ionic strength), the prediction of its transport through NF/RO membranes should be based on a combination of various transport models which encompass both steric-hindrance and charged repulsion mechanisms. There also exist arguments about whether diffusion or convection transport is more suitable to describe boron transport in NF/RO membranes. The answer is likely membrane-dependent. Diffusion transport would be dominant in low-flux RO membranes, whereas convection transport would play an important role in NF and high-flux RO membranes. Consequently, transport models which encompass both diffusion and convection, similar to the irreversible thermodynamic models, should have merit.

Studies on boron rejection by NF/RO membranes to date have exclusively focused on the membrane performance in virgin condition. Nevertheless, given the fact that chemical treatment is inevitable in all current membrane installations, changes in the membrane performance due to chemical exposure are practically expected.

Understanding the impacts of typically used chemicals on membrane integrity would help to predict the performance of aged membrane modules, and also help to improve the current standard procedures for chemical treatment, such as chemical cleaning and membrane preservation, therefore lengthening the membrane lifespan. Future studies on boron rejection by NF/RO membranes should take into account the impacts of chemical exposure on membrane performance.

CHAPTER 3: ENHANCED BORON REJECTION BY COMPLEXATION WITH POLYOLS

This chapter has been published as:

Tu, K.L., A.R. Chivas, and L.D. Nghiem, Enhanced boron rejection by NF/RO membranes by complexation with polyols: Measurement and mechanisms. *Desalination*, 2013. 310: 115–121.

3.1 Introduction

As discussed in Chapter 2 (Section 2.7), it is desirable to improve boron rejection efficiency in RO desalination and wastewater treatment industries. This chapter aims to provide an examination of an innovative method to improve boron rejection by RO membrane based on the complexation between boron and polyols which was mentioned in Section 2.1.3. Although this reaction has been successfully employed as the basis of selective ion exchange [188-190] and supported liquid membranes [191] for boron removal, it has not been utilised in RO technology to improve boron rejection. In a pioneering work on this topic, Geffen et al. [192] proposed the addition of D-mannitol to the feed solution to increase boron rejection via the complexation between D-mannitol and boric acid. Geffen et al. reported [192] that the reactant's concentration has a strong influence on boron rejection, whereas the reactant's ratio exhibited a slighter effect. Dydo et al. [193] found that N-methylglucamine resulted in a higher boron rejection improvement than using mannitol and sodium D-gluconate. In the former, mannitol was chosen as the model polyol due to its high equilibrium constant [192]. In the latter, N-methylglucamine was selected to represent weakly basic compounds that can be ionised to a significant extent under acidic conditions only [193]. Both studies [192, 193] reported a correlation between boron rejection and solution pH. While these two studies demonstrated the potential of using polyols to increase boron rejection by RO and possibly NF membranes, the underlying mechanisms of the interactions between boron, polyol, and the membrane remain poorly understood.

In this study, boron rejection in the presence of polyols was examined as a function of solution pH and boron:polyol molar ratios. The experimental results were mechanistically explained on the basis of the complexation equilibrium and the

properties of boric acid and polyols. Subsequent to the discussion of experimental results, potential applications of the technique are also discussed.

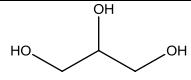
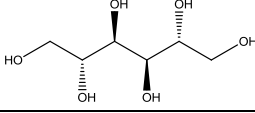
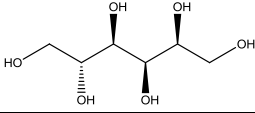
3.2 Materials and methods

3.2.1 Chemical and reagents

Suprapur HNO₃ was purchased from Merck Co. (Darmstadt, Germany). All other chemicals used were purchased from Sigma-Aldrich (Castle Hill, Australia) at reagent grade. NaCl, CaCl₂, NaHCO₃, and B(OH)₃ were used to prepare feed solution. NaOH and HCl were used for pH adjustment. Suprapur HNO₃ was used for sample dilution and preparation prior to ICP-MS analysis. Milli-Q water (Millipore, Billerica, MA, USA) was used for the preparation of all stock and feed solutions.

Glycerol, D-mannitol and D-sorbitol were used as model polyols because of their high boron-complexation stability constants (Table 5). These polyols are relatively inexpensive and can be available as food grade chemicals. For simplicity, D-mannitol and D-sorbitol will be referred to as mannitol and sorbitol hereafter. Mannitol and sorbitol are isomers; the only difference is the orientation of the hydroxyl group on carbon 2. The polyols used in this study possess low log K_{ow} values which imply a low hydrophobicity (Table 5). Stability constants of borate complexes (K₃ and K₄) have been investigated by several studies [48-50], whereas those of boric complexes (K₁ and K₂) are not available in the literature. The reported K₃ of glycerol, mannitol and sorbitol is considerably higher than K₄ (Table 5), and the overall complexation yield is in the order glycerol < mannitol < sorbitol. It is noteworthy that K₂ and K₄ would be promoted when molar concentration of the polyol is in excess of that of boron.

Table 5. Properties of the polyols used in this study [46, 48-50]

Polyol	Molecular weight (g.mol ⁻¹)	pK _a	Stability constant (L.mol ⁻¹)				Log K _{ow}	Molecular structure
			K ₁	K ₂	K ₃	K ₄		
Glycerol	92	13.68	na	na	16-25	2.6-3	-1.85	
Mannitol	182	13.14	na	na	1,060	150	-3.26	
Sorbitol	182	13.14	na	na	6,840	80	-3.26	

na: not available

3.2.2 Selected membranes

A nanofiltration membrane (NF90) and a reverse osmosis membrane (ESPA2) were used in this study. Both are thin-film composite membranes whose rejection capacity is accomplished by a thin polyamide layer which is mechanically supported by a porous polysulfone layer. The NF90 membrane (Dow FilmTec, Minneapolis, MN, USA) is a tight NF membrane which is usually used for water softening or brackish water treatment. The ESPA2 membrane (Hydranautics, Oceanside, CA, USA) is a low pressure RO membrane which can be used for the second pass of RO seawater desalination systems for boron removal. The recommended pH range for this membrane is between 2-10.6 for normal operation and 1-12 for cleaning events depending on the operating temperature [194]. Both membranes were received as flat sheet samples and were stored dry. Detailed properties of the membranes are shown in Table 6.

Table 6. Properties of the membranes used in this study

Membrane	Average pore diameter ^a (nm)	Na ⁺ rejection ^b (%)	Ca ²⁺ rejection ^b (%)	Pure water permeability (L.m ⁻² .h ⁻¹ .bar ⁻¹)	Contact angle (°)
NF90	0.68	87.2	88.6	10.5	50.9
ESPA2	na	98.3	99.5	4.0	43.3

^a Ref [195].

^b Rejection data were recorded at pH 8.

na: not available.

3.2.3 Cross-flow membrane filtration system

A laboratory-scale, cross-flow membrane filtration system is used in this study (Figure 9). The membrane cell was made of stainless steel and had an effective membrane area of 40 cm² (4 cm x 10 cm). The channel height of the cell was 2 mm. The unit utilised a Hydra-Cell pump (Wanner Engineering Inc., Minneapolis, MN, USA). Feed pressure and cross-flow velocity were controlled by a bypass valve and a back-pressure regulator. The temperature of the test solution was kept constant using a chiller/heater (S200 AquaCooler, Chester Hill, Australia) equipped with a stainless steel heat exchanger coil, which was submerged in a stainless steel reservoir. Permeate flow was measured by a digital flow meter (Optiflow 1000, Agilent Technologies, Palo Alto, CA, USA) connected to a computer, and the cross-flow rate was monitored by a rotameter. Permeate and retentate flows were recycled back to the feed reservoir.

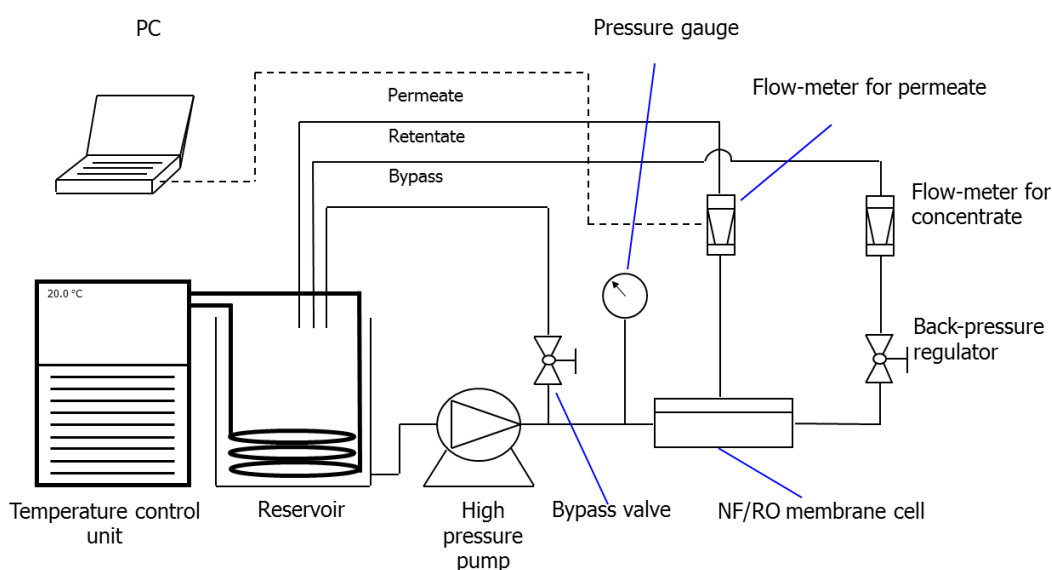


Figure 9. Schematic diagram of the NF/RO filtration system used in this study

3.2.4 Experimental protocol

Prior to each experiment, the membrane sample was rinsed with milli-Q water to remove any preservative coating layer, then the membrane was compacted using 9 L milli-Q water at a pressure of approximately 1,000 kPa higher than the normal operating pressure of each membrane. Membrane compaction was conducted for at least 1 h until a stable baseline flux was obtained. The electrolyte solution, which

contains 10 mM NaCl, 1 mM CaCl₂, 1 mM NaHCO₃, predetermined concentration of B(OH)₃ and one of the polyols, was then added to the feed reservoir making up to the total feed volume of 10 L. For all experiments, the cross-flow velocity and permeate flux were adjusted to be 42 cm.s⁻¹ and 42 LMH respectively. The temperature of the feed solution was kept constant at 20 ± 0.1 °C during the experiment. The feedwater pH was raised to 10 by adding 1M NaOH, and then was incrementally dropped to pH 6 by adding 1M HCl. The system was operated under a recirculation mode where both permeate and retentate were recirculated to the feed tank. Feed and permeate samples (25 mL each) were collected for analysis once the filtration system had been stabilised for 1 h at each investigated condition.

Experiments were conducted at two different boron concentrations: 0.43 mM (4.6 mg.L⁻¹ B) and 0.093 mM (1 mg.L⁻¹ B) in order to verify the results and also the application range of the technique. Boron rejection at 0.43 mM boron was tested with glycerol and mannitol at 1:1 and 1:5 molar ratios, and sorbitol at 1:1, 1:2 and 1:5 molar ratios. Boron rejection at 0.093 mM boron was tested with sorbitol at 1:0.2, 1:1, 1:2 and 1:5 molar ratios. The rejection (R) was calculated from the measured concentrations in the feed (C_f) and permeate (C_p) as:

$$R(\%) = 100 \times \left(1 - \frac{C_p}{C_f} \right) \quad \text{Eq.25}$$

3.2.5 Analytical methods

The concentrations of boron, sodium and calcium were analysed using an Agilent 7500cs ICP-MS (Agilent Technologies, Wilmington, DE, USA). Concentrations of the ¹¹B, ²³Na and ⁴⁴Ca isotope were acquired and reported as the overall concentrations of boron, sodium and calcium. Detection limits for ¹¹B, ²³Na and ⁴⁴Ca (expressed as total B, Na and Ca) were approximately 50 ng.L⁻¹, 140 ng.L⁻¹ and 1,800 ng.L⁻¹, respectively. Samples of the feedwater and permeate were diluted respectively 400 and 200 times using a 2% Merck Suprapur nitric acid. A Merck ICP multi-element standard solution was used for calibration. Calibration was conducted prior to each batch of analysis. The linear regression coefficients (R²) for all calibration curves were greater than 0.990 for all elements. To avoid contamination, only plastic apparatus was used for sample preparation and was

soaked in 5% Suprapur nitric acid for at least 24 h before being used. Prior to each batch of analyses, the ICP-MS was tuned by a multi-element tuning solution containing $1 \mu\text{g.L}^{-1}$ of lithium, yttrium, cerium, thallium and cobalt. Each analysis was conducted in triplicate and the variation was always less than 5%. Any instrumental drift during the analysis was corrected by analyzing a $5 \mu\text{g.L}^{-1}$ calibration standard every five samples.

Conductivity and pH were measured using an Orion 4-Star Plus pH/conductivity meter (Thermo Scientific, Beverly, MA, USA). The concentration of glycerol, mannitol and sorbitol was determined using a Shimadzu TOC V_{CSH} analyser (Shimadzu, Kyoto, Japan).

3.3 Results and discussions

3.3.1 Boric acid – polyol complexation

The complexation capability of each polyol with boron appeared in the order sorbitol > mannitol > glycerol (Figure 10). This is also the order of the complexation stability constants at high pH when boron exists exclusively as borate ion (Table 5). Considerable changes in the conductivity and pH (Figure 10) imply that negatively charged complexes and protons were produced (Eq.3), and therefore K_1K_2 was significant especially when either sorbitol or mannitol was used as the complexing reagent. The complexation occurred almost spontaneously within the first 5 seconds (data not shown). It is noteworthy that these complexations occurred at $\text{pH} < 6$ where boron existed exclusively as boric acid.

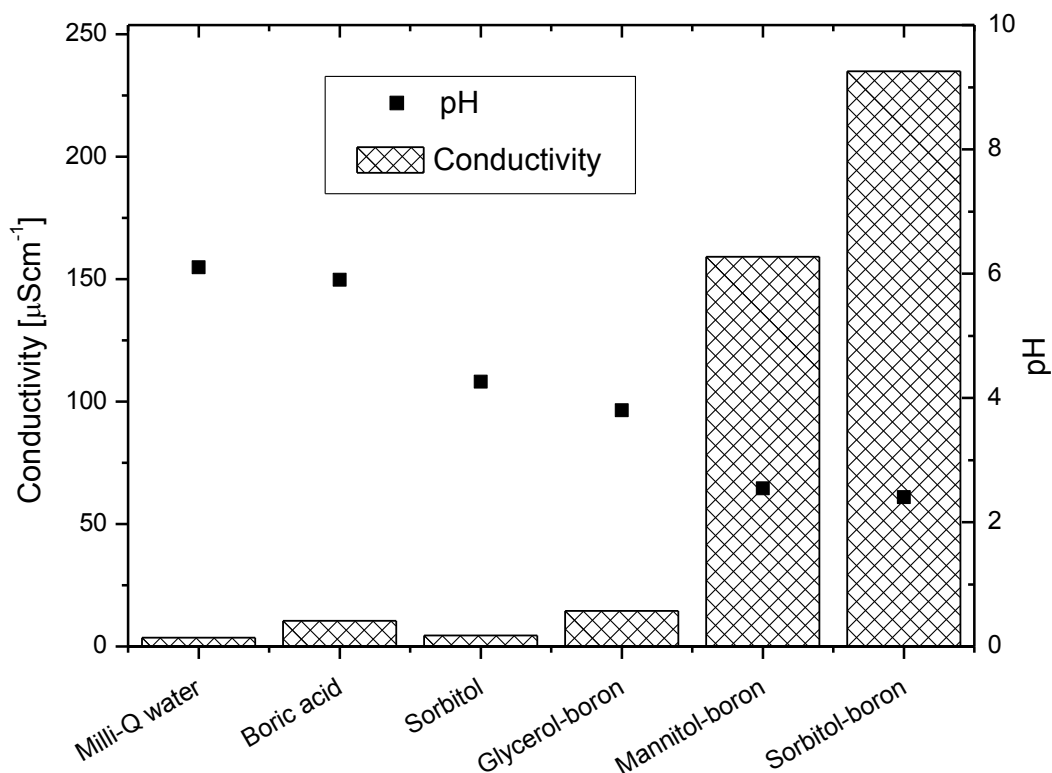


Figure 10. Changes in pH and conductivity as a result of complexation between 10 mM boric acid and 2 M glycerol, mannitol or sorbitol.

3.3.2 The rejection of boron and polyols

The rejections of boron and three polyols were found in the order sorbitol = mannitol > glycerol > boron (Figure 11) which is also the order of their molecular weights. Boron rejection was constant at $\text{pH} \leq 8$ and rapidly increased as the solution pH increased beyond 8, whereas polyol rejections appeared to be pH independent. This observation can be attributed to the dissociation of boron and polyols which governs their rejection by charged repulsion mechanism. Possessing pK_a values greater than 13 (Table 5), the polyols remained in the undissociated form in the investigated pH range and therefore their rejections by the membranes remained constant. On the other hand, the proportion of borate ions increased rapidly as the solution pH increased beyond the pK_a 9.23 of boric acid and resulted in the substantial increase in boron rejection. The changes in boron rejection as a function of pH reported here are consistent with previous studies in the literature [15, 16].

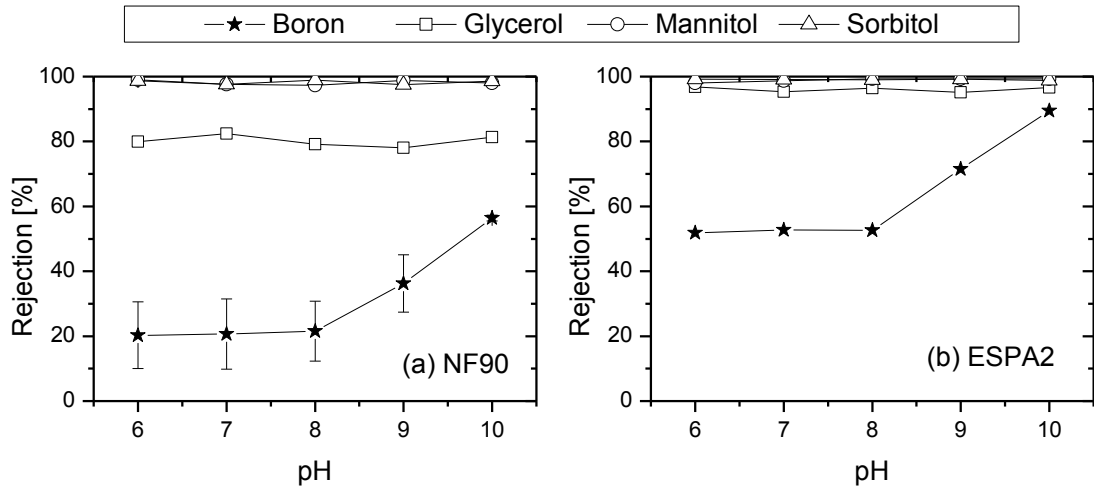


Figure 11. The rejection of boron and polyols by the (a) NF90 and (b) ESPA2 membranes. Feedwater contains 10 mM NaCl, 1 mM CaCl₂, 1mM NaHCO₃, either 0.43 mM B(OH)₃ or 0.43 mM polyol. Feedwater temperature 20 °C, permeate flux 42 LMH, cross-flow velocity 42 cm.s⁻¹. The error bars show the standard deviations of two repetitive experiments.

3.3.3 The effects of polyol addition

The rejection of sodium and calcium without the presence of any polyols slightly increased with increasing pH (Figure 12). This result is consistent with several previous studies [85, 86], and could be attributed to the increase in the membrane surface charge at increasing pH. This trend can still be observed in the presence of polyols; however, the rejections of sodium and calcium were slightly higher than that in the polyol-free condition, especially in the presence of mannitol or sorbitol (Figure 12). This phenomenon can be attributed to the ability of polyols to complex with cations Na⁺ and Ca²⁺ as previously reported [196].

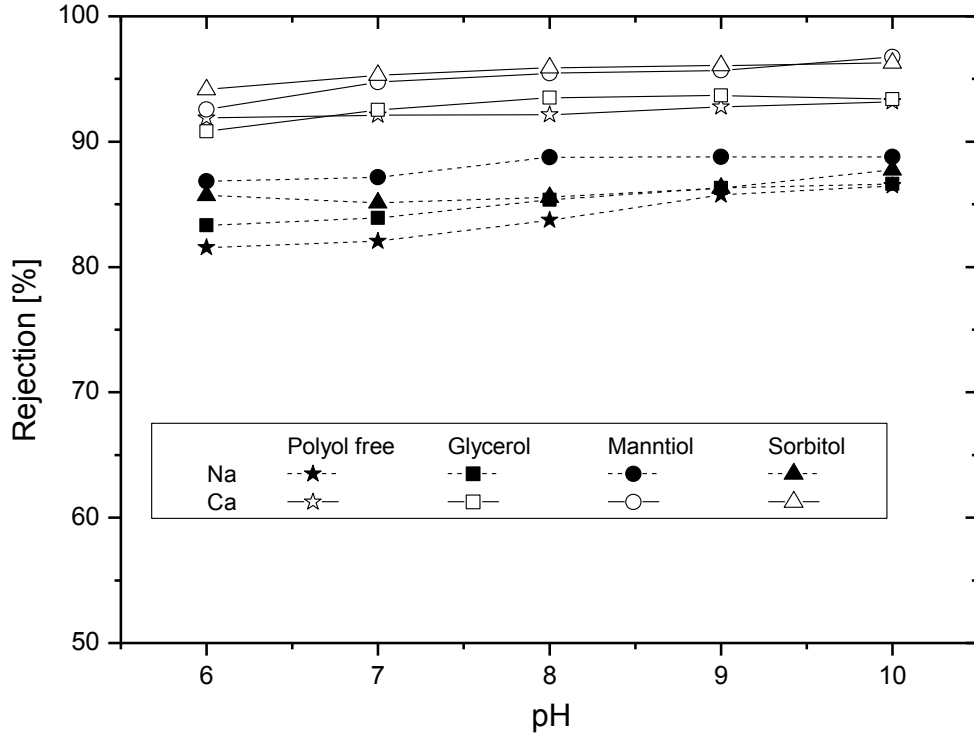


Figure 12. The rejection of sodium and calcium by the NF90 membrane in polyol-free and polyol-present conditions. The feedwater contains 0.43 mM B(OH)₃, 2.15 mM polyol (corresponding to a boron:polyol molar ratio of 1:5). Other constituents include 10 mM NaCl, 1 mM CaCl₂ and 1 mM NaHCO₃. Feedwater temperature 20 °C, permeate flux 42 LMH, cross-flow velocity 42 cm.s⁻¹.

It is noteworthy that during the experiment, a stable water flux was obtained after five hours of filtration by both membranes regardless of the polyols and their dosage (Figure 13). All three polyols used in this study are hydrophilic (Table 5) and thus their hydrophobic interactions with the membrane surface are expected to be negligible. Although the NF90 membrane showed slightly more permeate fluctuation than the ESPA2 membrane, this fluctuation was less than 2% (Figure 13) indicating that the addition of polyol to the feed did not lead to significant membrane fouling.

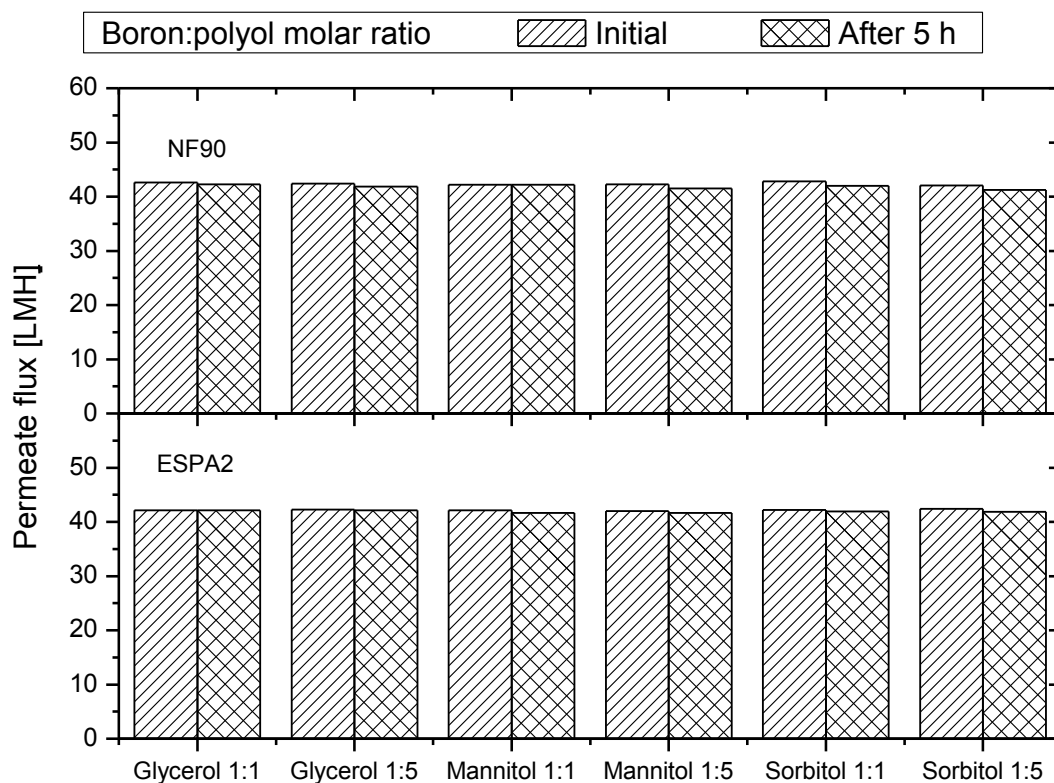


Figure 13. Membrane fouling propensity of the NF/RO filtration experiments. Feedwater contains 0.43 mM $B(OH)_3$, either 0.43 mM or 2.15 mM polyol, 10 mM NaCl, 1 mM $CaCl_2$ and 1 mM $NaHCO_3$. Feed temperature 20 °C, cross-flow velocity 42 $cm.s^{-1}$.

A significant improvement in boron rejection was achieved in the presence of polyols in the feed solution (Figure 14). At the same polyol dose and pH value, higher increases in boron rejection were obtained generally in the order sorbitol > mannitol > glycerol (Figure 14) which is also the order of the stability constant of the boron-polyol complexes (Table 5). The result implies that boron-polyol complexes were formed and their rejection is directly related to the stability constant of the complexes.

Boron rejection by the NF90 membrane in the presence of polyol appeared to be more sensitive to pH and the type of polyols than that by the ESPA2 membrane. The highest improvement in boron rejection by the NF90 membrane (at pH 9 using sorbitol) was 45%; whereas it was only 20% by the ESPA2 membrane at the same condition (Figure 14). This is because the ESPA2 membrane has a significantly higher rejection of plain boron than the NF90 membrane. The presence of polyol

resulted in a less apparent increase in boron rejection by the ESPA2 compared to the NF90 membrane, particularly at pH 6 and 7 (Figure 14).

Rejection of the boron-polyol complex appeared to be strongly affected by the solution pH. An increase in the solution pH leads to an increase in boron rejection regardless of the membrane, type of polyols and their dose (Figure 14). This is not solely due to the speciation of boric acid as a function of pH but also because of the complexation between boron and the polyol. At pH below the pK_a 9.23 of boric acid, boron exists predominantly as boric acid. According to Eq.3, the complexation between boric acid and polyol can produce protons, and thus lead to a decrease in pH (Figure 10). As a result, the complexation reaction is more favorable at high pH. In other words, the complexation efficiency increases as the solution pH increases, leading to a higher boron rejection. It is noted that the complexation between boric acid and polyol was not complete even when the molar concentration of the polyol was five times that of boric acid. Boron rejection in the presence of sorbitol ranged from 45 to 98% (Figure 14a), whereas the rejection of sorbitol was 98% (Figure 11a). A similar observation can also be made with mannitol and glycerol. Results reported here indicate that the increase in boron rejection in the presence of polyol depends mostly on the complexation efficiency.

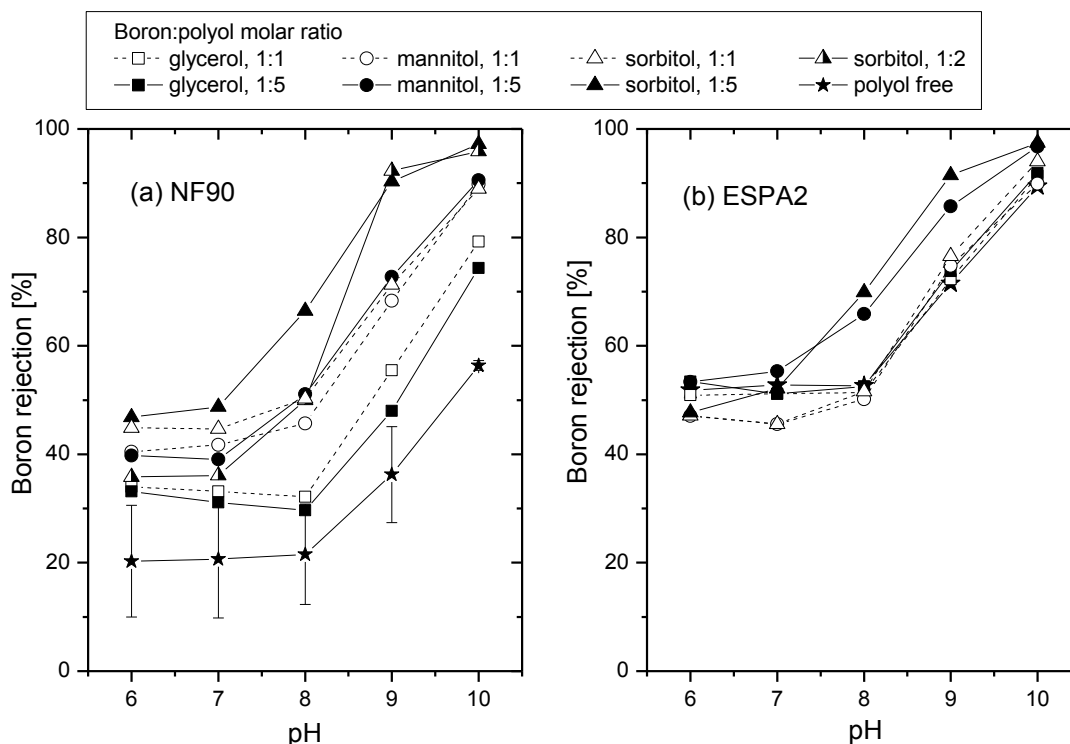


Figure 14. Boron rejection by the (a) NF90 and (b) ESPA2 membrane with feedwater containing different boron:polyol molar ratios. The feedwater contains 0.43 mM $B(OH)_3$, 10 mM NaCl, 1 mM $CaCl_2$ and 1 mM $NaHCO_3$. Feed temperature 20 °C, permeate flux 42 LMH, cross-flow velocity 42 $cm.s^{-1}$. The error bars show the standard deviations of two repetitive experiments.

Although a high pH condition was more favourable for the complexation between boron and polyols, the increase in boron rejection due to the addition of polyol to the feed solution was relatively uniform within the pH range of 6 to 10 investigated here, particularly for the NF90 membrane (Figure 14). For instance, the increase in boron rejection by the NF90 membrane due to sorbitol addition was approximately 35% throughout the pH range of 6 and 10 (Figure 14a). A possible explanation for this observation is the interplay between the speciation of boric acid and the complexation between boric acid and the polyol as the feed solution pH increases. At pH from 6 to 8, boric acid is dominantly present. The rejection of boron is low whereas the rejection of boron in the presence of a polyol depends on the efficiency of the complexation reaction. As the solution pH increases, the complexation efficiency increases; however, the rejection of boron also increases because of the

speciation of boric acid. As a result, the net increase in boron rejection appears to be constant over the entire pH range investigated in this study (Figure 14a).

Although the boron:polyol molar ratio could affect the types of complex formed (Section 2.1.3), there was no discernible difference in boron rejection between sufficient and excess sorbitol concentrations. The boron:sorbitol molar ratio of 1:1, 1:2 and 1:5 showed a similar boron rejection across the whole pH range (Figure 15). This can be attributed to the high rejection of sorbitol by the NF90 membrane (Figure 11). It is noteworthy that even at a very low sorbitol concentration (i.e. boron:sorbitol molar ratio of 1:0.2), a considerable increase in boron rejection could be observed (Figure 15). Nevertheless, at pH 10, the increase in boron rejection at the boron:sorbitol molar ratio of 1:0.2 was substantially lower than that at the ratio of 1:1. This is because at high pH, the complexation between boron and sorbitol is complete and boron rejection is governed mostly by the molar ratio between boron and sorbitol. Results reported here indicate that a small dosage sorbitol (i.e. in the range of 3.4 to 17 mg.L⁻¹ corresponding to boron:sorbitol molar ratio of 1:0.2 to 1:1) could be adequate to achieve a significant increase in boron rejection by the NF90 membrane. According to the market overview by ICIS (www.icis.com/chemicals/sorbitol/), the cost of sorbitol in the first quarter of 2012 is from 0.82 – 0.91 US\$/kg. Therefore, the addition of polyols such as sorbitol to feedwater to improve the rejection of boron by a NF membrane can be a practical approach for the removal of boron.

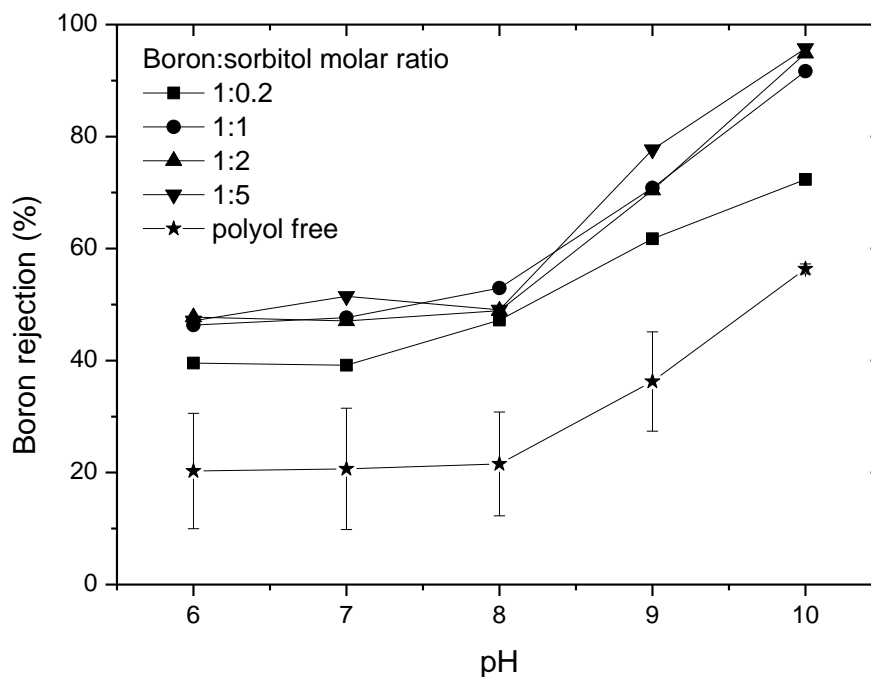


Figure 15. Boron rejection by the NF90 membrane with feedwater containing different boron:sorbitol molar ratios. The feed solution contains 0.093 mM $B(OH)_3$, 10 mM NaCl, 1 mM $CaCl_2$ and 1 mM $NaHCO_3$. Feed temperature 20 °C, permeate flux 42 LMH, cross-flow velocity 42 $cm.s^{-1}$. The error bars show the standard deviations of two repetitive experiments.

3.4 Conclusions

The addition of polyols including glycerol, mannitol or sorbitol to the feed can substantially improve boron rejection. The efficiency of each polyol to improve boron rejection was directly related to the stability constant of their complexation with boron. Polyols could complex with boron in either the boric acid or borate anion form; however the complexation between polyol and boric acid appeared to be incomplete. The increase in boron rejection due to polyol addition was higher for the NF membrane compared to the RO membrane. A boron:polyol molar ratio of 1:1 appeared to be adequate and a higher concentration of polyol did not lead to any further increase in boron rejection. A considerable improvement in boron rejection was observed even when the boron:sorbitol molar ratio was as low as 1:0.2. The presence of polyols did not cause any observable membrane fouling issue. Results reported here suggest that the addition of polyols could allow NF membranes to be effectively used for boron removal.

CHAPTER 4: EFFECTS OF CHEMICAL CLEANING ON BORON REJECTION

This chapter has been published as:

Tu, K.L., A.R. Chivas, and L.D. Nghiem, Effects of chemical cleaning on separation efficiency of a reverse osmosis membrane. *Membrane Water Treatment*. Accepted manuscript.

4.1 Introduction

As discussed in Chapter 2 (Section 2.4.1), chemical cleaning is a regular practice of all RO installations; however, it has the potential to alter the membrane performance. Given that the impacts of chemical cleaning, especially sequential cleaning, on the rejection of small and neutrally charged solutes by RO membranes have not been thoroughly understood, this study aims to investigate the effects of single and sequential membrane cleaning cycles on boron rejection by RO membranes. Membrane cleaning agents used in this study include citric acid, sodium hydroxide, SDS, EDTA, a mixture of SDS and EDTA, and two commercial membrane cleaning formulations, namely MC3 and MC11. Changes in the water permeability and the rejections of boron and sodium are elucidated by any modifications in the membrane surface charge, hydrophobicity, and chemical composition.

4.2 Materials and methods

4.2.1 Membrane and chemicals

The ESPA2 membrane was used in this study. Basic properties of this membrane have been given in Section 3.2.2.

Analytical grade NaCl, CaCl₂, NaHCO₃, and B(OH)₃ were used to prepare the feed solution. Merck Suprapur nitric acid was used for sample dilution prior to analysis. Milli-Q water was used for the preparation of all stock and feed solutions. Chemicals used for simulating membrane cleaning include citric acid, sodium hydroxide, SDS, EDTA, a mixture of SDS and EDTA, and two proprietary membrane cleaning formulations namely MC3 and MC11 (IMCD, Mulgrave, Victoria, Australia). The properties of these solutions are presented in Table 7. EDTA and SDS solutions are

prepared approximately five times more concentrated than the typically recommended values in order to accelerate any impact on the membrane. The MC3 and MC11 solutions are used at the supplier-recommended concentration.

Table 7. Solutions used for membrane cleaning simulation in this study

Chemical/commercial name	Chemical formula/ Ingredient	Concentration	pH
Citric acid (CA)	$C_6H_8O_7$	---	3
Sodium hydroxide (SH)	NaOH	---	11
Surfactant (SDS)	$NaC_{12}H_{25}SO_4$	0.15%	11
Chelating agent (EDTA)	$C_{10}H_{16}N_2O_8$	5%	11
Mixture of surfactant and chelating agent (SDS+EDTA)		0.15% SDS + 5% EDTA	11
MC3	Organic acid, detergent builders, and chelating agents	25 g.L^{-1}	3
MC11	pH buffer, detergent builders, and chelating agents	25 g.L^{-1}	11

4.2.2 Cross-flow membrane filtration system and experimental protocol

This study used the RO filtration system which was described in detail in Section 3.2.3.

At the beginning of each experiment, the membrane sample was compacted by using Milli-Q water at 30 bar for 18 h. A stable flux was usually obtained within the first 10 h run. Following the membrane compaction, pure water permeability of the membrane was measured from 5 to 30 bar with 5 bar increments (at 20 °C). Electrolyte solution was then added to the feed reservoir making up a 10 L feedwater containing 10 mM NaCl, 1 mM $CaCl_2$, 1 mM $NaHCO_3$, and 0.43 mM $B(OH)_3$ (or 4.6 $mg.L^{-1}$ B). Rejections were obtained at permeate fluxes of 10, 20, 42, and 60 LMH, temperatures of 10, 20, 30, and 40 °C, and pH values of 7, 8, 9.5, and 11. Unless otherwise stated, the standard testing condition is 20 LMH flux, 20 °C, pH 8, and 42

cm.s⁻¹ cross-flow velocity. The pH value was adjusted using either 1 M NaOH or 1 M HCl solution. In all experiments, once the target operational parameters had been obtained, the system was stabilised for 60 min before feed and permeate samples of 20 mL each were taken for analysis.

4.2.3 Simulation of membrane cleaning

Chemical cleaning was simulated by soaking flat-sheet virgin membrane samples in a sealed glass bottle containing a prepared cleaning solution for 25 h. The bottle was immersed in a temperature-controlled water bath (SWB1, Stuart, Staffordshire, UK) and the temperature was maintained at 30 ± 0.5 °C. The 25-h exposure was chosen to simulate the cumulative membrane cleaning period over three years of operation. Similar simulated membrane cleaning protocol has been used elsewhere [143]. After 25-h exposure to cleaning chemical, the membrane sample was removed from the solution and thoroughly rinsed with copious amount of Milli-Q water before being tested for surface properties and separation efficiency. Impacts of sequential cleaning on the membrane performance were investigated by soaking a virgin membrane in a cleaning solution for 25 h followed by another cleaning solution for 25 h. The membrane was thoroughly rinsed with Milli-Q water between the two cleaning cycles.

The membrane cleaning protocol used in this study differs somewhat from that used in practice. Membrane cleaning in full-scale RO membrane plants usually includes circulations of cleaning solution which results in rigorous mixing of the solution to improve the cleaning efficiency. In addition, the fouling layer on a used membrane may partially shield the membrane from direct exposure to the cleaning agents. Despite these differences in the membrane cleaning regime, the protocol used in this study is probably the most appropriate for simulating the impacts of chemical cleaning under controlled conditions and has been widely used in other studies [142, 143, 145].

4.2.4 Membrane characterisation methods

The electro-kinetic property of the virgin and chemically cleaned membranes was measured using a SurPASS streaming potential analyser (Anton Paar GmbH, Graz,

Austria). The zeta potential of the membrane surface was calculated from the measured streaming potential using the Fairbrother–Mastin approach [197]. All streaming potential measurements were conducted in a background electrolyte solution containing 1 mM KCl, at 500 mbar streaming pressure, and room temperature of approximately 25 °C. Analytical grade HCl and KOH were used to adjust the pH by means of automatic titration.

The hydrophobicity of the membrane surface was measured using a Rame-Hart goniometer (Model 250, Rame-Hart, Netcong, NJ) following the standard sessile drop method. Prior to each measurement, the membrane sample was dried in air for approximately 5 h. Five Milli-Q water droplets were applied to each membrane sample and the contact angle was immediately measured on both sides of the droplet. Measurements were conducted at room temperature (ca. 25 °C).

FTIR analysis was conducted using a Shimadzu IRAffinity-1 (Kyoto, Japan) spectrometer to determine major functional groups of the virgin and chemically cleaned membranes. Membrane samples were placed on the ATR crystal and pressed onto the surface with a plate press. The measured spectrum was between 600 cm⁻¹ and 1750 cm⁻¹ at a resolution of 2 cm⁻¹. Each scan was performed 20 times. Background correction was performed at the beginning of each measuring batch.

4.2.5 Chemical analytical methods

The concentrations of boron and sodium were analysed using an ICP-MS system. The method has been thoroughly described in Section 3.2.5. Conductivity and pH were measured using an Orion 4-Star Plus pH/conductivity meter.

Solute rejection was calculated using Eq.25.

Changes in membrane performance (contact angle, water permeability) were calculated using:

$$\text{Relative change (\%)} = \frac{X_{\text{tr}} - X_{\text{vir}}}{X_{\text{vir}}} \times 100 \quad \text{Eq.26}$$

Where X_{tr} and X_{vir} are the performance parameters (i.e. contact angle or water permeability) of the treated (cleaned) membrane and virgin membrane, respectively.

4.3 Results and discussion

4.3.1 Charge density

The charge density of a polymeric membrane surface may influence its pore structure and Donnan equilibrium which govern the rejection efficiency, particularly of charged solutes [198]. Charge density of the membrane was evaluated through the zeta potential value which indicates a net interaction between the membrane surface and an electrolyte [179]. In this study, the solution pH appeared to have a significant impact on the zeta potential of the ESPA2 membrane (Figure 16). The influence of solution pH on the membrane zeta potential can be explained by the dissociation of functional groups on the membrane active layer (i.e. carboxylic and amine groups) [197]. As the pH of the electrolyte increased from 3 to 11, the zeta potential of virgin ESPA2 membrane shifted from +30 mV to -42 mV with an isoelectric point at pH 4 where minimum salt rejection and maximum water permeability is usually observed [85, 199, 200]. The 25-h acidic cleaning (pH 3) did not cause any considerable impact on the charge density of the ESPA2 membrane. On the other hand, the caustic cleaning (pH 11) made the membrane slightly more negatively charged at pH between 6 and 11 (Figure 16). According to Elimelech et al. [170], the charged profile of a membrane can be affected by the adsorption of ions on the membrane surface, which subsequently changes the dissociation of the membrane functional groups.

The SDS cleaning resulted in a decrease in the charge density of the membrane surface over the entire pH range, both positive and negative charge (Figure 16). It appeared that the SDS molecules were adsorbed on the membrane surface and inhibited the impact of pH on the dissociation groups of the membrane surface. Similar results have been reported by Simon et al. [140]; however, opposite results were observed by Al-Amoudi et al. [142] who found that an over-night exposure to SDS would make the NF membranes more negatively charged from pH 3 to 10. The discrepancy may be attributed to the different conformations of the membranes used. The acidic cleaning conducted after SDS cleaning partially recovered the negative charge of the membrane (i.e. closer to the charge of virgin membrane) (Figure 16). However, the isoelectric point was not recovered and was equal to that of the SDS

cleaned membrane. It is hypothesised that the association between SDS and membrane surface has been weakened by the citric acid solution. It is also noteworthy that there might be some modifications within the membrane pores but such changes could not be detected by the streaming potential measurement [173]. In fact, it was suggested that the charge within membrane pores, rather than that on the membrane surface, would have a significant impact on the separation efficiency of the membrane [85].

The impact of EDTA on the membrane charge was opposite to that of SDS cleaning, although these solutions had the same pH condition (pH 11). This result confirms that the membrane charge density is more significantly impacted by the surfactant or chelating agent rather than the pH of the cleaning solution. The zeta potential of the EDTA cleaned membrane was slightly more negative than that of the virgin membrane (Figure 16). The isoelectric point was also shifted to a lower pH value. The adsorption of EDTA on the membrane surface might have introduced more carboxylic groups on the membrane surface, and thus increased the negative charge of the membrane. The application of a subsequent acidic cleaning seemed not to considerably affect the membrane charge density (Figure 16), which implies that EDTA molecules were still adsorbed on the membrane surface. At $\text{pH} < 5.5$, the zeta potential of the SDS+EDTA-cleaned membrane was comparable to that of those cleaned by either SDS or EDTA solution. However, at $\text{pH} > 5.5$, the zeta potential of the SDS+EDTA-cleaned membrane was equal to that of the virgin ESPA2 membrane (Figure 16). It appeared that the charge density of the SDS+EDTA-cleaned membrane was the result of a neutralisation impact of individual cleaning agents. The mechanism of this effect has not been reported in the literature. The subsequent acidic cleaning led to a significant decrease in the negative charge of the SDS+EDTA cleaned membrane (Figure 16).

The formulated MC3 cleaning solution did not cause any considerable impact on the charge density of the ESPA2 membrane, whereas the MC11 solution led to a more negative membrane charge (Figure 16). A similar result has been reported elsewhere [143]. The subsequent caustic cleaning did not impact the charge of the MC3-cleaned membrane; however, it slightly decreased the negative charge of the MC11-cleaned

membrane (Figure 16). Since the exact composition of these solutions is proprietary, the mechanism of their impacts on the membrane charge cannot be elucidated.

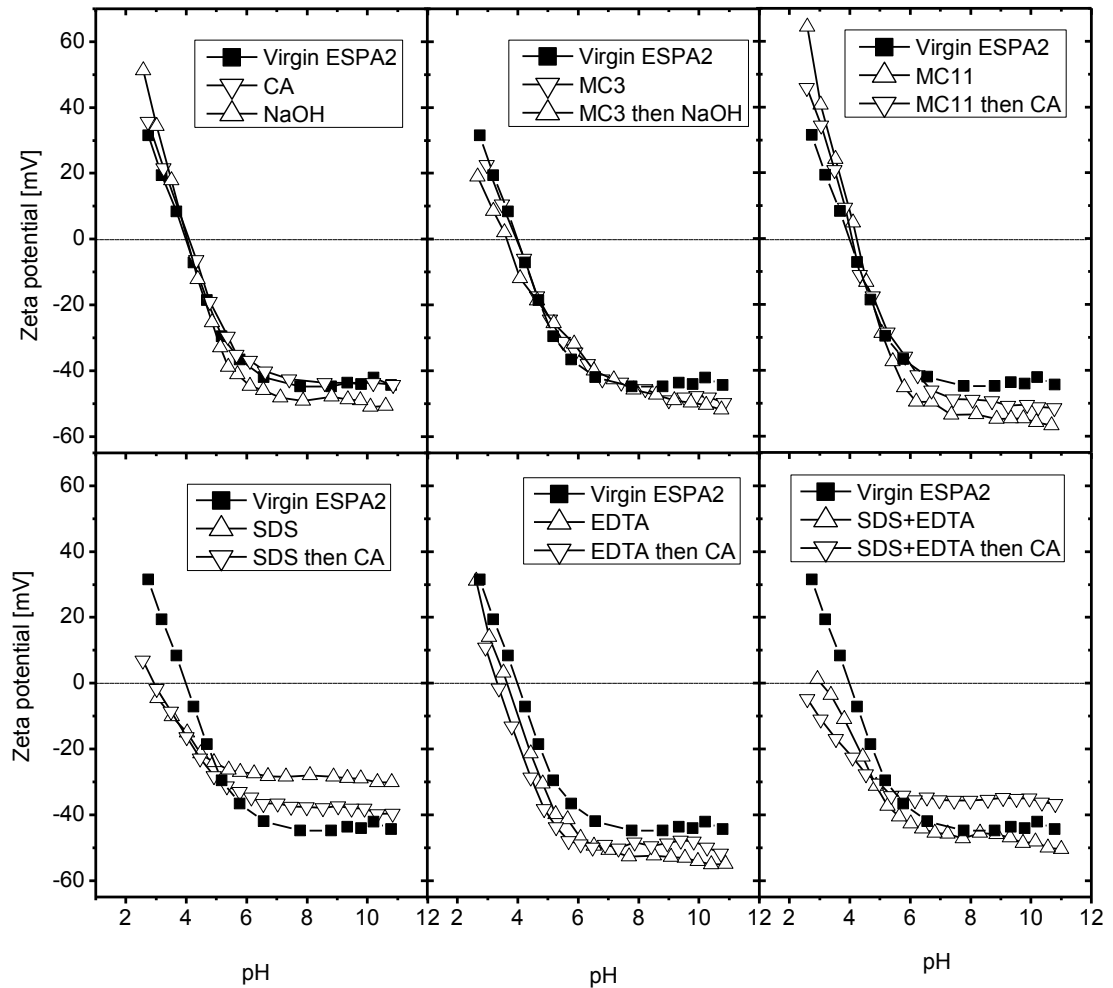


Figure 16. Changes in zeta potential of the ESPA2 membrane as a consequence of single and sequential chemical cleaning. The measurements were conducted at room temperature (ca. 25 °C) in a 1 mM KCl solution.

4.3.2 Hydrophobicity and surface bonding

Chemical cleaning using either citric acid (pH 3) or sodium hydroxide (pH 11) rendered the ESPA2 membrane slightly more hydrophobic (Figure 17). Similar results have been reported by Simon et al. [140]. Tian et al. [144] hypothesised that sodium hydroxide could increase the membrane surface hydrophobicity by reacting with hydrophilic functional groups in the active layer. Some studies [176, 179] found that changes in the contact angle would indicate changes in the membrane

conformation and also the charge density. However, in this study, the zeta potential (Figure 16) and FTIR (Figure 18) measurements did not detect any changes in the conformation of the membranes cleaned by either citric acid or sodium hydroxide. On the other hand, chemical cleaning using either SDS or EDTA rendered the membrane more significantly hydrophilic (Figure 17). This observation is consistent with the literature, and was attributed to the adsorption of hydrophilic SDS and EDTA molecules on the membrane polyamide structure [140, 201, 202]. A study conducted by Kim et al. [203] suggested that under extreme conditions, the polyamide active skin layer can be hydrolysed to carboxylic acid derivatives, resulting in an increase in surface hydrophilicity. Nevertheless, the FTIR data (Figure 18) does not detect that any hydrolysis occurred on the membrane surface. There was no surprise that the mixture of SDS and EDTA increased the membrane's hydrophilicity (Figure 17), given that these individual chemicals were found to cause the same effect. The formulated cleaning chemicals MC3 and MC11 shifted the membrane hydrophobicity in opposite directions. The MC3 rendered the membrane more hydrophilic, whereas the MC11 made it substantially more hydrophobic (Figure 17). Similar results have been reported by Simon et al. [145]. The high hydrophilicity of the MC3-cleaned membrane can be explained by the presence of hydrophilic chelating agents in the MC3 formula (Table 7). The MC11 may contain hydrophobic ingredients but the specific formula is unidentified.

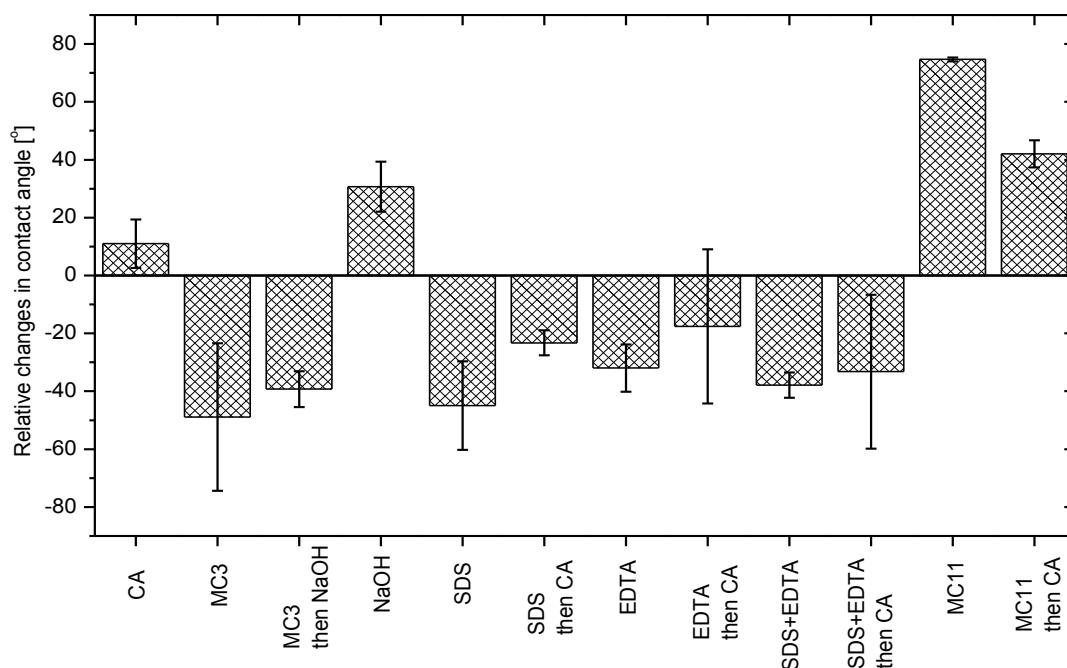


Figure 17: Changes in contact angle values of the ESPA2 membrane as a consequence of single and sequential chemical cleaning. A positive value indicates an increase in the hydrophobicity, and vice versa. The measurements were conducted at room temperature (ca. 25 °C) with Milli-Q water used as a reference solvent. The error bars show the standard deviation of five replicated measurements.

It is interesting to note that the subsequent cleanings counteracted the impacts of the first cleaning chemical on the membrane hydrophobicity, and thus changes in the membrane hydrophobicity were diminished. A similar phenomenon with respect to the zeta potential of the chemically cleaned membranes could be observed in Figure 16. Results reported here suggest the wash-out effect of the subsequent cleaning on the first one. Changes in the membrane hydrophobicity may result in changes in the membrane performance. For example, it was reported that a more hydrophilic membrane would have a higher water permeability [204, 205] and a lower fouling propensity [174]. In addition, Bernstein et al. [206] reported that a decrease in hydrophobicity would lead to a decrease in boron rejection, although the reason for such observation was not provided.

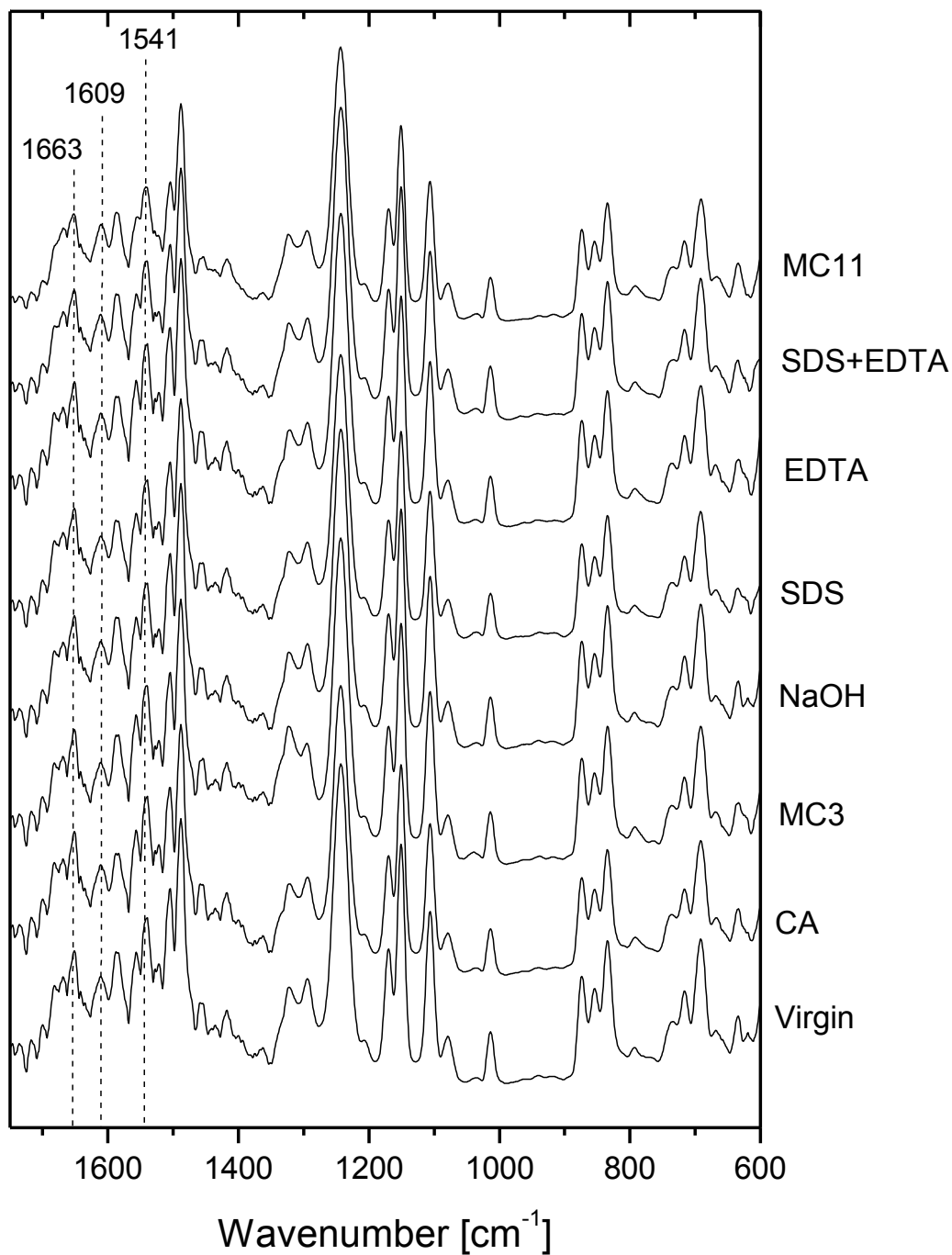


Figure 18. FTIR absorption spectra of virgin and chemically cleaned ESPA2 membranes at 2 cm⁻¹ resolution.

4.3.3 Water permeability

Some studies reported that the water permeability of NF/RO membranes would be either decreased or increased as a consequence of exposure to either strong acidic or caustic conditions, respectively [88, 133, 140, 142]. Similar results were found in this

study. The 25-h acidic cleaning decreased the water permeability of the ESPA2 membrane by more than 10%, whereas the caustic cleaning resulted in a 5% water permeability increase (Figure 19). Fundamental research conducted by Braghetta et al. [88] attributed the increase in the water permeability of NF membranes in caustic conditions to the enhanced internal electrostatic charged repulsion within the membrane matrix which increased the membrane porosity and so the water permeability. This explanation is supported by the increase in charge density of the NaOH-cleaned membrane as observed in Figure 16. Interestingly, Childress and Elimelech [85] reported that the pore size of membranes would be reduced at both low and high pH, which resulted in the decrease in water permeability in both acidic and caustic conditions. Considering the above discrepant results, the impact of pH on the membrane water permeability seems to be membrane-dependent.

The 25-h membrane cleaning using either SDS or EDTA in caustic conditions resulted in a significant increase (ca. 15%) in the water permeability of the ESPA2 membrane. A similar result has been reported in the literature [140, 142, 207], and was attributed to the adsorption of SDS or EDTA molecules on the membrane surface. The adsorption of these hydrophilic agents renders the membrane surface more hydrophilic thus leads to an increase in its water permeability. This explanation is supported by the increase in the hydrophilicity of the SDS-cleaned membrane and the EDTA-cleaned membrane as observed in Figure 17. In addition, Liikanen et al. [133] suggested that at high pH, EDTA could complex with some membrane constituents, resulting in an increase in the membrane porosity and so an increase in the water permeability. As expected, the mixture of SDS and EDTA in caustic conditions increased the water permeability of the cleaned membrane (Figure 19). It is interesting to note that the correlation between increased hydrophilicity and increased water permeability was not seen with the formulated cleaning chemicals MC3 and MC11. The MC3-cleaned membrane and MC11-cleaned membrane obtained lower and higher water permeability, respectively (Figure 19), even though the MC3-cleaned membrane was very hydrophilic and the MC11-cleaned membrane was highly hydrophobic (Figure 17). Similar results were reported by Simon et al. [145]. However, this phenomenon cannot be thoroughly explained since the exact

compositions of these two commercially available formulated chemical cleaning solutions are not known.

It is interesting to note that the impacts of the chemical cleaning on the water permeability, either positive or negative, can be mitigated or even inverted by applying a subsequent cleaning step with a pH condition opposite to that of the initial cleaning solution. For example, cleaning with MC3 in acidic conditions decreased 6% of the water permeability of the virgin membrane, and the subsequent caustic cleaning led to a 25% increase in water permeability compared to the virgin membrane (Figure 19). A similar observation was reported by Fujioka et al. [143]. It appears that the pH of the cleaning solutions has a strong impact on the water permeability of the membrane.

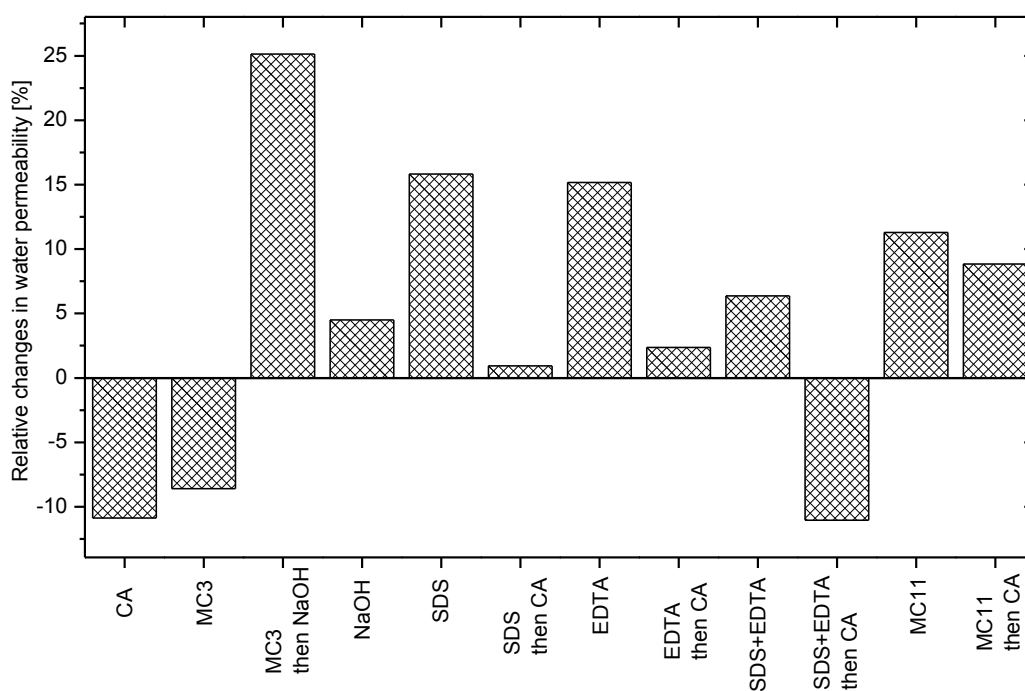


Figure 19. Relative change in the water permeability of ESPA2 membranes as a consequence of single and sequential chemical cleaning. The water permeability was measured with Milli-Q water from 5 to 30 bar with 5 bar increments and at 20 °C; cross-flow velocity 42 cm.s⁻¹.

4.3.4 The rejection of boron and sodium

Membrane cleaning solutions usually contain surfactant and chelating agents in either caustic or acidic condition. For a systematic investigation of the impacts of membrane cleaning on the membrane integrity, the impacts of caustic and acidic conditions are first examined in this study. The rejections of boron and sodium by virgin and cleaned membranes were investigated as functions of permeate flux, temperature, and solution pH. In good agreement with the literature [73, 79], boron rejection was strongly affected by flux, temperature and feed solution pH. Boron rejection by the virgin ESPA2 varied from 45 to 72% when the permeate flux increased from 10 to 60 LMH. Similarly, the increase in water temperature from 10 to 40 °C caused a decrease in boron rejection from 69 to 40% (Figure 20). In particular, boron rejection by the virgin ESPA2 reached 90% at the water pH of 11. On the other hand, sodium rejection was higher than 95% and marginally affected by the operating condition changes (Figure 20). Transport mechanisms and the impacts of flux, temperature and pH on boron and sodium rejection have been well deliberated in the literature [123, 208]. Possessing a pK_a of 9.2, the boric acid molecule is poorly hydrated in aqueous solutions having a pH lower than this value. Boron rejection by commercial RO membranes is relatively low because the boric acid molecule is small in size (its Stokes radius is approximately double that of the water molecule) and neutrally charged (Section 2.1.3). The transformation from boric acid to borate species explains the increase in boron rejection as the pH increased [86]. On the other hand, being a hydrated and charged species at all pH values, the sodium ion can be efficiently removed by a RO membrane regardless of operating condition changes [86].

Several studies have been dedicated to investigate the impacts of acidic and caustic cleaning on the separation efficiency of NF/RO membranes. Although using different membranes and different targeted solutes, there is a good agreement amongst studies that caustic cleaning would markedly decrease the rejection efficiency of the membranes, whereas acidic cleaning did not cause any considerable impacts. Caustic cleaning was reported to decrease the rejection of NDMA [143], $MgCl_2$ [139] and carbamazepine [140] by various NF/RO membranes. In this study, the 25-h caustic cleaning with sodium hydroxide (pH 11) resulted in an approximately 10% decrease

in boron rejection, whereas sodium rejection was unaffected (Figure 20). The boron rejection loss was consistently observed at various testing permeate fluxes, temperatures, and pH values, which indicated that the changes were caused by the modification of the membrane surface. In practice, caustic cleaning is a typical membrane cleaning procedure because it is very useful to remove many types of foulant [202, 207]. The loss of boron rejection efficiency as seen on Figure 20 may raise major concerns of inadequate boron level in permeate water produced by aged membrane installations. The decrease in boron rejection, together with the increase in water permeability (Figure 19) of the caustic-cleaned membrane, can be attributed to an increase in the membrane porosity which is caused by an increased internal charged repulsion [88]. Sodium rejection is unaffected by this mechanism because the increased internal charged repulsion would help to sustain or even improve the rejection of hydrated sodium molecules in the solution [88].

Acidic cleaning was reported to cause negligible impacts on the rejection of NDMA [143] and $MgCl_2$ [139] by NF/RO membranes. In this study, the 25-h acidic cleaning with citric acid (pH 3) led to an approximate 10% decrease in boron rejection and 5% decrease in sodium rejection (Figure 20). This rejection loss indicates major conformational changes occurred within the membrane polymer structure. It is noteworthy that such rejection decrease was coupled with a 10% decrease in water permeability of the acidic-cleaned membrane (Figure 19). The concurrent loss of water permeability and solute rejection was reported elsewhere in the literature [152], and was attributed to the transformation from crystalline regions to an amorphous state of the membrane polymer structure. According to Kang et al. [152], this transformation led to a cleavage of the polyamide structure which decreased solute rejection and created a “soft barrier layer” which was compacted under operating pressure and consequently resulted in a flux decline. However, FTIR analysis in this study is not adequately sensitive to detect these changes (Figure 18) and thus the exact mechanisms accounting for this phenomenon cannot be verified.

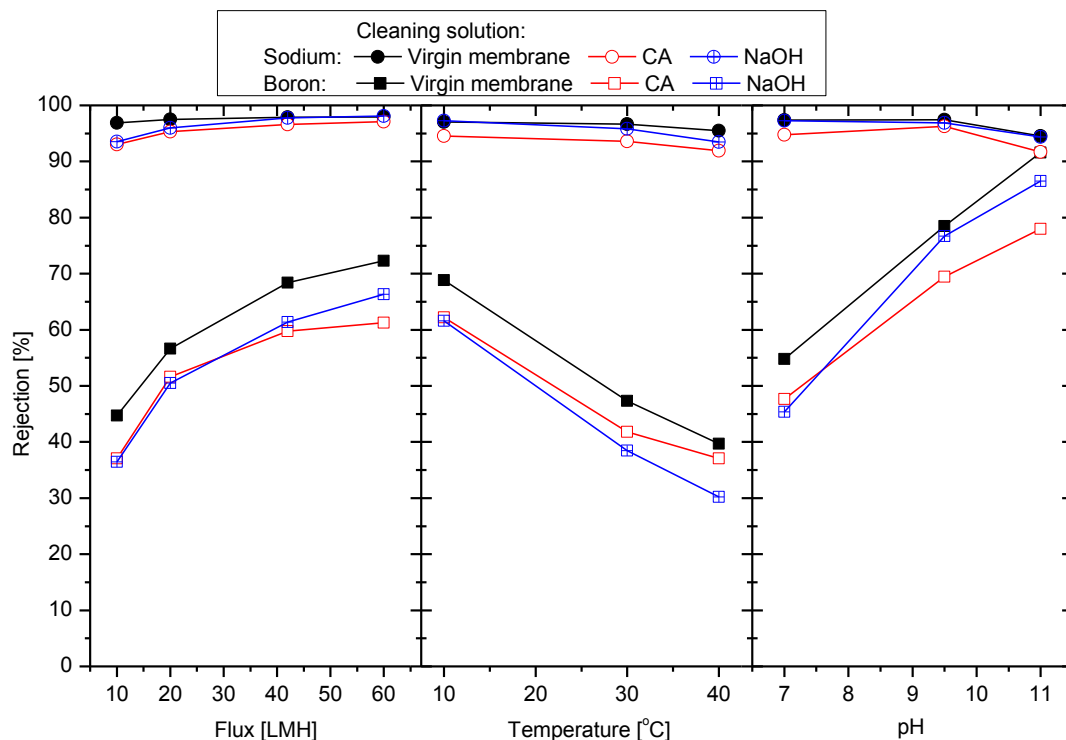


Figure 20. Changes in boron and sodium rejections by the ESPA2 membrane as a consequence of acidic (citric acid, CA) or caustic (NaOH) cleaning. Unless otherwise stated, the testing conditions are: pH 8, feedwater contains 0.43 mM B(OH)₃, 10 mM NaCl, 1 mM NaHCO₃, and 1 mM CaCl₂; temperature 20 °C, permeate flux 20 LMH, cross-flow velocity 42 cm.s⁻¹.

The reported results regarding the impacts of SDS cleaning on the membrane performance are discrepant and appear to be strongly membrane-dependent [85, 139, 146]. In this study, the rejections of boron and sodium by the SDS-cleaned membrane were comparable to that by the NaOH-cleaned membrane (Figure 21). This result implies that SDS itself does not cause any negative impact on the rejection efficiency of the membrane. The SDS-cleaned membrane had a lower boron and sodium rejection than the virgin ESPA2 membrane because of the caustic condition as discussed previously (Figure 20). The application of an acidic cleaning after SDS cleaning caused a substantial decrease in sodium rejection and sustained the boron rejection of the cleaned membrane (Figure 21). This phenomenon has not been reported in the literature. As discussed in Section 3.2.1, the application of citric acid could remove the adsorbed SDS from the membrane surface. It is hypothesised that this process also changes the internal pore structure of the membrane, likely the

charge within pores which is not detected by the streaming potential measurement. The decrease in sodium rejection is a result of the decrease in charged repulsion between sodium molecules and internal membrane pores.

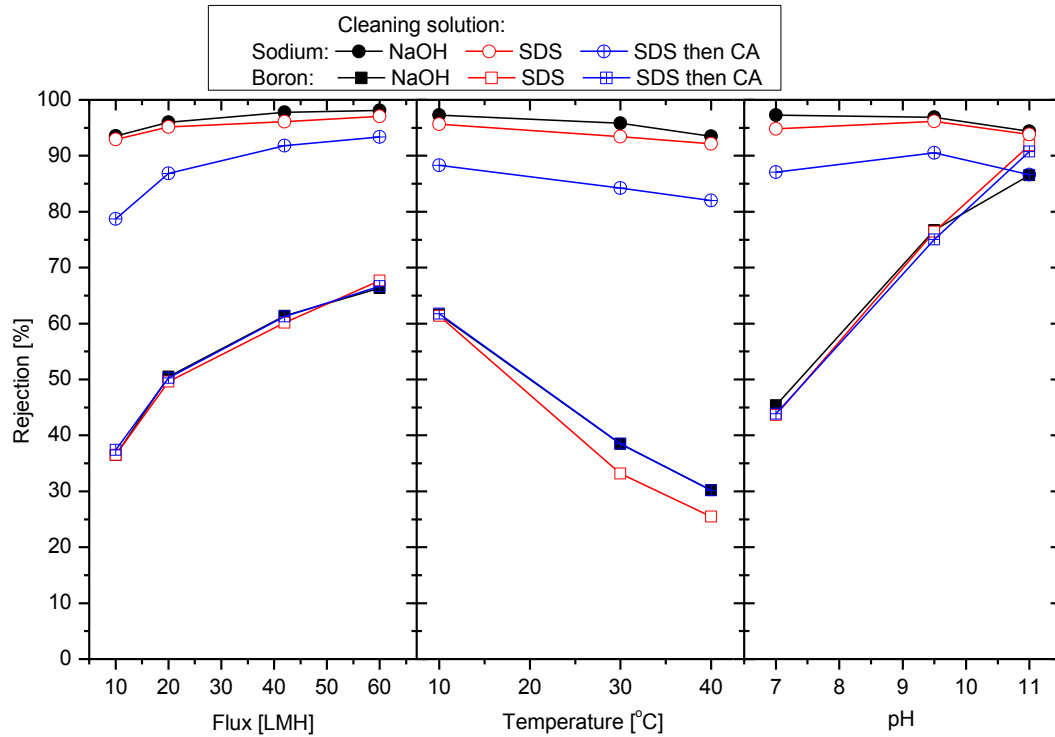


Figure 21. Changes in boron and sodium rejections by the ESPA2 membrane after membrane cleaning with SDS solution (pH 11) and SDS solution followed by citric acid solution (pH 3). Unless otherwise stated, the testing conditions are: pH 8, feedwater contains 0.43 mM $B(OH)_3$, 10 mM NaCl, 1 mM $NaHCO_3$, and 1 mM $CaCl_2$; temperature 20 °C, permeate flux 20 LMH, cross-flow velocity 42 $cm.s^{-1}$.

Compared to the NaOH-cleaned membrane, the EDTA-cleaned membrane obtained a marginally lower sodium rejection (i.e. 5% lower) and a comparable boron rejection (Figure 22). This result is consistent with previous studies [140, 146] which found that EDTA cleaning in caustic conditions does not cause considerable impact on the separation efficiency of membranes. However, in contrast with SDS, the application of an acidic cleaning after EDTA cleaning recovered the rejection of sodium to the level of the NaOH-cleaned membrane (Figure 22). It is noteworthy that this sodium rejection was still lower than that by the virgin membrane. Consistent with the surface analysis results (i.e. charge and hydrophobicity), it appears that the adsorbed EDTA on the membrane surface has been removed by the

acidic cleaning and this process does not negatively affect the membrane polymer structure.

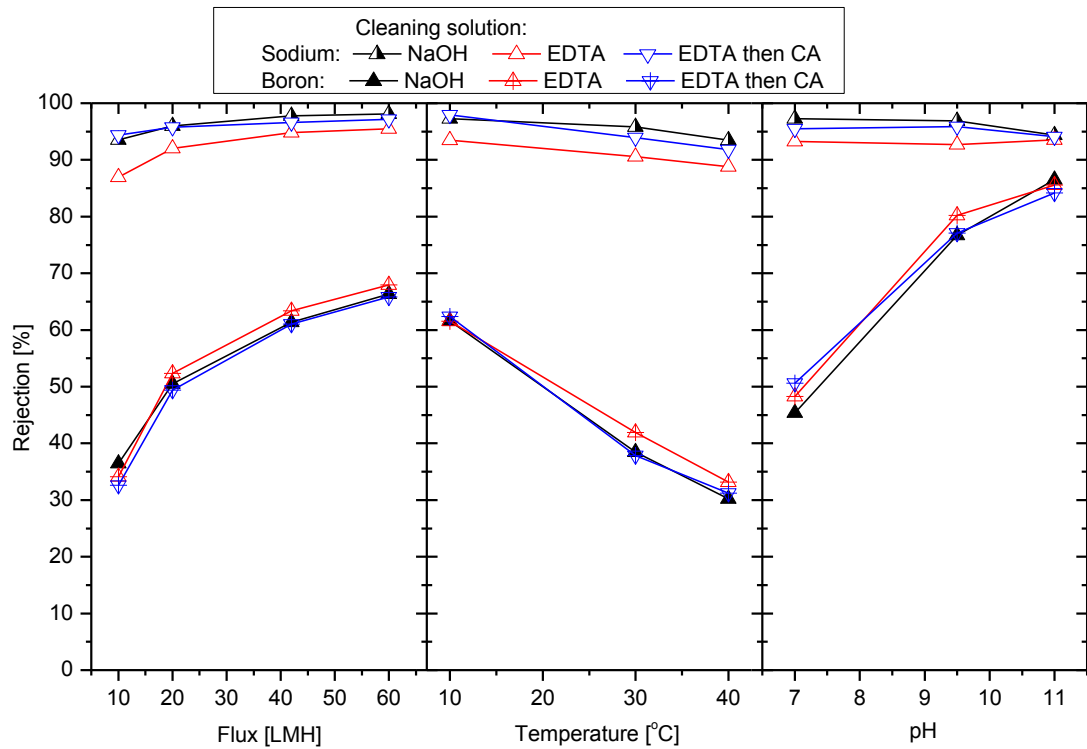


Figure 22. Changes in boron and sodium rejections by the ESPA2 membrane after membrane cleaning with EDTA solution (pH 11) and EDTA solution followed by citric acid solution (pH 3). Unless otherwise stated, the testing conditions are: pH 8, feedwater contains 0.43 mM B(OH)₃, 10 mM NaCl, 1 mM NaHCO₃, and 1 mM CaCl₂; temperature 20 °C, permeate flux 20 LMH, cross-flow velocity 42 cm.s⁻¹.

Impacts of the combined SDS and EDTA in a caustic solution on the membrane performance have not been reported in the literature, although this mixture was found to be more effective to mitigate membrane fouling than individually used [134]. In this study, the SDS+EDTA-cleaned membrane had approximately 8% lower boron rejection than the caustic-cleaned membrane (Figure 23), and consequently about 18% lower than that of the virgin membrane (Figure 20 and Figure 23). Sodium rejection appeared to be unaffected by the SDS+EDTA cleaning solution (Figure 23). This impact is different from that caused by separated SDS cleaning and EDTA cleaning, which implies that there probably are mutual interactions amongst SDS, EDTA, and the membrane surface when SDS and EDTA are used simultaneously.

Because boron rejection is mainly governed by the sieving effect, the decrease in boron rejection indicates an increase in the pore size of the SDS+EDTA-cleaned membrane. Nevertheless, this expansion of the membrane pores appears to be retreated when an acidic cleaning was subsequently applied, indicating through the recovery of boron rejection (Figure 23). However, the application of acidic cleaning could not recover the boron rejection by the SDS+EDTA-cleaned membrane back to level of the virgin membrane (Figure 20 and Figure 23).

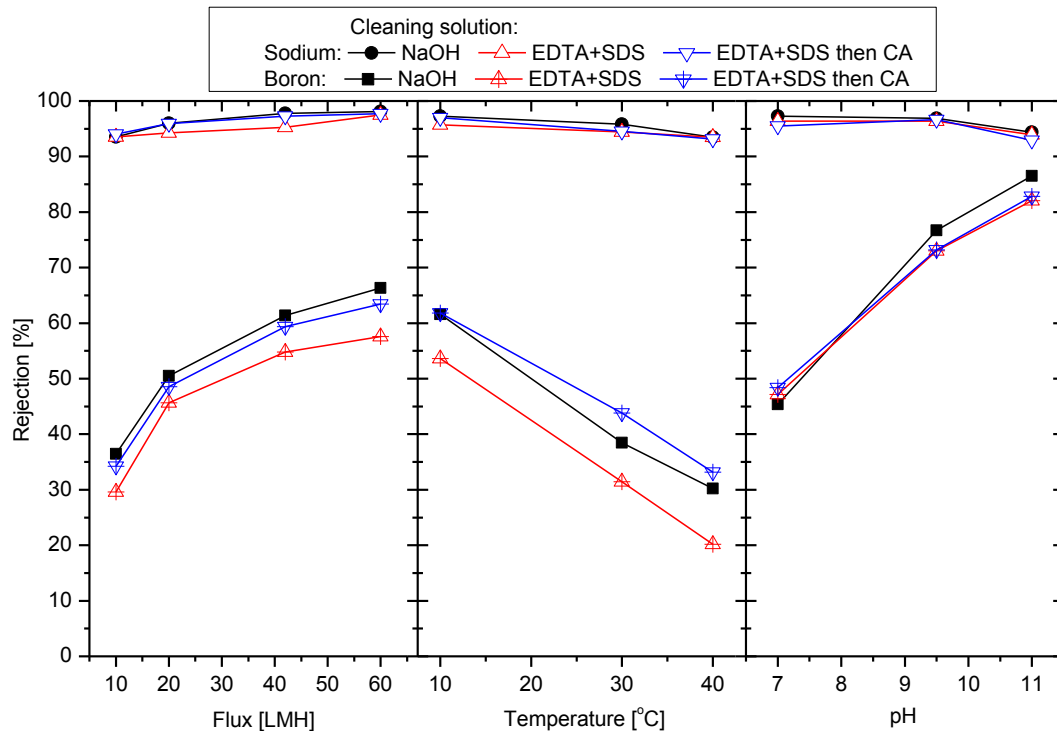


Figure 23. Changes in boron and sodium rejections by the ESPA2 membrane after membrane cleaning with EDTA+SDS solution (pH 11) and EDTA+SDS solution followed by citric acid solution (pH 3). Unless otherwise stated, the testing conditions are: pH 8, feedwater contains 0.43 mM B(OH)₃, 10 mM NaCl, 1 mM NaHCO₃, and 1 mM CaCl₂; temperature 20 °C, permeate flux 20 LMH, cross-flow velocity 42 cm.s⁻¹.

Boron rejection by the MC11-cleaned membrane was comparable to that of the caustic cleaned membrane (Figure 24), which was approximately 10% lower than boron rejection of the virgin membrane (Figure 20). A similar result was reported by Fujioka et al. [143] who found that the rejection of NDMA – a compound having similar molecular property to boron, would be decreased when the ESPA2 membrane

was cleaned by MC11. In good agreement with a previous study result [145], the rejection of sodium by the MC11-cleaned membrane was equivalent to that of the caustic-cleaned and also of the virgin ESPA2 (Figure 20 and Figure 24). The acidic cleaning following the MC11 cleaning did not cause any impacts on boron and sodium rejection, and thus a 10% lower boron rejection than the virgin membrane still remained (Figure 20 and Figure 24).

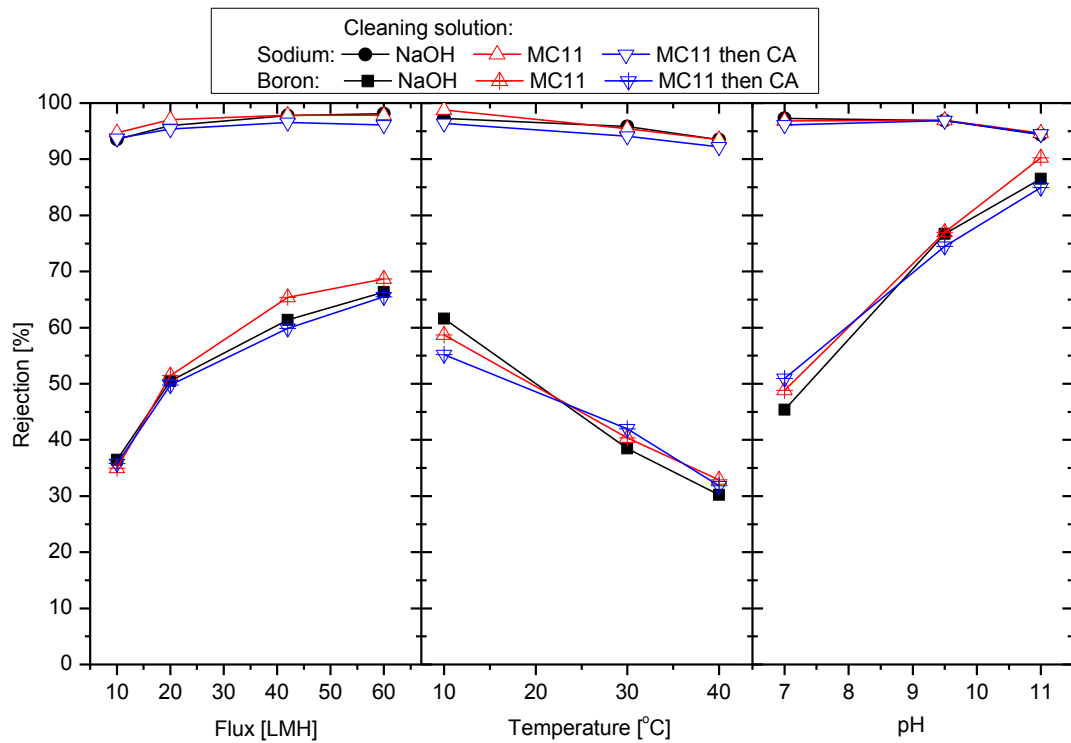


Figure 24. Changes in boron and sodium rejections by the ESPA2 membrane after membrane cleaning with MC11 solution (pH 11) and MC11 solution followed by citric acid solution (pH 3). Unless otherwise stated, the testing conditions are: pH 8, feedwater contains 0.43 mM B(OH)₃, 10 mM NaCl, 1 mM NaHCO₃, and 1 mM CaCl₂; temperature 20 °C, permeate flux 20 LMH, cross-flow velocity 42 cm.s⁻¹.

Interestingly, the MC3 appeared to be the only cleaning chemical tested in this study which could recover the decreased boron rejection caused by acidic/caustic solutions, thus preserved boron and sodium rejections of the cleaned membrane as high as that of the virgin membrane (less than 5% variation) (Figure 20 and Figure 25). In other studies, membrane cleaning using MC3 was found to cause discernable impacts on the rejections of organic compounds and inorganic salts [143, 145]. The application of a caustic cleaning after the MC3 cleaning did not cause any impacts on the

rejections (Figure 25) although this cleaning process causes major changes on the membrane water permeability (Figure 19).

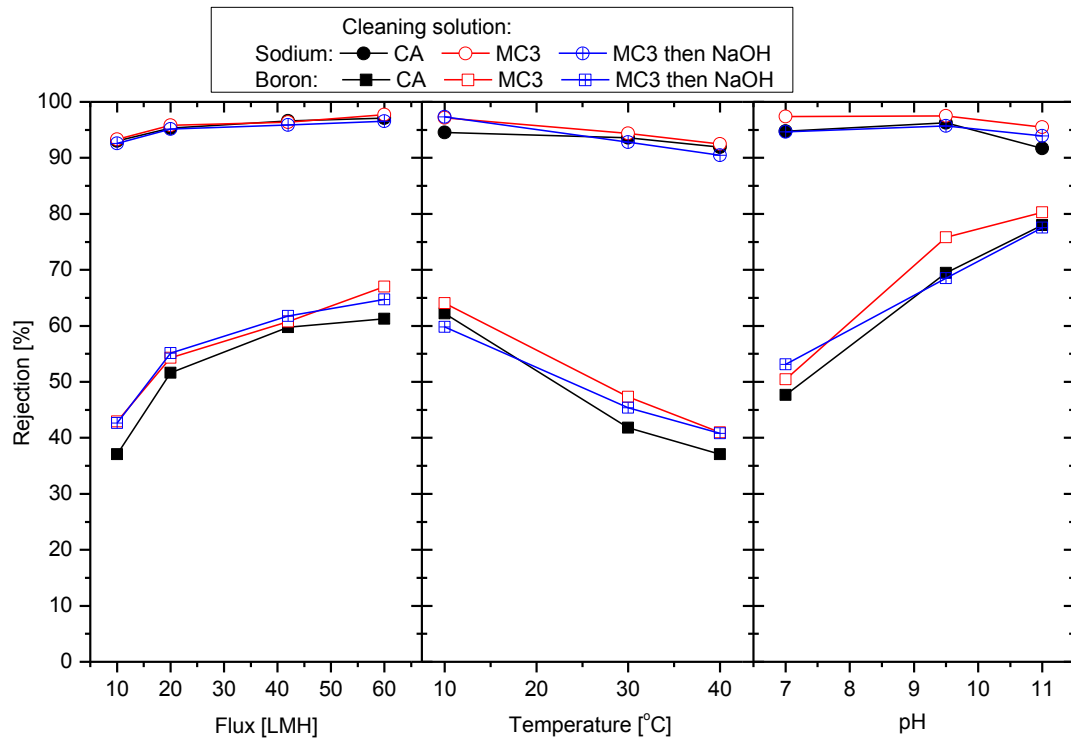


Figure 25. Changes in boron and sodium rejections by the ESPA2 membrane after membrane cleaning with MC3 solution (pH 3) and MC3 solution followed by sodium hydroxide solution (pH 11). Unless otherwise stated, the testing conditions are: pH 8, feedwater contains 0.43 mM $B(OH)_3$, 10 mM NaCl, 1 mM $NaHCO_3$, and 1 mM $CaCl_2$; temperature 20 °C, permeate flux 20 LMH, cross-flow velocity 42 $cm.s^{-1}$.

4.4 Conclusions

Membrane cleaning can substantially alter the hydrophobicity and water permeability of the RO membrane; however, its impacts on the rejections of boron and sodium are much less. This finding implies that water and solutes (boron and sodium) transport through RO membranes by different mechanisms. Different behaviours of boron rejection and sodium rejection were also observed in some cases (i.e. EDTA, SDS+EDTA, MC3), which underlined the difference between boron and sodium transport mechanisms through RO membranes. Although the presence of surfactant or chelating agent may cause some decreases in the rejections, solution pH was

found to be the key factor responsible for the loss of membrane separation and surface properties. Strong acidic or caustic cleaning, respectively, would decrease or increase the water permeability. However, the impacts of solution pH on the water permeability could be reversed by applying a subsequent cleaning with the opposite pH condition. On the other hand, the impacts of solution pH on boron and sodium rejections were irreversible in most cases. The results of this study imply that in order to minimise the impacts of chemical cleaning on the membrane performance, the cleaning solution either with or without the addition of surfactant and chelating agent should be used at less harsh pH conditions where possible. In addition, the strong impact of the cleaning solution on the water permeability suggests that a typical method to evaluate cleaning efficiency, which is based on the water permeability recovery, is of low reliability. A recovery in water permeability after membrane cleaning can be observed even when the fouling layer is not thoroughly removed, which may cause more severe fouling afterwards.

CHAPTER 5: EFFECTS OF MEMBRANE PRESERVATION ON BORON REJECTION

This chapter has been published as:

Tu, K.L., A.R. Chivas, and L.D. Nghiem, Effects of chemical preservation on flux and solute rejection by reverse osmosis membranes. *Journal of Membrane Science*, 2014. 472: 202-209.

5.1 Introduction

Despite the need to operate small-scale RO systems on an intermittent basis and to occasionally mothball large-scale RO plants, there has been very little research work on membrane preservation. The literature review undertaken as part of this study revealed that there has been only one report [209] on this topic in the peer reviewed literature. Thus, this study aims to investigate the impacts of chemical preservation of RO membranes on water permeability and solute rejection including boron and sodium. Three preservative chemicals, namely formaldehyde, SMBS, and DBNPA, were evaluated for membrane preservation at pH 3 and 7. Impacts of chemical preservation on the membrane performance were evaluated at various operating fluxes, temperatures and pH values. Changes in the membrane performance were thoroughly explained by changes in the membrane surface properties.

5.2 Materials and methods

5.2.1 Membranes and chemicals

The ESPA2 and SWC5 membranes were used in this study. Basic properties of the ESPA2 membrane have been given in Section 3.2.2. The SWC5 (Hydranautics) is a high-pressure seawater RO membrane.

Analytical grade SMBS (Chem-Supply, SA, Australia), formaldehyde (BDH Prolabo, VWR, QLD, Australia) and DBNPA (Sigma-Aldrich, MO, USA) were used as membrane preservative chemicals. Analytical grade NaCl, CaCl₂, NaHCO₃, and B(OH)₃ were used to prepare the feed solution. Suprapur nitric acid was used for sample dilution prior to analysis. Milli-Q water was used for the preparation of all stock and feed solutions.

5.2.2 Cross-flow membrane filtration system

This study used the RO filtration system which was described in detail in Section 3.2.3.

At the beginning of each experiment, the membrane sample was compacted by using Milli-Q water at 30 bar for 18 h. A stable flux was usually obtained within the first 10 h run. Following the membrane compaction, pure water permeability of the membrane was measured at 5, 10, 15, 20, 25, and 30 bar (at 20 °C). Electrolyte solution was then added to the feed reservoir making up a 10 L feedwater containing 10 mM NaCl, 1 mM CaCl₂, 1 mM NaHCO₃, and 0.43 mM B(OH)₃ (or 4.6 mg.L⁻¹ B). Boron and sodium rejections were obtained at permeate fluxes of 10, 20, 42, and 60 LMH, temperatures of 10, 20, 30, and 40 °C, cross-flow velocity of 42 cm.s⁻¹, and pH values of 7, 8, 9, and 11. The permeate flux and the cross-flow velocity were controlled by adjusting the bypass valve and the back-pressure regulator. The applied pressure was linearly proportional to permeate flux, reversely proportional to temperature and independent to the feedwater pH (Appendix, Figure A1). Unless otherwise stated, the standard testing condition is 20 LMH flux, 20 °C, pH 8, and 42 cm.s⁻¹ cross-flow velocity. The pH value was adjusted using either 1 M NaOH or 1 M HCl solution. In all experiments, once the target operational parameters had been obtained, the system was stabilised for 60 min before feed and permeate samples of 20 mL each were taken for analysis.

5.2.3 Membrane preservation protocol

A virgin membrane sample was first evaluated for pure water permeability and salt rejection. The sample was then removed from the membrane cell for preservation. Membrane preservation was simulated by submerging a membrane sample in the preservative solution in a 600 mL air-tight glass bottle for 14 days. SMBS and formaldehyde preservative solutions were prepared at a strength of 5% (wt/wt) in Milli-Q water and were adjusted to either pH 3 or 7. These conditions represent a chemical preservation period from 2 months to up to 2 years. DBNPA preservative solution was prepared at a strength of 1% (wt/wt) in Milli-Q water and was adjusted to pH 7. The bottle was completely filled with the preservative solution to eliminate any head space and was placed in the dark. The pH of the preserving solution was

monitored during the preservation period. At the end of the simulated preservation period, the preserved membrane samples were rinsed with copious amounts of Milli-Q water and then evaluated again for water permeability and salt rejection.

It is noted that the permeate flux of different elements of the same membrane name may vary up to 20% due to variation in the manufacturing process [210]. In fact, by testing seven 10 cm × 4 cm membrane samples, variations of 9% and 17% in water permeability of the ESPA2 and SWC5 membrane, respectively, were observed in this study. On the other hand, the mounting and dismounting of the membrane sample to the RO cell did not result in any discernible variation in permeate flux and salt rejection as can be seen from three repeated cycles of filtration after sample mounting and dismounting (Appendix, Figure A2). By using a single membrane sample for evaluating permeate flux and salt rejection before and after preservation, the impact of individual preservative chemicals on the membrane can be accurately examined. However, it is noteworthy that inconsistency among different membrane samples used for different preserving chemicals may still occur. In addition, this study used virgin membranes for the investigation. In practice, chemical preservation would be applied to used membranes, which have been exposed to various chemicals (e.g. cleaning and disinfection agents) and thus their surface properties and separation performance may differ from those under virgin condition [145, 211]. As such, changes in the performance of the used membrane due to preservation may be quantitatively different to this study. Similarly, the occurrence of foulants such as colloidal particles and organic matter on the membrane surface may also influence the impact of preserving chemicals.

5.2.4 Membrane characterisation methods

Membrane characterisation methods used in this study include streaming potential, hydrophobicity, and FTIR. Details of these methods have been given in Section 4.2.4.

5.2.5 Analytical methods

The concentrations of boron and sodium were analysed using an ICP-MS system. The method has been thoroughly described in Section 3.2.5. Conductivity and pH

were measured using an Orion 4-Star Plus pH/conductivity meter. Redox potential was measured by an ORP meter model TPS WP-80D (Thermo Fisher Scientific).

The rejections of boron and sodium were calculated using the Eq.25.

Changes in membrane performance (rejection or flux) were calculated using the Eq.26. Where X_{ir} and X_{vir} are the performances (rejection or flux) of the preserved membrane and the virgin membrane, respectively.

5.3 Result and discussion

5.3.1 Charge density

As the solution pH increases from 3 to 11, the membrane surface charge changed from slightly positive to negative (Figure 26). This is a well-known phenomenon and is attributed to the deprotonation of the carboxylic and amine groups in polyamide active layer at increasing pH [170]. Furthermore, results reported here also show that the membrane surface charge can be significantly altered after chemical preservation (Figure 26). Changes in the membrane surface charge appeared to be driven by both the solution pH and the preserving chemicals. After being exposed to a pH 7 solution (without any preservative chemicals) for 14 days, the zeta potential profiles of both the ESPA2 and SWC5 were identical to those under the virgin condition. In contrast, before and after 14 days of exposure to a pH 3 solution (without any preservative chemicals), when measured at pH 8, the zeta potentials of the ESPA2 and SWC5 changed from -45 to -23 mV and -50 to -14 mV, respectively. Changes in the membrane surface charge after exposure to the preservative chemicals used in this study could also be observed. In general, the membrane became less negatively charged in comparison to the virgin condition. However, there seems to be a combined effect of the solution pH and preservative chemical on the membrane surface charge. After 14 days of exposure to a pH 3 solution that did not contain any preservative chemicals, the most significant decrease in the membrane negative surface charge (when measured at pH 7-8) could be observed with both the ESPA2 and SWC5. On the other hand, both the ESPA2 and SWC5 were less negatively charged after 14 days of exposure to preservative solution (which was maintained at pH 7). Changes in the membrane surface charge due to chemical preservation

reported here may influence the rejection of ionic (or charged) solutes. More importantly, these changes imply that there could be chemical and/or physical transformation of the membrane active skin layer in response to chemical preservation. Changes in the membrane charged profile may indicate an absorption of free ions on the membrane surface [170], or even a cleavage of functional groups within the membrane structure such as carboxylic and amine groups [212]. The charge profile of the SWC5 membrane appeared to be more affected by the chemical preservation than that of the ESPA2 membrane, probably because the SWC5 has a greater charge density (Figure 26) which encourages the absorption of counter-ions on the membrane surface. It is noteworthy that the measured zeta potential values could be affected by the membrane surface roughness, in which lower zeta potential values would be obtained as the surface roughness increased [213].

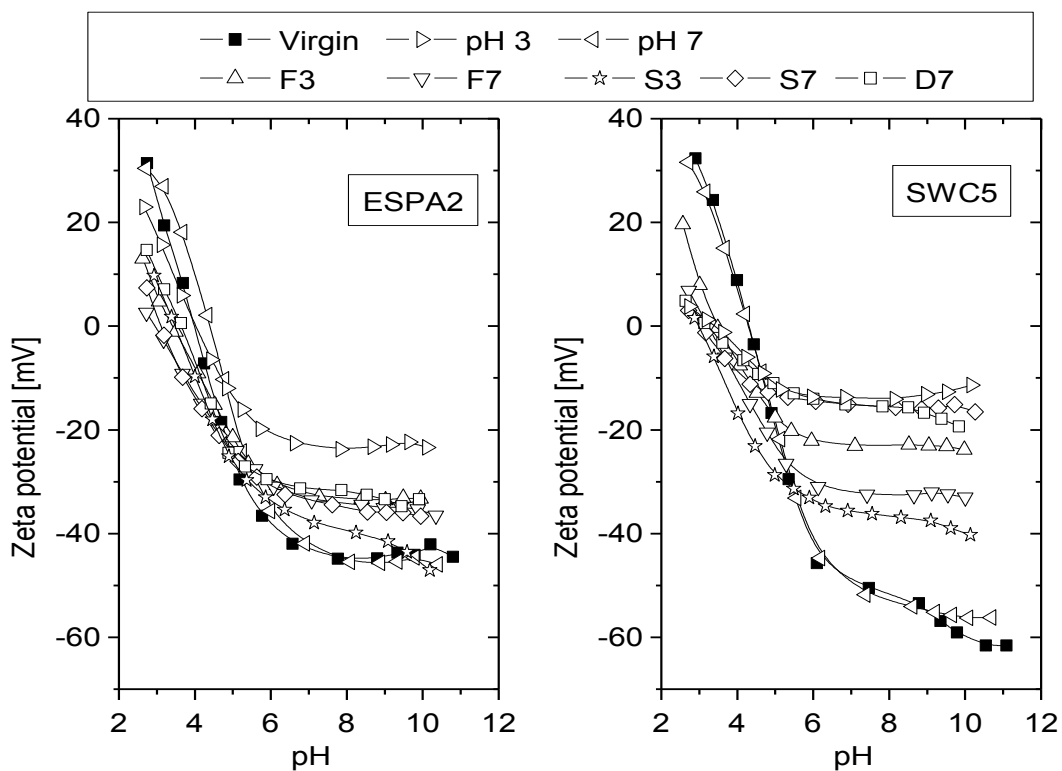


Figure 26. Zeta potential of virgin and preserved ESPA2 and SWC5 membranes. Measurements conducted at room temperature (ca. 25 °C) in a 1 mM KCl solution. Abbreviations: S7 for SMBS at pH 7, S3 for SMBS at pH 3, F7 for formaldehyde at pH 7, F3 for formaldehyde at pH 3, D7 for DBNPA at pH 7.

5.3.2 Hydrophobicity

The contact angles of the virgin ESPA2 and SWC5 membranes were 55° and 50°, respectively. In all cases, the membrane contact angle decreased and the membrane became less hydrophobic after chemical preservation. The decrease in the membrane hydrophobicity was more severe when the preservative chemical solution was maintained at pH 3 compared to pH 7. In addition, the effect of chemical preservation on the membrane surface hydrophobicity decreased in the order formaldehyde, SMBS, and DBNPA. These observations were consistent for both the ESPA2 and SWC5 membranes (Figure 27). The large standard deviations in the contact angle of the SWC5 membrane indicate that this membrane surface is less homogeneous than the ESPA2. Changes in the membrane hydrophobicity indicate modifications in the membrane surface chemistry or conformation [176]. The decrease in hydrophobicity observed here can be attributed to the dissociation of

carboxyl and amine groups which produced hydrophilic $[\text{COO}^-]$ and $[-\text{NH}_2]$ groups or adsorption of preservative chemicals to the membrane surface. The decrease in hydrophobicity of preserved membranes may result in an increase in the water permeability [204] and a decrease in the fouling propensity of the membrane [174]. In addition, Bernstein et al. [206] reported that a decrease in hydrophobicity would lead to a decrease in boron rejection, although the reason for such observation was not provided.

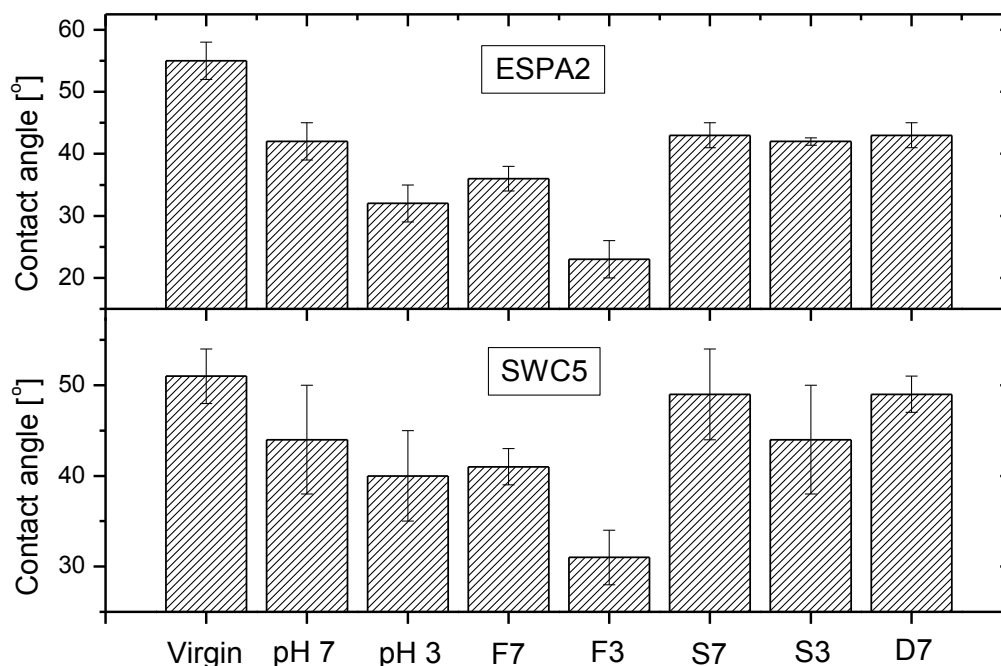


Figure 27. Contact angle values of virgin and preserved ESPA2 and SWC5 membranes. Measurements conducted at room temperature (approximately 25 °C), Milli-Q water used as reference solvent. The error bars show the standard deviation of five replicate measurements. Abbreviations: S7 for SMBS at pH 7, S3 for SMBS at pH 3, F7 for formaldehyde at pH 7, F3 for formaldehyde at pH 3, D7 for DBNPA at pH 7.

5.3.3 Chemical composition

The impact of chemical preservation on chemical composition of the membrane surface was qualitatively examined by FTIR analysis (Figure 28). In the wavenumber region of $1800\text{-}600\text{ cm}^{-1}$, both the polyamide active layer and the polysulfone support layer are sampled due to the penetration depth ($> 300\text{ nm}$) of this technique

compared to the thickness of the membrane active layer [182]. According to Tang et al. [182], polyamide functional groups are represented at wavenumbers 1663, 1609, and 1541 cm^{-1} , and polysulfone groups are represented at 1587, 1504, 1488, 1365, 1350-1280, 1245, 1180-1145, and 830 cm^{-1} . These peaks are clearly observed on Figure 3. The FTIR spectra of the ESPA2 and SWC5 membranes are generally identical, except the appearance of a peak at 1700 cm^{-1} on the SWC5 which can be assigned to the stretching of C=O bonding within either the carbonyl or carboxylic acid groups [214]. It is interesting that this peak lost its intensity as the SWC5 membrane is preserved in formaldehyde pH 7 and SMBS pH 7. The polyamide-represented peaks of the ESPA2 membrane seem not to be affected by the preservative chemicals, however, for the SWC5, some changes are clearly observed at the region 1560-1541 cm^{-1} (Figure 28). The spectra of the SWC5 samples preserved in formaldehyde pH 3, SMBS pH 3 and DBNPA pH 7 show an additional peak at 1560 cm^{-1} which is not seen at the virgin SWC5 and those preserved in formaldehyde pH 7 and SMBS pH 7 (Figure 28). The presence of this peak (1560 cm^{-1}) is hardly reported in the literature, and was assigned to the amorphous phase of an unassociated amide [215]. There seems to be a hydrolysis of the amide groups in the membrane active layer under the effects of formaldehyde pH 3, SMBS pH 3 and DBNPA pH 7 solutions. For both virgin and preserved ESPA2 and SWC5 membranes, peaks assigned to polysulfone groups were not affected by preserving chemicals (Figure 28).

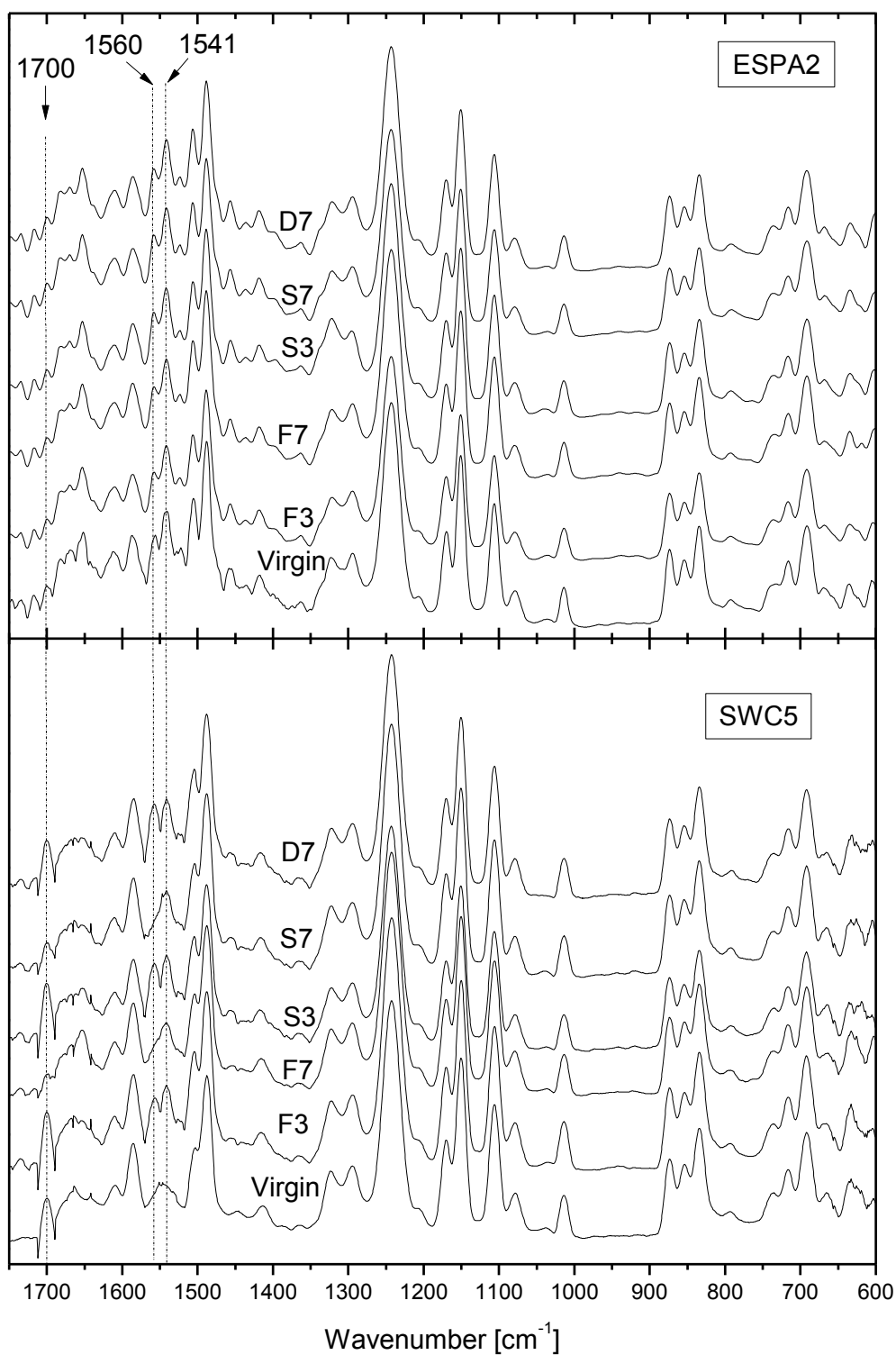


Figure 28. FTIR absorption spectra of virgin and preserved ESPA2 and SWC5 membranes obtained at 2 cm⁻¹ resolution. Abbreviation: F3 for formaldehyde at pH 3, F7 for formaldehyde at pH 7, S3 for SMBS at pH 3, S7 for SMBS at pH 7, D7 for DBNPA at pH 7.

5.3.4 The rejection of boron and sodium by virgin RO membranes

The rejections of boron, sodium, and conductivity by the ESPA2 and SWC5 membranes were determined as a function of permeate flux, temperature, and solution pH to establish the referencing baseline for subsequent evaluation of the impact of chemical preservation. As expected, sodium and conductivity rejections by the ESPA2 and SWC5 were high (Figure 29). As a result, the effects of these operating conditions on sodium and conductivity rejection were negligible (Figure 29). In good agreement with the literature [73, 79], boron rejection was strongly affected by flux, temperature and feed solution pH. The increase in permeate flux from 10 to 60 LMH led to an increase in boron rejection by the ESPA2 membrane from 30 to 72% (Figure 29). Likewise, the increase in water temperature from 10 to 40 °C resulted in a decrease in boron rejection by the ESPA2 membrane from 67 to 17%. Similar results were observed with the SWC5 membrane, although the changes in boron rejection were considerably smaller compared to the ESPA2. Boron rejections were comparable at pH 7 and 8, rapidly increased at pH > 8 and approached sodium rejection at pH 11.

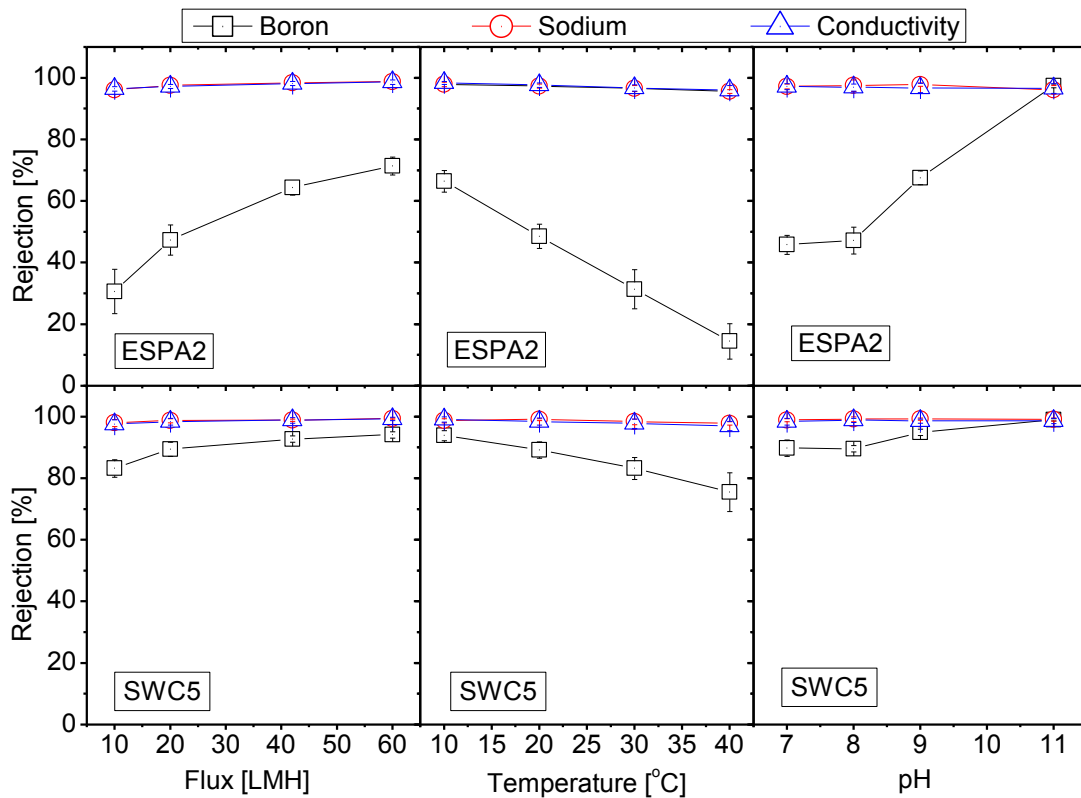


Figure 29. The rejection of boron, sodium and conductivity by the virgin ESPA2 and SWC5 membranes at various operating conditions. Unless otherwise stated, the testing conditions are: pH 8, feedwater contains 0.43 mM B(OH)₃, 10 mM NaCl, 1 mM NaHCO₃, and 1 mM CaCl₂; temperature 20 °C, permeate flux 20 LMH, cross-flow velocity 42 cm.s⁻¹. The error bars indicate the standard deviation of seven replicate experiments.

The effects of flux, temperature and pH on boron and sodium rejection have been previously discussed in the literature. According to the irreversible thermodynamic model, as the permeate flux increases, convective transport of water through the membrane increases while diffusive transport of boron remains constant, resulting in a lower boron concentration in the permeate or a higher boron rejection [123]. The effect of temperature on boron rejection could be attributed to the expansion of the membrane structure and the increase in boron permeability as the solution temperature increases [208]. Boron rejection is governed by steric hindrance mechanism at pH < 9.2 (pK_a of boric acid), and by both steric hindrance and charged repulsion at pH > 9.2 [86]. The speciation transformation from B(OH)₃ to B(OH)₄⁻ throughout this pH value explains the increase in boron rejection as the pH increased.

On the other hand, being a hydrated and charged species at all pH values, sodium ion can be efficiently removed by RO membrane regardless of operating condition changes [86]. It is therefore suggested that to maintain the rejection efficiency of the membrane, a proper preservation condition should not cause the risk of membrane swelling and not decrease the surface charged density of the membrane. The former would sustain the efficiency of the size-exclusion mechanism, and the latter facilitates the charged repulsion rejection mechanism.

5.3.5 Changes in the membrane performance

As can be seen in Figure 30, small variations in water permeability as well as boron and sodium rejection were observed with the blank experiment (in which the membrane was submerged in pH 7 solution without any preservative chemicals for 14 days). These variations can be used as the baseline for assessing the impact of chemical preservation on water permeability and separation efficiency.

The impacts of chemical preservation on water permeability and separation efficiency of both ESPA2 and SWC5 are dependent on the solution pH and the preservative itself. At pH 7, chemical preservation using DBNPA led to a severe impact on the membrane separation efficiency. On the other hand, the impacts caused by formaldehyde and SMBS solution at pH 7 on the rejection of boron and sodium was small and was comparable to that of the blank experiment (Figure 30). When the pH of the SMBS and formaldehyde solutions was reduced to 3, the impacts of chemical preservation on both boron and sodium rejections were significant. For the SWC5 membrane, the decrease in rejections of the samples preserved in formaldehyde pH 3, SMBS pH 3 and DBNPA pH 7 solutions is consistent with the hydrolysis of these membrane surfaces as observed for the FTIR spectra (Figure 28). Nevertheless, for the ESPA2, the loss of performance is not reflected for the FTIR data. It is noteworthy that while the rejection of sodium was less sensitive to the variation in operating conditions than that of boron (Section 5.3.4), both sodium and boron rejections were strongly impacted by chemical preservation. In addition, the impact of chemical preservation on boron and sodium rejections was more significant than that on the membrane water permeability.

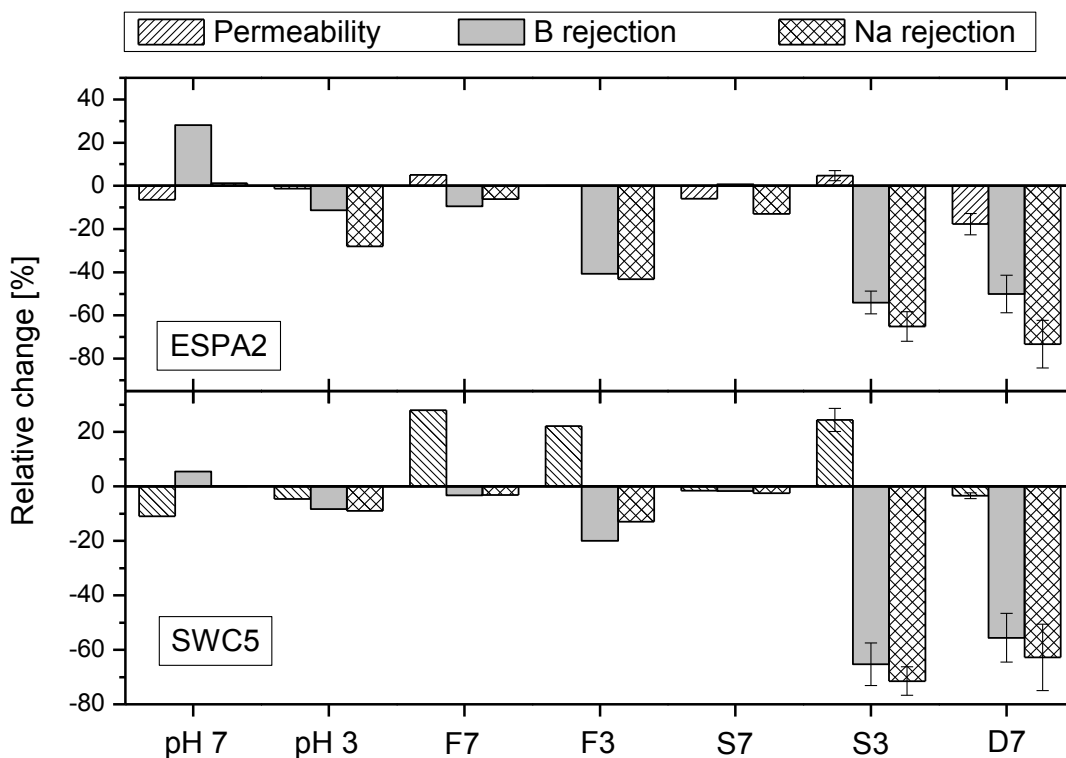


Figure 30. Relative change in pure-water permeability and rejection of boron and sodium by ESPA2 and SWC5 membranes after exposure to preservatives. Standard test conditions: pH 8, feedwater contains 0.43 mM B(OH)₃, 10 mM NaCl, 1 mM NaHCO₃, and 1 mM CaCl₂; temperature 20 °C, permeate flux 20 LMH, cross-flow velocity 42 cm.s⁻¹. The error bars show the standard deviation of two replicate experiments. Abbreviations: S7 for SMBS at pH 7, S3 for SMBS at pH 3, F7 for formaldehyde at pH 7, F3 for formaldehyde at pH 3, D7 for DBNPA at pH 7.

For virgin RO membranes, water permeability is inversely proportional to boron rejection and vice versa [206, 216]. This phenomenon could be observed with the ESPA2 and SWC5 membranes preserved in formaldehyde solution at pH 3 and 7 and in SMBS solution at pH 3 (Figure 30). Similar results were reported when nanofiltration and RO membranes were exposed to either cleaning or disinfecting agents [140, 211]. The phenomenon was attributed to the cleavage of polyamide bonding which increased the nominal membrane pore size and so encouraged both water and solute molecules passing through the membrane. In contrast, the DBNPA preservative solution caused a decrease in both water permeability and solute rejection at the same time (Figure 30). The concurrent loss of water permeability and

solute rejection was reported elsewhere in the literature [152], and was attributed to the transformation from crystalline regions to an amorphous state. Kang et al. [152] suggested that this transformation led to a cleavage of the polyamide structure which decreased solute rejection, meanwhile created a “soft barrier layer” which was compacted under operating pressure and consequently resulted in a flux decline. This explanation is supported by the FTIR data in Figure 3 which indicate a hydrolysis of the SWC5 membrane polymeric structure under the effect of DBNPA solution.

It is interesting to note that although the ESPA2 and SWC5 membranes were affected at similar magnitude regarding boron and sodium rejections, the water permeability of the SWC5 was more severely impacted than that of the ESPA2. For instance, when preserved in formaldehyde solutions at pH 7 and pH 3 and SMBS solution at pH 3, water permeability of the SWC5 membrane increased more than 20%, whereas only less than 10% permeability increase was observed for the ESPA2 membrane (Figure 30). This may probably be attributed to the lower contact angle (more hydrophilic) of the preserved SWC5 membranes than that of the ESPA2 membrane as seen in Figure 27.

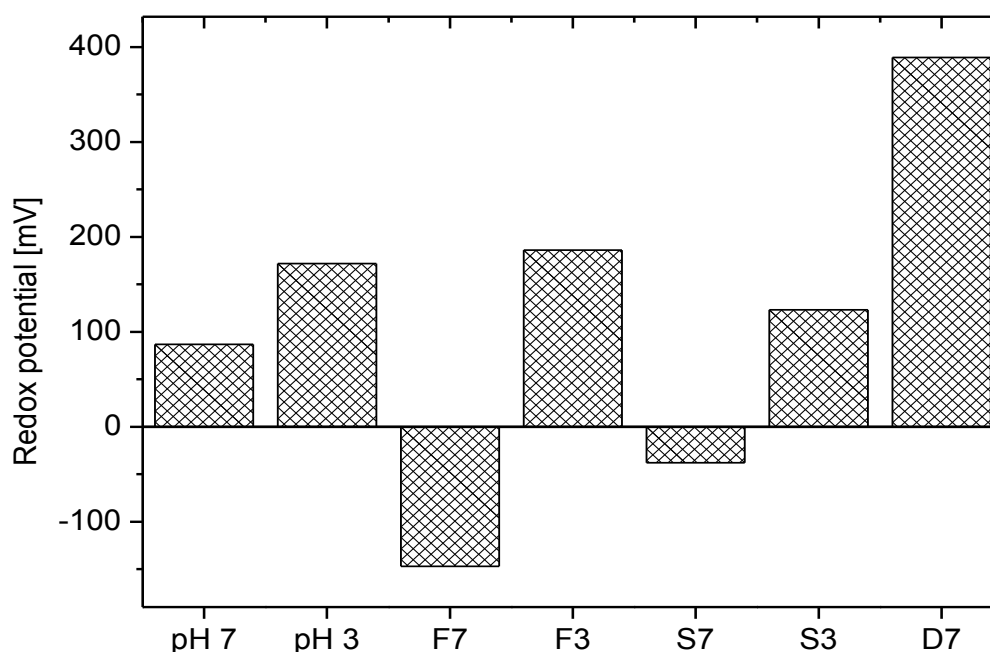


Figure 31. Redox potential of the preserving solutions. Abbreviations: S7 for SMBS at pH 7, S3 for SMBS at pH 3, F7 for formaldehyde at pH 7, F3 for formaldehyde at pH 3, D7 for DBNPA at pH 7.

Of particular note, the impacts of chemical preservation on membrane performance appear to be associated with the redox potential of the preservative solution. The redox potential of the preservative solutions is pH dependent (Figure 31). In general, the redox potential decreases as the solution pH increases. At pH 3, the redox potentials of the formaldehyde and SMBS solutions were 186 and 123 mV, respectively. At pH 7, the redox potentials of these solutions were -147 and -38 mV, respectively. On the other hand, the DBNPA solution had a high redox potential of 389 mV at pH 7. Results reported here are consistent with previous studies [217, 218] in which an increase in pH was shown to result in a decrease in the solution redox potential. The strong oxidation potentials of the formaldehyde pH 3, SMBS pH 3 and DBNPA pH 7 solutions also explain the hydrolysis of the SWC5 samples preserved in these solutions. Results from Figure 30 and Figure 31 suggest that a reducing condition is necessary to minimise the impacts of chemical preservation on membrane performance. There are currently no specifications about the redox potential of the preservative solution. In addition, it is advisable that the pH of SMBS and formaldehyde solutions be maintained at near-neutral rather than the recommended pH value of above 3 currently specified by membrane manufacturers.

The effects of membrane preservation on boron rejection efficiency were further investigated at different operating conditions (Figure 32 and Figure 33). Boron rejection was selected because it could be strongly affected by operating condition changes (Figure 29). Similar to the results obtained at standard testing fluxes, temperatures, and pH values (Figure 30), the results obtained at other testing conditions show that preservation in the SMBS solution and formaldehyde solution at pH 3 and DBNPA solution at pH 7 caused the most profound effect on the boron rejection (Figure 32 and Figure 33). This result confirms that the membrane polymeric structure was modified by the preservative chemicals and that this impact is irreversible. At various fluxes, pH values, and temperatures, comparable changes in boron rejection were observed as consequences of membrane preservation. As a result, boron rejection by the preserved ESPA2 and SWC5 membranes responded to changes in operating conditions in a similar manner to that obtained by the virgin membranes. This result implies that boron rejection by the preserved and virgin membranes is governed by the same mechanisms which have been elucidated in

Section 5.3.4. The membranes obtained lower boron rejections because its pores became more open as an impact of the preservative chemicals.

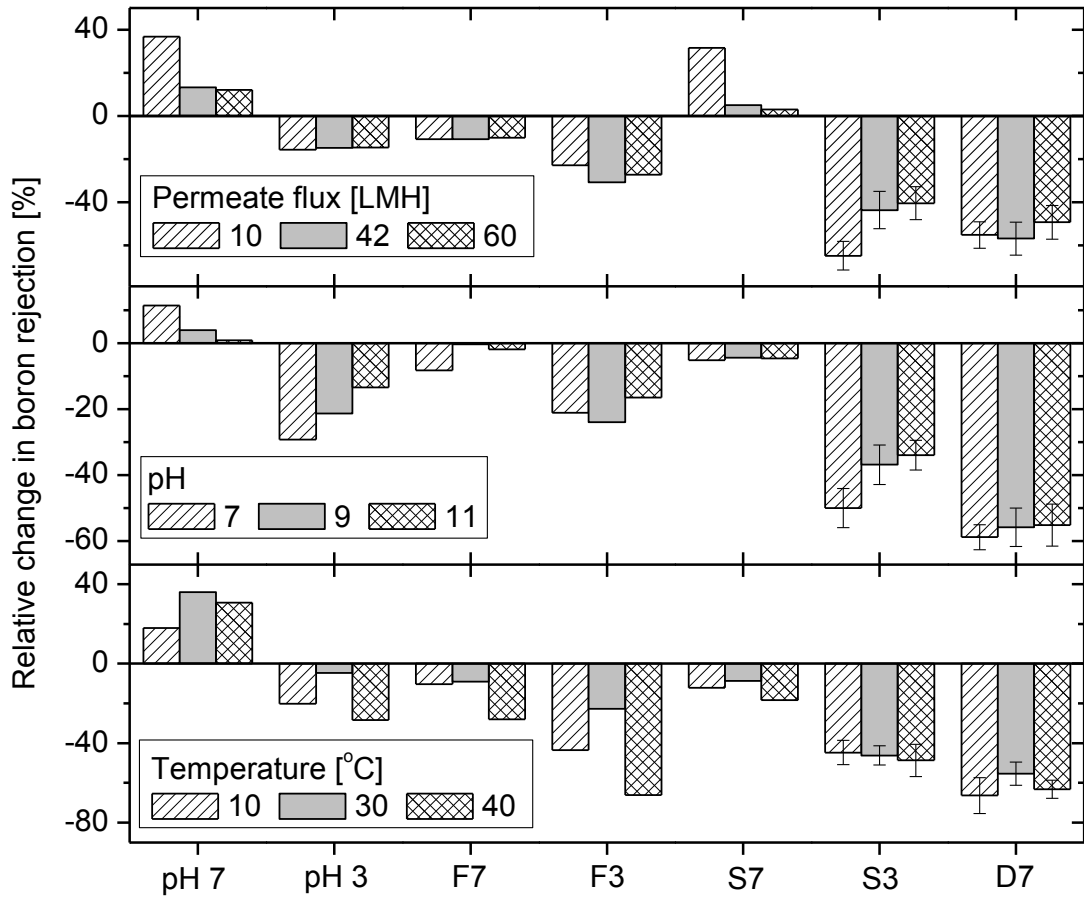


Figure 32. Relative change in boron rejection by the ESPA2 membrane at different testing fluxes, temperatures, and pH values. Standard test conditions: pH 8, feedwater contains 0.43 mM $B(OH)_3$, 10 mM NaCl, 1 mM $NaHCO_3$, and 1 mM $CaCl_2$; temperature 20 °C, permeate flux 20 LMH, cross-flow velocity 42 $cm.s^{-1}$. Abbreviations: S7 for SMBS at pH 7, S3 for SMBS at pH 3, F7 for formaldehyde at pH 7, F3 for formaldehyde at pH 3, D7 for DBNPA at pH 7.

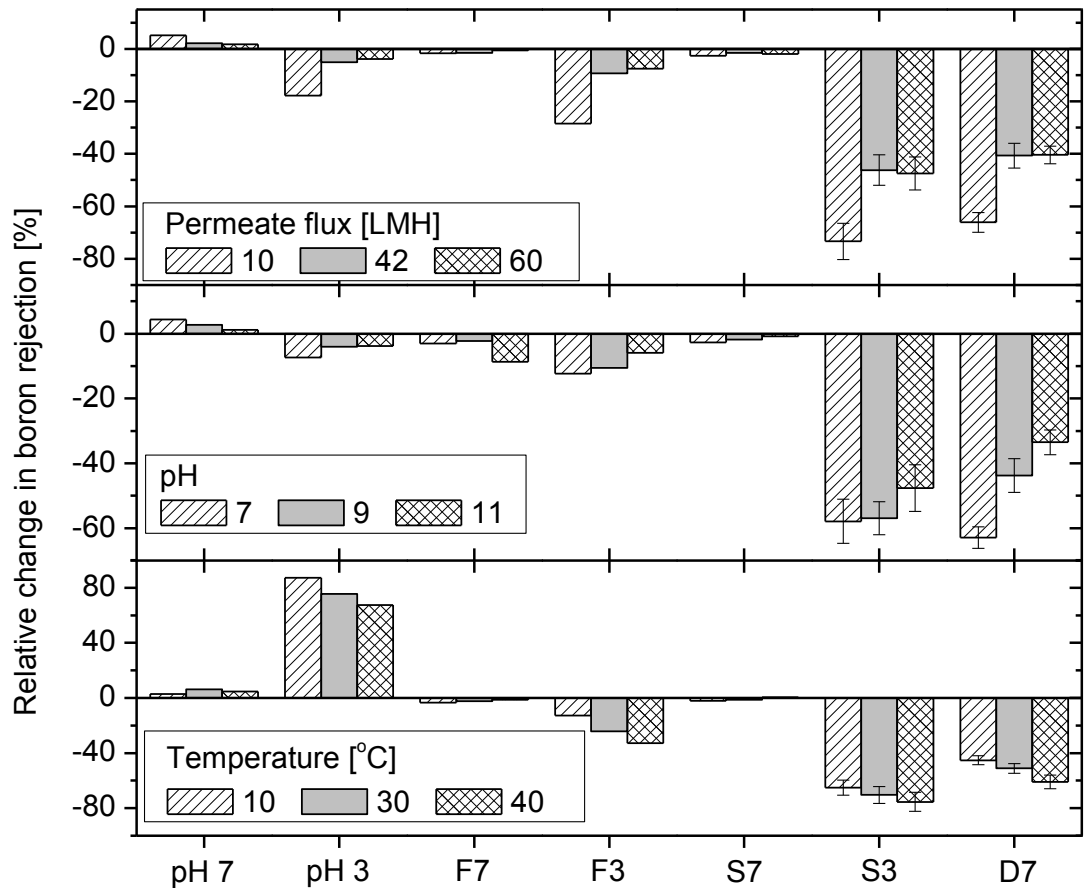


Figure 33. Relative change in boron rejection by the SWC5 membrane at different testing fluxes, temperatures, and pH values. Standard test conditions: pH 8, feedwater contains 0.43 mM $B(OH)_3$, 10 mM NaCl, 1 mM $NaHCO_3$, and 1 mM $CaCl_2$; temperature 20 °C, permeate flux 20 LMH, cross-flow velocity 42 $cm.s^{-1}$. Abbreviations: S7 for SMBS at pH 7, S3 for SMBS at pH 3, F7 for formaldehyde at pH 7, F3 for formaldehyde at pH 3, D7 for DBNPA at pH 7.

5.4 Conclusion

Results reported here show that chemical preservation of polyamide RO membranes may alter the membrane surface properties (i.e., surface charge and hydrophobicity) and subsequently result in negative impacts on both water permeability and solute rejection. Moreover, the effect of chemical preservation on boron and sodium rejections is comparable and more significant than the impact on the membrane water permeability. The impact of chemical preservation on the membrane performance is dependent on the solution pH and the preservative itself. The results

demonstrate that the undesirable impacts of chemical preservation can be minimised by appropriate selection of the preservatives and by preserving the membrane in a reducing condition. Our results suggest that formaldehyde and sodium metabisulfite may be used as preservative chemicals; however, it is necessary to maintain the preservative solution at near-neutral pH.

CHAPTER 6: BORON AS A SURROGATE FOR NDMA REJECTION

This chapter has been published as:

Tu, K.L., T. Fujioka, S.J. Khan, Y. Poussade, A. Roux, J.E. Drewes, A.R. Chivas, and L.D. Nghiem, Boron as a surrogate for N-nitrosodimethylamine rejection by reverse osmosis membranes in potable water reuse applications. *Environmental Science & Technology*, 2013. 47: 6425-6430.

6.1 Introduction

In wastewater reclamation scheme, there exist several pollutants of concern beside boron. Among them, NDMA attracts significant attention not only because of its carcinogenic property but also because it is difficult to be removed by commercial RO membranes. NDMA is poorly rejected by RO membranes because it has a small and neutral charge molecular, similar to boric acid. Nevertheless, the monitoring of NDMA in wastewater treatment plants is a major challenge because reliable chemical analysis technique for NDMA requires sophisticated instruments and expert labour. Furthermore, a commercial package for simulating NDMA rejection by RO membranes is not yet available.

On the other hand, boron concentration in aqueous solutions can be readily measured using a range of conventional analytical techniques including ion chromatography [128, 219] or online probes [220]. In addition, boron rejection can also be modelled and simulated using currently available commercial software packages (e.g. ROSA, TorayDS/DS2, and IMSDesign provided by Dow FilmTec, Toray, and Hydranautics, respectively).

Given the co-occurrence of NDMA and boron in wastewater effluents and the similarities between NDMA and boric acid molecules, the aim of this study was to demonstrate the prospect of using boron as a viable surrogate for NDMA rejection by RO membranes. Boron rejections by six different RO membranes were correlated to those of NDMA under similar operating conditions. The impact of permeate flux and temperature on the rejection of both boron and NDMA was also evaluated.

6.2 Materials and methods

6.2.1 Chemicals and reagents

Stock solution of 10 mg.L⁻¹ of NDMA (Sigma–Aldrich, St Louis, MO, USA) was prepared in pure methanol, in the dark at -18 °C, and was used within one month. B(OH)₃, NaCl, CaCl₂, NaHCO₃, NaOH, and HCl were used for preparing the feed solution. Suprapur nitric acid was used for sample dilution prior to ICP-MS analysis. Milli-Q water was used for the preparation of stock and feed solutions. All chemicals used are analytical grade. Tertiary treated effluent was collected from a water reclamation plant in New South Wales, Australia which was comprised of primary screening followed by an activated sludge treatment process and microfiltration. The tertiary treated effluent sample was collected after microfiltration. The effluent had a boron concentration of 0.1 mg.L⁻¹, conductivity of 720 μS.cm⁻¹ and a pH of 7.1. The detailed characteristics of this tertiary treated effluent have been reported elsewhere [221].

6.2.2 Membranes

Six RO membranes were used in this study, including BW30 (Dow FilmTec, Minneapolis, MN, USA), ESPA1, ESPA2, ESPAB, SWC5 (Hydranautics, Oceanside, CA, USA), and TFC-HR (Koch Membrane Systems, San Diego, CA, USA) membranes. The SWC5 is a high-pressure seawater RO membrane and the others are low-pressure RO membranes commonly used for water reuse applications. These are thin-film composite membranes consisting of an ultra-thin polyamide (or polyamide derivative) skin layer on top of a micro-porous support layer. Key properties of these membranes are summarised in Table 8.

Table 8. Water permeability and salt rejection of the selected RO membranes

Membrane	Water permeability ^a [L.m ⁻² .h ⁻¹ .bar ⁻¹]	TDS rejection ^b [%]	Na rejection ^b [%]
SWC5	2.63	99.2	99.3
TFC-HR	3.12	98.8	99.2
BW30	3.88	92.8	93.3
ESPAB	4.55	98.4	98.5
ESPA2	6.15	95.8	96.1
ESPA1	7.80	95.5	95.8

^a Measured with Milli-Q water at 1,000 kPa and 20 °C.

^b Measured at 20 LMH permeate flux, 20 mmol.L⁻¹ NaCl and pH 8.

6.2.3 NF/RO filtration system and experimental protocol

This study used the RO filtration system which was described in detail in Section 3.2.3.

Prior to each experiment, the membrane sample was rinsed with Milli-Q water to remove any preservative chemicals. Membrane compaction was then conducted using Milli-Q water at 1,800 kPa for at least 1 h until a stable permeate flux had been achieved. Following the membrane compaction, the pressure was reduced to 1,000 kPa for the pure water permeability measurement. The Milli-Q water was then replaced by a 10 L standard feed solution containing 250 ng.L⁻¹ NDMA, 5.75 mg.L⁻¹ B(OH)₃ (1 mg.L⁻¹ B), 20 mmol.L⁻¹ NaCl, 1 mmol.L⁻¹ CaCl₂, and 1 mmol.L⁻¹ NaHCO₃. The NDMA and boron concentrations were chosen to represent concentrations previously observed in secondary treated effluent. The pH of the feed solution was adjusted and kept constant at pH 8 by adding a small volume of either 1 mol.L⁻¹ NaOH or 1 mol.L⁻¹ HCl solution. When tertiary treated effluent was used as the feed, an appropriate volume of NDMA stock solution was used to obtain of concentration of 250 ng.L⁻¹ NDMA in the feed; no further chemical addition or pH adjustment were required. The operational parameters were set at 20 LMH permeate flux, 20 °C temperature, and 42 cm.s⁻¹ cross-flow velocity unless otherwise stated. These parameters are similar to those commonly used in full-scale RO installations

for wastewater reclamation [186]. Permeate and retentate were circulated back to the feed reservoir to maintain the same feed solution composition throughout the experiment. Experiments with variable permeate flux were conducted by first adjusting the permeate flux to 60 LMH followed by a stepwise reduction in 5 LMH increments. For experiments with variable temperature, the feed temperature was incrementally increased from 10 to 40 °C. The permeate flux and feed solution temperature were selected for further examination since these two parameters are known to have strong effects on the rejection of boric acid and NDMA [15, 186]. In all experiments, once the target operational parameters were achieved, the filtration system was operated at steady state for 1 h prior to the collection of feed and permeate samples for analysis. At each sampling event, 200 mL of feed and permeate samples were collected simultaneously. Isotope standard (50 ng) of NDMA was added to the samples and solid phase extraction (SPE) was conducted immediately.

6.2.4 Chemical analytical methods

The concentration of NDMA was determined using an Agilent 7890A gas chromatograph (GC) coupled with an Agilent 7000B triple quadrupole mass spectrometer (MS/MS) (Agilent Technologies, Wilmington, DE, USA). The obtained limit of quantification of NDMA by this analytical method is 0.45 ng.L⁻¹ in ultrapure water [222]. Details of the SPE procedure and validation of the methods in different matrix solutions are available elsewhere [222]. The concentrations of boron and sodium were analysed using an Agilent 7500cs ICP-MS. The details of this analytical method have been described in Section 3.2.5. Conductivity and pH were measured using an Orion 4-Star Plus pH/conductivity meter.

6.3 Result and discussion

6.3.1 Correlation between boron and NDMA rejection by RO membranes

The RO membranes used in this study were systematically selected to span a wide range of permeability (Table 8). As a result, the rejection values of boron also covered a large range from approximately 10% (by the ESPA1 membrane which has the highest water permeability) to as high as 80% (by SWC5 which is a seawater RO membrane). The range of NDMA rejection by these membranes was similar to that

of boron, ranging from 22-74%. The linear correlation ($R^2 = 0.95$) between the rejection values of boron and NDMA shown in Figure 34 has an F-value of 104 corresponding to a p-value of 0.000517. In addition, the slope of the linear regression is 0.82 indicating that the absolute values of boric acid rejection and NDMA rejection by a specific membrane are comparable to each other, especially by the higher-rejection membranes such as ESPAB and SWC5.

The strong correlation between boron and NDMA rejections by RO membranes observed here can be attributed to the similarity in their molecular dimensions, charge, and rejection mechanism. Possessing a pK_a value of 9.2 (Table 9), boric acid can speciate and transform from its neutral boric acid form to the negatively charged borate species as a function of pH (Figure 35). As a result, in aqueous solution, boron exists predominantly (> 90%) in the neutral boric acid form at or below pH 8 (Figure 35). On the other hand, NDMA only exists as an uncharged species in the normal wastewater pH range due to its negative pK_b value (Table 9). As a result, at or below pH 8, both boron and NDMA exist in their uncharged forms and steric hindrance is the only mechanism governing their rejection by RO membranes [87, 187, 223]. With the steric hindrance rejection mechanism, rejection is governed by the size of the solute. Boric acid and NDMA have comparable molecular dimensions (Table 9) and thus their rejection values as well as behaviour are comparable. In addition, boric acid and NDMA are both hydrophilic (Table 9) and thus are not expected to adsorb to the membrane polymeric matrix. It is noteworthy that NDMA has a significantly higher dipole moment than that of boric acid (Table 9). The dipole moment can influence the orientation of cylindrical molecules as they approach the membrane surface [224]. NDMA and boric acid have comparable molecular length and height (Table 9) and since the relative rejection for both solutes was similar the influence of dipole moment on their rejection appears to be insignificant.

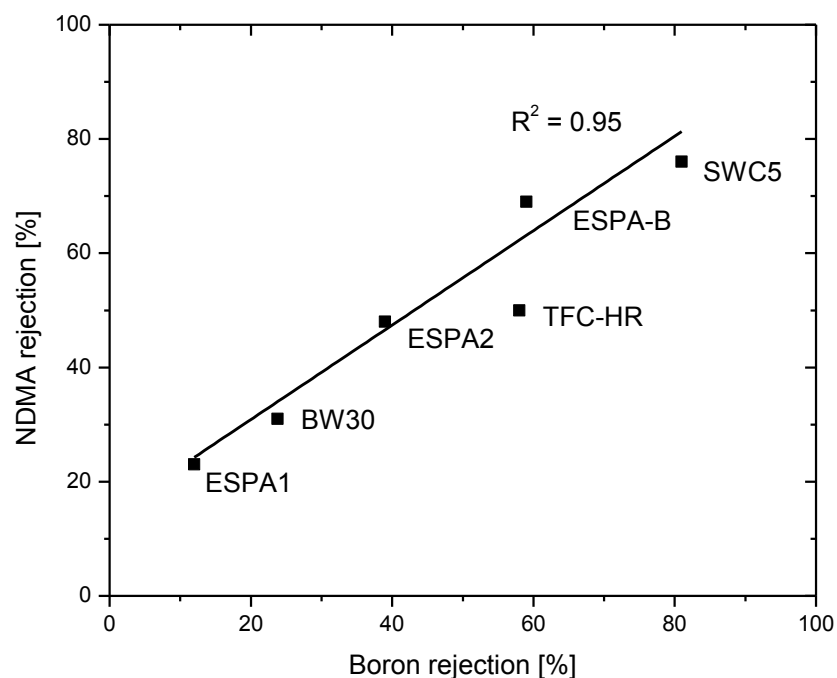
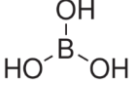
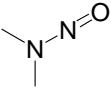


Figure 34. The correlation between the rejections of boron and NDMA by different membranes at pH 8. Feedwater contains 250 ng.L⁻¹ NDMA, 5.75 mg.L⁻¹ B(OH)₃, 20 mmol.L⁻¹ NaCl, 1 mmol.L⁻¹ NaHCO₃, and 1 mmol.L⁻¹ CaCl₂; temperature 20 °C, permeate flux 20 LMH, cross-flow velocity 42 cm.s⁻¹.

Table 9. Properties of boric acid and NDMA.

	Boric acid	NDMA
Molecular weight [g.mol ⁻¹]	61.83	74.05
Molecular dimensions [Å] ^a		
Length	4.52	4.10
Height	3.08	3.46
Width	0.85	1.73
Molecular structure		
pK _a /pK _b ^b	9.2	-3.63
LogK _{ow} ^b	-0.64	-0.50
Dipole moment [D] ^c	1.11	3.71

^a Calculated using the ChemBio3D Ultra software.

^b From SciFinder Scholar (obtained from the *Advanced Chemistry Development Software*).

^c Calculated using the Millsian 2.1 software.

The correlation between boron and NDMA rejections reported in Figure 34 creates a perspective for monitoring and predicting the fate and transport of NDMA during RO membrane filtration using boron rejection as a surrogate. Boron rejection could serve as a reference for selecting membranes for NDMA removal purposes. However, the correlation shown in Figure 34 was obtained under a specific filtration operating condition. By contrast, the operating condition in full-scale RO installations may vary quite significantly. Thus, it is necessary to establish a range where the above correlation is valid.

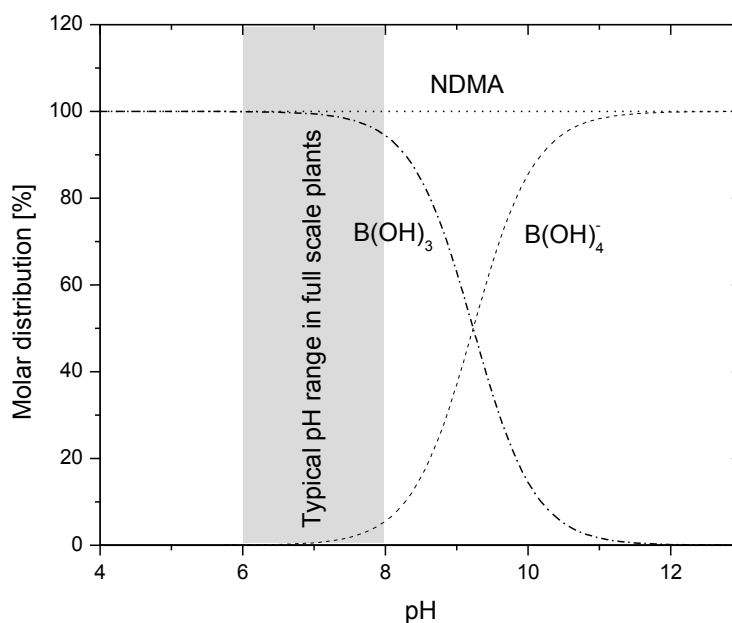


Figure 35. The speciation of boric acid and NDMA in de-ionised water matrix, temperature 25 °C, pressure 1 atm.

6.3.2 Effects of operating conditions on boron and NDMA rejection

In a full-scale RO installation, in addition to the solution pH, temporal variation in other operating parameters including solute concentration, ionic strength, permeate flux and temperature can be expected. Some of these parameters do not affect solute rejection while others can exert a significant impact on the separation efficiency of RO membranes. It has been consistently reported that the rejections of boron and NDMA by RO membranes are independent of their concentrations in the feedwater [15, 186]. Thus, the concentration is not expected to affect the correlation between NDMA and boron rejection. Similarly, it has also been revealed that the impact of ionic strength variation on the rejection of neutral solutes is not significant [197,

225]. NDMA rejection by RO membranes was reported to decrease by only 17% as the feed ionic strength increased from 26 to 260 mmol.L⁻¹ [187]. Steinle-Darling et al. [226] reported a 15% decrease in NDMA rejection by the ESPA3 membrane when the NaCl concentration increased from 0 to 100 mmol.L⁻¹. Similarly, the impact of ionic strength (within the range encountered during water reuse) on boron rejection was not significant. Tu et al. [86] reported a slight increase in boron rejection when the feedwater ionic strength was raised from 16 to 43 mmol.L⁻¹, and there exists a coupling effect between the water ionic strength and pH on boron rejection. Given the small impact of feed concentration and ionic strength on the rejection of boron and NDMA reported in the literature, the influence of these two parameters on the correlation between boron and NDMA rejections was not examined here. Instead, we have sought to demonstrate the correlation between boron and NDMA rejections under a range of permeate fluxes and feed solution temperatures since these parameters are known to exert a significant impact on the rejection of boron and NDMA.

An increase in the permeate flux led to a substantial increase in the rejection of both boron and NDMA (Figure 36a). This result is consistent with the literature [187, 227] and can be systematically described by the irreversible thermodynamic model [187] wherein solute rejection approaches the intrinsic membrane reflection coefficient (σ) as the permeate flux increases. As a result, an increase in permeate flux will result in an increase in solute rejection. At pH 8, a linear correlation ($R^2 = 0.99$) between the rejections of boron and NDMA at various permeate flux was observed (Figure 36b). However, it is noteworthy that the boron rejection can significantly increase when boron exists as the negatively charged borate ion at pH values above 8. At pH 6 and 8, NDMA and boron rejections were comparable, whereas at pH 10.5, boron rejection was substantially higher (Figure 36a). This result implies that boron can only be used as a surrogate for NDMA rejection at pH values equal or below 8.

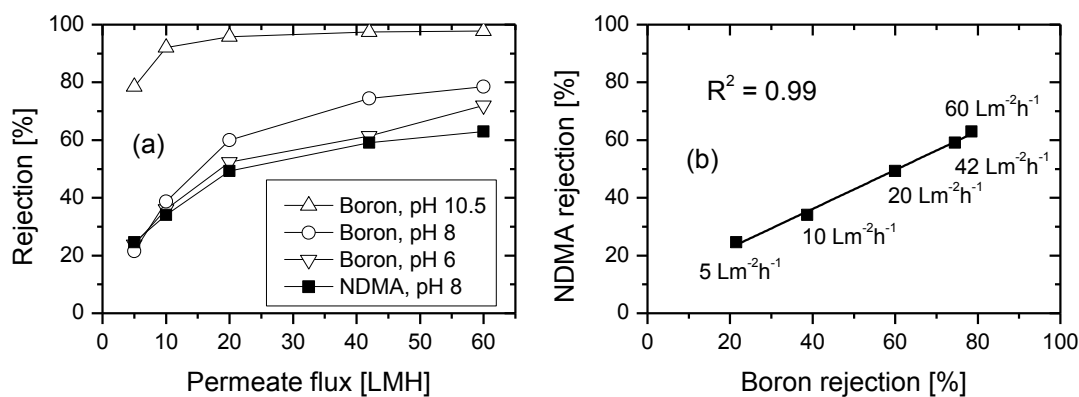


Figure 36. (a) The rejection of boron and NDMA as functions of permeate flux at different pH values; and (b) the correlation between boron and NDMA rejections at various permeate fluxes at pH 8. The TFC-HR membrane was used; feedwater contains 250 ng.L^{-1} NDMA, 5.75 mg.L^{-1} B(OH)_3 , 20 mmol.L^{-1} NaCl, 1 mmol.L^{-1} NaHCO_3 , and 1 mmol.L^{-1} CaCl_2 ; temperature $20 \text{ }^\circ\text{C}$, cross-flow velocity 42 cm.s^{-1} .

The rejections of boron and NDMA decreased linearly as a function of feed solution temperature (Figure 37a). Similar results have also been reported elsewhere [73, 187] and were attributed to the swelling of the membrane structure [93, 208] as well as the increase in the solute diffusivities [94]. Boron rejection at pH 6 and 8 and NDMA rejection at pH 8 appeared to be comparable at various feedwater temperatures (Figure 37a). Indeed, a linear correlation ($R^2 = 0.98$) between boron rejection and NDMA rejection at various feedwater temperatures can be observed at pH 8 (Figure 37b). However, once again, at pH 10.5, boron rejection as a function of feedwater temperature exhibited a very different behaviour (Figure 37a). These results reaffirmed that boron can only be used as a surrogate for NDMA rejection at pH 8 or below when both boron and NDMA exist as neutral species.

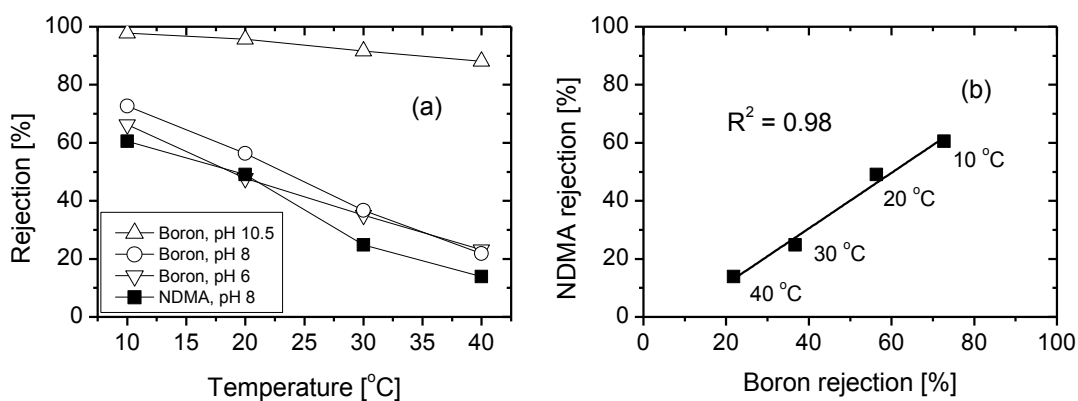


Figure 37. (a) The rejection of boron and NDMA as functions of temperature at different pH values; and (b) the correlation between boron and NDMA rejections at various temperatures at pH 8. The TFC-HR membrane was used; feedwater contains 250 ng.L^{-1} NDMA, 5.75 mg.L^{-1} B(OH)_3 , 20 mmol.L^{-1} NaCl, 1 mmol.L^{-1} NaHCO_3 , and 1 mmol.L^{-1} CaCl_2 ; permeate flux 20 LMH , cross-flow velocity 42 cm.s^{-1} .

The correlation between boron and NDMA rejections at different temperatures was also validated using a tertiary treated effluent matrix. The tertiary treated effluent had a pH value of 7.1 and thus both boron and NDMA exist in their neutral forms. As expected, a linear correlation between boron and NDMA rejections was observed with a correlation coefficient (R^2) of 0.94 as the feed solution temperature increased from 10 to 40 °C (Figure 38a). However, it is noteworthy that the rejections of both boron and NDMA differ slightly from values reported in Figure 37. This variation can be attributed to the compositional difference between the tertiary treated effluent and the synthetic feedwater solution used in this study [228].

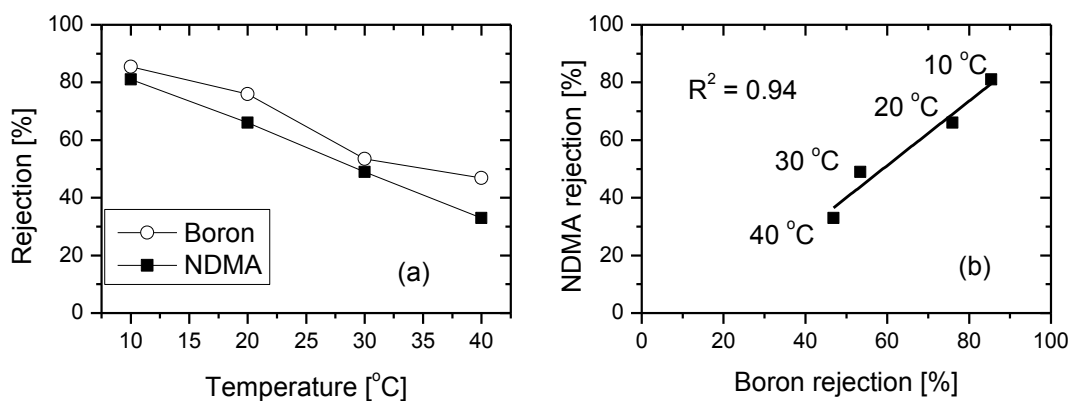


Figure 38. (a) The rejection of boron and NDMA as functions of temperature; and (b) the correlation between boron and NDMA rejections at various temperatures. The TFC-HR membrane was used. Tertiary treated effluent dosed with 250 ng.L^{-1} NDMA was used as feed solution. Permeate flux 20 LMH, cross-flow velocity 42 cm.s^{-1} .

The strong correlation between boron and NDMA rejections reported in this study is valid at pH 8 or lower where boron exists in the form of boric acid (Figure 35). It is noteworthy that in full-scale RO plants for water reclamation applications, the feedwater pH is usually in the range of pH 6-7.5 to minimise the precipitation of partially-soluble salts [186]. Thus, our proposal to use boron as a surrogate for NDMA rejection can be applied in the typical context of water reclamation. Given the recent availability of online boron monitoring techniques (i.e. online ion chromatography and boron-specific probe), boron can be a viable surrogate for NDMA rejection. Thus, the rejection of NDMA by RO membranes can be predicted without the burden of NDMA analysis. Nevertheless, this approach does not eliminate the need for compliance monitoring of NDMA in the RO permeate. Furthermore, caution is necessary when using boron as a surrogate for NDMA rejection. For example, the established correlation may be influenced by the interactions between boric acid with other constituents present in the water matrix. A notable example is the complexation between boric acid and poly-alcohols which can substantially increase boric acid rejection by RO membranes (Section 2.1.3). Further studies are necessary to assess the validity of this concept in pilot- and full-scale operations and under the influence of parameters that have not been investigated in

this study, such as the interaction of boric acid with traces of poly-alcohols in the feed solution.

6.4 Conclusion

Results reported in this study revealed a strong linear correlation ($R^2 = 95\%$) between boron and NDMA rejections by RO membranes. In addition, at pH 8 when both boron and NDMA exist as neutral solutes, the variation in their rejection as a function of permeate fluxes and feed solution temperatures resemble each other very closely. Boron rejection increased from 21 to 79% and the correlation coefficient of the linear regression between boron and NDMA rejections was 0.99 as the permeate flux varied from 5 to 60 LMH. Similarly, boron rejection decreased from 73 to 22% and the correlation coefficient of determination of the linear regression between boron and NDMA rejections was 0.98 as the feed solution temperature varied from 10 to 40 °C. This observed correlation can be attributed to the similarity in molecular dimensions between boric acid and NDMA. A good correlation between boron and NDMA rejections was also achieved when tertiary treated effluent was used as feedwater. These results suggest that boron can be used as a surrogate for the rejection of NDMA within the pH range typically used in RO plants for water reclamation applications (pH 6-8). Further studies are necessary to assess the validity of this concept in pilot- and full-scale operations and under the influence of operating parameters that have not been investigated in this study, such as membrane fouling, chemical cleaning, and the interaction of boric acid with traces of poly-alcohols in the feed.

CHAPTER 7: CONCLUSIONS AND RECOMMENDATIONS

This dissertation provided further insights to the understanding of boron rejection by NF/RO membranes. Chapter 2 reviewed the current state-of-the-art understanding of boron rejection by NF/RO membranes.

The literature review conducted as part of this dissertation suggests that the mechanisms governing boron transport through NF/RO membranes were described and simulated by numerous phenomenological-based and mechanistic-based models. The phenomenological-based models have relatively simple algorithms so they have been widely applied in laboratory-scale and industry-scale to predict and optimise boron rejection of RO installations. On the other hand, the mechanistic-based models are able to provide insight into the transport mechanism and the solute-membrane interaction thus these models are useful in optimising the membrane design. The modelling of boron transport is more complicated than for other solutes since boron is a special solute which exists in both neutral and charged forms depending on the chemistry of the environment. The simulation of boron rejection therefore should take into account both boron species whose transport is governed by different mechanisms.

The review also shows that a large number of studies in the last ten years have been dedicated to examine important chemical and operational factors affecting boron rejection by NF/RO membranes. As a result, various technical solutions have been employed by full-scale RO water treatment plants to produce permeate satisfying the targeted boron levels for different applications. The most commonly used method to improve boron rejection in contemporary full-scale RO plants is the double-pass membrane configuration in which pH of the first-pass permeate is increased to above pH 10 prior to the second pass. The addition of a second membrane pass entails a significant capital and operational cost increase thus renders the overall process less economical. In this dissertation, an alternative approach of adding polyols to the feed for improving boron rejection was explored.

Chapter 3 provided an experimental-based research to evaluate the technical feasibility of improving boron rejection by NF/RO membranes by adding polyols into the feed. Experiments conducted on three selected polyols, namely glycerol,

mannitol, and sorbitol indicated that choosing the polyol used in the complexation is the foremost factor to improve boron rejection because the overall boron rejection enhancement is directly proportional to the stability constant of the boron-polyol complexes. Amongst the three polyols tested in this study, sorbitol, which has the highest complexation constant with boron, was found to increase boron rejection by approximately 20% at a boron:sorbitol molar ratio as low as 1:0.2. Given the relatively low market price of sorbitol, the addition of sorbitol at such ratio could be an economical solution. The econo-technical efficiency of this method can be further improved by recovering and regenerating the used polyol in the brine stream. Future research is needed to examine other potentially suitable polyol compounds which have a high complexation constant with boron and are also easy to be recovered.

Chapters 4 and 5 of this dissertation fulfilled another knowledge gap identified from the literature review. These two chapters elucidated the effects of chemical cleaning and membrane ageing due to chemical preservation on boron rejection. In Chapter 4, the impacts of chemical cleaning on boron rejection and water permeability of a BWRO membrane (ESPA2) were investigated. Various typically used cleaning chemicals were selected to simulate membrane cleaning, including citric acid, sodium hydroxide, SDS, EDTA, a mixture of SDS and EDTA, and two commercial formulations, namely MC3 and MC11. The study found that chemical cleaning can decrease the rejection of boron and sodium by the membrane. The water permeability and surface properties of the membrane can also be significantly affected by chemical cleaning. Such changes in the membrane performance and surface properties were attributed to the pH condition of the cleaning chemical rather than the cleaning chemical itself. Interestingly, whereas the impacts of the cleaning chemical on the membrane water permeability were found reversible, the impacts on boron and sodium rejection were irreversible in most cases. The results of this study imply that in order to minimise the impacts of chemical cleaning on the membrane performance, the cleaning solution should be used at less harsh pH conditions where possible.

In Chapter 5, boron rejection by chemically preserved BWRO and SWRO membranes was experimentally investigated. Three preservative chemicals, namely formaldehyde, SMBS, and DBNPA, were evaluated for membrane preservation at

pH 3 and 7. The study found that the redox potential of the preserving chemical, which is dependent on the pH and the preservative itself, is the key factor governing its impacts on the preserved membrane. The preserving chemicals having high oxidation potentials would cause more negative impacts on the boron rejection by the preserved membrane, and vice versa. The result implies that the undesirable impacts of chemical preservation on RO membranes can be minimised by appropriate selection of the preservatives and by preserving the membrane in a reducing condition.

Chapter 6 demonstrated an initiative to use boron rejection data as a surrogate for NDMA rejection in RO wastewater treatment plants. This proposed approach is based on the premise that boron and NDMA have similar molecular properties when the solution pH is equal to or lower than 8, thus can be rejected by RO membranes at a comparable magnitude. Using six RO membranes covering a wide range of permeability, the study found a strong linear correlation ($R^2 = 95\%$) between boron and NDMA rejection, which indicates that boron can be used as a viable surrogate for NDMA rejection at pH 8 or lower. The correlation was validated in different operating fluxes and temperatures, and also in a tertiary treated wastewater matrix. Nevertheless, the concept still requires further studies before its industrial application occurs. The boron-NDMA rejection correlation needs to be validated in pilot- and full-scale processes, and also under impacts of practical membrane operations such as fouling and chemical cleaning.

Driven by the inevitable tendency of utilising seawater and reclaimed wastewater – high boron level sources for agricultural irrigation, the requirement for boron removal is projected to be perpetual. RO membrane, thanks to its overwhelming techno-economic advantages in water treatment, has attracted enormous studies for boron removal in the last decade. Nevertheless, satisfying stringent regulated boron standards meanwhile sustaining the economic benefit of membrane installations is still far from accomplishment. Ultimately, boron removal by RO membranes relies on two principle factors: the membrane characteristic and pH of the feedwater. There seems to be little room for novel membranes which achieve high boron rejection without scarifying its water permeability. On the other hand, pH elevation, which can substantially improve boron rejection of the membrane, is constrained by the

membrane scaling propensity. Recently, research on reducing the scaling propensity has achieved numerous advancements which facilitate high pH operation of RO membrane installations. As a result, boron rejection enhancement using high pH operation is becoming more practical. This is believed to be the most simple and practical solution for improving boron rejection by RO membranes.

REFERENCES

1. Gleick, P.H., ed. *Water Resources in Encyclopedia of Climate and Weather*. ed. S.H. Schneider. Vol. 2. 1996, University Press: New York.
2. UNESCO, *Water for People, Water for Life*, in *United Nations World Water Development*. 2003.
3. Fry, A., *Water facts and trends*. August 2005, World Business Council for Sustainable Development: Geneva.
4. Nair, M. and D. Kumar, *Water desalination and challenges: The Middle East perspective: A review*. *Desalination and Water Treatment*, 2013. **51**(10-12): p. 2030-2040.
5. Greenlee, L.F., et al., *Reverse osmosis desalination: Water sources, technology, and today's challenges*. *Water Research*, 2009. **43**(9): p. 2317-2348.
6. Fritzmann, C., et al., *State-of-the-art of reverse osmosis desalination*. *Desalination*, 2007. **216**(1-3): p. 1-76.
7. The-U.S.-National-Research-Council, . *Desalination: A national perspective*. 2008, Washington D.C.: National Academies Press.
8. Hoang, M., et al., *Desalination in Australia - National Research Flagships*, in *National Research Flagships*. 2009, CSIRO Materials Science and Engineering: Clayton, Victoria.
9. El Saliby, I., et al., *Desalination plants in Australia, review and facts*. *Desalination*, 2009. **247**(1-3): p. 1-14.
10. Nghiem, L.D., et al., *Treatment of coal seam gas produced water for beneficial use in australia: A review of best practices*. *Desalination and Water Treatment*, 2011. **32**(1-3): p. 316-323.
11. Sauvet-Goichon, B., *Ashkelon desalination plant - A successful challenge*. *Desalination*, 2007. **203**(1-3): p. 75-81.
12. Harris, C., *Modular desalting for specialized applications*. *Desalination*, 2000. **132**(1-3): p. 269-274.
13. Altman, S.J., et al., *Membrane treatment of side-stream cooling tower water for reduction of water usage*. *Desalination*, 2012. **285**: p. 177-183.
14. Massot, A., et al., *Nanofiltration and reverse osmosis in winemaking*. *Desalination*, 2008. **231**(1-3): p. 283-289.
15. Tu, K.L., L.D. Nghiem, and A.R. Chivas, *Boron removal by reverse osmosis membranes in seawater desalination applications*. *Separation and Purification Technology*, 2010. **75**: p. 87-101.
16. Hilal, N., G.J. Kim, and C. Somerfield, *Boron removal from saline water: A comprehensive review*. *Desalination*, 2011. **273**: p. 23-35.
17. Parks, J.L. and M. Edwards, *Boron in the Environment*. *Critical Reviews in Environmental Science and Technology*, 2005. **35**: p. 81-114.

18. Coughlin, J.R., *Sources of human exposure: Overview of water supplies as sources of boron*. Biological Trace Element Research, 1998. **66**(1-3): p. 87-100.
19. Argust, P., *Distribution of boron in the environment*. Biological Trace Element Research, 1998. **66**: p. 131-143.
20. Howe, P.D., *A review of boron effects in the environment*. Biological Trace Element Research, 1998. **66**(1-3): p. 153-166.
21. Butterwick, L., N.d. Oude, and K. Raymond, *Safety assessment of boron in aquatic and terrestrial environments*. Ecotoxicology and Environmental Safety, 1989. **17**(3): p. 339-371.
22. WHO, *Guidelines for Drinking Water Quality 4th Edition*. 2011, Geneva.
23. *Health effects support document for boron*. 2008, U.S. Environmental Protection Agency.
24. Melnyk, L., et al., *Boron removal from natural and wastewaters using combined sorption/membrane process*. Desalination, 2005. **185**(1-3): p. 147-157.
25. Dyer, S.D. and R.J. Caprara, *A method for evaluating consumer product ingredient contributions to surface and drinking water: Boron as a test case*. Environmental Toxicology and Chemistry, 1997. **16**(10): p. 2070-2081.
26. Fox, K.K., et al., *Measured variation in boron loads reaching European sewage treatment works*. Chemosphere, 2002. **47**(5): p. 499-505.
27. Neal, C. and A.J. Robson, *A summary of river water quality data collected within the Land-Ocean Interaction Study: Core data for eastern UK rivers draining to the North Sea*. Science of the Total Environment, 2000. **251-252**: p. 585-665.
28. Moore, J.A. and C. Expert Scientific, *An assessment of boric acid and borax using the IEHR Evaluative process for assessing human developmental and reproductive toxicity of agents*. Reproductive Toxicology, 1997. **11**(1): p. 123-160.
29. Gupta, U.C., et al., *Boron toxicity and deficiency - A review*. Canadian Journal of Soil Science, 1985. **65**(3): p. 381-409.
30. Linden, C.H., et al., *Acute ingestions of boric acid*. Journal of Toxicology-Clinical Toxicology, 1986. **24**(4): p. 269-279.
31. WHO, *Trace Elements in Human Nutrition and Health*. 1996, Geneva: World Health Organization.
32. Birge, W.J. and J.A. Black, *Sensitivity of vertebrate embryos to boron compounds*, in EPA-560/1-76-008. 1977, EPA.
33. Eisler, R., *Boron hazards to fish, wildlife, and invertebrates: a synoptic review*. Biological Report - US Fish & Wildlife Service, 1990. **85**(1 .20).

34. Bick, A. and G. Oron, *Post-treatment design of seawater reverse osmosis plants: boron removal technology selection for potable water production and environmental control*. Desalination, 2005. **178**(1-3): p. 233-246.
35. Farhat, A., et al., *Boron removal in new generation reverse osmosis (RO) membranes using two-pass RO without pH adjustment*. Desalination, 2013. **310**: p. 50-59.
36. WHO, WHO 2008. *Final Regulatory Determinations for the Second Drinking Water Contaminant Candidate List*. 2008.
37. Glueckstern, P. and M. Priel, *Boron removal in brackish water desalination systems*. Desalination, 2006. **205**: p. 178-184.
38. Kurihara, M., et al., *Advancement of RO Membrane for Seawater Desalination and Wastewater Reclamation*. 2008, Toray Industries.
39. National Library of Medicine's TOXNET system, *Hazardous Substance Data Bank 2006. Boron. Generate from the Hazardous Substances Data Bank (HSDB)*.
40. Health Canada. *Summary of Guidelines for Canadian Drinking Water Quality*. 2003, Ottawa: Health Canada, Editor. 2003.
41. Council of the European Union. *Council Directive 98/83/EC, November 3, 1998, on the quality of water intended for human consumption*.
42. Ministry of Environment, Republic of Korea 2009. *Management of Drinking Water Quality*.
43. Park, J.K. and K.J. Lee, *Diffusion coefficients for aqueous boric acid*. Journal of Chemical & Engineering Data, 1994. **39**(4): p. 891-894.
44. Choi, W.W. and K.Y. Chen, *Evaluation of boron removal by adsorption on solids*. Environmental Science & Technology, 1979. **13**(2): p. 189-196.
45. Owen, B.B., *The Dissociation Constant of Boric Acid from 10 to 50°C*. Journal of the American Chemical Society, 1934. **56**(8): p. 1695-1697.
46. Power, P.P. and W.G. Woods, *The chemistry of boron and its speciation in plants*. Plant and Soil, 1997. **193**: p. 1-13.
47. Belcher, R., G.W. Tully, and G. Svehla, *A comparative study of various complexing agents (polyols) used in the titration of boric acid*. Analytica Chimica Acta, 1970. **50**(2): p. 261-267.
48. Van Duin, M., et al., *The pH dependence of the stability of esters of boric acid and borate in aqueous medium as studied by ¹¹B NMR*. Tetrahedron, 1984. **40**(15): p. 2901-2911.
49. Van Duin, M., et al., *Studies on borate esters II . Structure and stability of borate esters of polyhydroxycarboxylates and related polyols in aqueous alkaline media as studied by ¹¹B NMR*. Tetrahedron, 1985. **41**(16): p. 3411-3421.

50. Makke M, Kieboom A. P. G., and Bekkum van H., *Studies on borate esters III. Borate esters of D-mannitol, D-glucitol, D-fructose and D-glucose in water*. Recueil des Travaux Chimiques des Pays-Bas, 1985. **104**: p. 230-235.
51. Arruda, M.A.Z. and E.A.G. Zagatto, *A simple stopped-flow method with continuous pumping for the spectrophotometric flow-injection determination of boron in plants*. Analytica Chimica Acta, 1987. **199**(C): p. 137-145.
52. López, F.J., E. Giménez, and F. Hernández, *Analytical study on the determination of boron in environmental water samples*. Fresenius' Journal of Analytical Chemistry, 1993. **346**(10-11): p. 984-987.
53. Hill, C.J. and R.P. Lash, *Ion chromatographic determination of boron as tetrafluoroborate*. Analytical Chemistry, 1980. **52**(1): p. 24-27.
54. Katagiri, J., T. Yoshioka, and T. Mizoguchi, *Basic study on the determination of total boron by conversion to tetrafluoroborate ion (BF_4^-) followed by ion chromatography*. Analytica Chimica Acta, 2006. **570**(1): p. 65-72.
55. Imato, T., T. Yoshizuka, and N. Ishibashi, *Potentiometric flow-injection determination of boron by using a flow-through tetrafluoroborate ion-selective poly(vinyl chloride) membrane electrode*. Analytica Chimica Acta, 1990. **233**(1): p. 139-141.
56. Sah, R.N. and P.H. Brown, *Boron Determination-A Review of Analytical Methods*. Microchemical Journal, 1997. **56**(3): p. 285-304.
57. Botelho, G.M.A., A.J. Curtius, and R.C. Campos, *Determination of boron by electrothermal atomic absorption spectrometry: Testing different modifiers, atomization surfaces and potential interferents*. Journal of Analytical Atomic Spectrometry, 1994. **9**(11): p. 1263-1267.
58. Papaspyrou, M., et al., *Determination of boron in cell suspensions using electrothermal atomic absorption spectrometry*. Journal of Analytical Atomic Spectrometry, 1994. **9**(7): p. 791-795.
59. Gregoire, D.C., *Determination of boron in fresh and saline waters by inductively coupled plasma mass spectrometry*. Journal of Analytical Atomic Spectrometry, 1990. **5**(7): p. 623-626.
60. Smith, F.G., et al., *Measurement of boron concentration and isotope ratios in biological samples by inductively coupled plasma mass spectrometry with direct injection nebulization*. Analytica Chimica Acta, 1991. **248**(1): p. 229-234.
61. Evans, S. and U. Krähenbühl, *Improved boron determination in biological material by inductively coupled plasma mass spectrometry*. Journal of Analytical Atomic Spectrometry, 1994. **9**(11): p. 1249-1253.
62. APHA, *Standard methods for the examination of water and wastewater*. 21 ed. 2005, Washington, D.C.: APHA-AWWA-WEF.
63. World Health Organisation, *Boron in Drinking Water-Background document for development of WHO Guidelines for Drinking water quality*, WHO, Editor. 2003.

64. Evans, S. and U. Krähenbühl, *Boron analysis in biological material: microwave digestion procedure and determination by different methods*. Fresenius' Journal of Analytical Chemistry, 1994. **349**(6): p. 454-459.
65. Fujita, Y., et al., *A study of boron adsorption onto activated sludge*. Bioresource Technology, 2005. **96**(12): p. 1350-1356.
66. Downing, R.G., et al., *Considerations in the determination of Boron at low concentrations*. Biological Trace Element Research, 1998. **66**(1-3): p. 3-21.
67. Green, G.H., C. Blincoe, and H.J. Weeth, *Boron contamination from borosilicate glass*. Journal of Agricultural and Food Chemistry, 1976. **24**(6): p. 1245-1246.
68. Al-Ammar, A.S., R.K. Gupta, and R.M. Barnes, *Elimination of boron memory effect in inductively coupled plasma-mass spectrometry by ammonia gas injection into the spray chamber during analysis*. Spectrochimica Acta Part B: Atomic Spectroscopy, 2000. **55**(6): p. 629-635.
69. Al-Ammar, A., R.K. Gupta, and R.M. Barnes, *Elimination of boron memory effect in inductively coupled plasma-mass spectrometry by addition of ammonia*. Spectrochimica acta, Part B: Atomic spectroscopy, 1999. **54**(7): p. 1077-1084.
70. Gregoire, D.C., *Determination of boron isotope ratios in geological materials by inductively coupled plasma mass spectrometry*. Analytical Chemistry, 1987. **59**(20): p. 2479-2484.
71. Huehmer, R.P., et al., *Enhancing boron rejection in seawater reverse osmosis facilities*. Water Science and Technology: Water Supply, 2008. **8**: p. 519-525.
72. Dydo, P., et al., *Boron removal from landfill leachate by means of nanofiltration and reverse osmosis*. Desalination, 2005. **185**: p. 131-137.
73. Hung, P.V.X., S.-H. Cho, and S.-H. Moon, *Prediction of boron transport through seawater reverse osmosis membranes using solution-diffusion model*. Desalination, 2009. **247**(1-3): p. 33-44.
74. Cengeloglu, Y., et al., *Removal of boron from water by using reverse osmosis*. Separation and Purification Technology, 2008. **64**: p. 141-146.
75. Faigon, M. and D. Hefer, *Boron rejection in SWRO at high pH conditions versus cascade design*. Desalination, 2008. **223**(1-3): p. 10-16.
76. Glueckstern, P. and M. Priel, *Optimization of boron removal in old and new SWRO systems*. Desalination, 2003. **156**(1-3): p. 219-228.
77. Gorenflo, A., et al., *High pH operation in seawater reverse osmosis permeate: First results from the world's largest SWRO plant in Ashkelon*. Desalination, 2007. **203**(1-3): p. 82-90.
78. Koseoglu, H., et al., *The effects of operating conditions on boron removal from geothermal waters by membrane processes*. Desalination, 2010. **258**(1-3): p. 72-78.

79. Koseoglu, H., et al., *Boron removal from seawater using high rejection SWRO membranes - impact of pH, feed concentration, pressure, and cross-flow velocity*. Desalination, 2008. **227**(1-3): p. 253-263.
80. Pastor, M.R., et al., *Influence of pH in the elimination of boron by means of reverse osmosis*. Desalination, 2001. **140**(2): p. 145-152.
81. Sagiv, A. and R. Semiat, *Analysis of parameters affecting boron permeation through reverse osmosis membranes*. Journal of Membrane Science, 2004. **243**(1-2): p. 79-87.
82. Taniguchi, M., et al., *Boron removal in RO seawater desalination*. Desalination, 2004. **167**: p. 419-426.
83. Taniguchi, M., M. Kurihara, and S. Kimura, *Boron reduction performance of reverse osmosis seawater desalination process*. Journal of Membrane Science, 2001. **183**(2): p. 259-267.
84. Oo, M.H. and S.L. Ong, *Implication of zeta potential at different salinities on boron removal by RO membranes*. Journal of Membrane Science, 2010. **352**(1-2): p. 1-6.
85. Childress, A.E. and M. Elimelech, *Relating nanofiltration membrane performance to membrane charge (electrokinetic) characteristics*. Environmental Science and Technology, 2000. **34**(17): p. 3710-3716.
86. Tu, K.L., L.D. Nghiem, and A.R. Chivas, *Coupling effects of feed solution pH and ionic strength on the rejection of boron by NF/RO membranes*. Chemical Engineering Journal, 2011. **168**: p. 700-706.
87. Oo, M.H. and L. Song, *Effect of pH and ionic strength on boron removal by RO membranes*. Desalination, 2009. **246**(1-3): p. 605-612.
88. Braghetta, A., F.A. DiGiano, and W.P. Ball, *Nanofiltration of natural organic matter: pH and ionic strength effects*. Journal of Environmental Engineering-Asce, 1997. **123**(7): p. 628-641.
89. Oo, M.H. and S.L. Ong, *Boron removal and zeta potential of RO membranes: Impact of pH and salinity*. Desalination and Water Treatment, 2012. **39**(1-3): p. 83-87.
90. Prats, D., M.F. Chillón-Arias, and M. Rodríguez-Pastor, *Analysis of the influence of pH and pressure on the elimination of boron in reverse osmosis*. Desalination, 2000. **128**(3): p. 269-273.
91. Koseoglu, H., et al., *The removal of boron from model solutions and seawater using reverse osmosis membranes*. Desalination, 2008. **223**(1-3): p. 126-133.
92. Kim, J., et al., *Boron Rejection By Reverse Osmosis Membranes: National Reconnaissance And Mechanism Study*. 2009, U.S. Department of the Interior, Bureau of Reclamation.
93. Sharma, R.R., R. Agrawal, and S. Chellam, *Temperature effects on sieving characteristics of thin-film composite nanofiltration membranes: pore size distributions and transport parameters*. Journal of Membrane Science, 2003. **223**(1-2): p. 69-87.

94. Hyung, H. and J.-H. Kim, *A mechanistic study on boron rejection by sea water reverse osmosis membranes*. Journal of Membrane Science, 2006. **286**: p. 269-278.
95. Redondo, J., M. Busch, and J.-P. De Witte, *Boron removal from seawater using FILMTECTM high rejection SWRO membranes*. Desalination, 2003. **156**(1-3): p. 229-238.
96. Tu, K.L., A.R. Chivas, and L.D. Nghiem, *Effects of membrane fouling and scaling on boron rejection by nanofiltration and reverse osmosis membranes*. Desalination, 2011. **279**(1-3): p. 269-277.
97. Huertas, E., et al., *Influence of biofouling on boron removal by nanofiltration and reverse osmosis membranes*. Journal of Membrane Science, 2008. **318**: p. 264-270.
98. Nadav, N., M. Priel, and P. Glueckstern, *Boron removal from the permeate of a large SWRO plant in Eilat*. Desalination, 2005. **185**(1-3): p. 121-129.
99. Wijmans, J.G. and R.W. Baker, *The solution-diffusion model - A review*. Journal of Membrane Science, 1995. **107**(1-2): p. 1-21.
100. Kimura, S. and S. Souriraj, *Analysis of data in reverse osmosis with porous cellulose acetate membranes used*. Aiche Journal, 1967. **13**(3): p. 497-503.
101. Burghoff, H., K. Lee, and W. Pusch, *Characterization of transport across cellulose acetate membranes in the presence of strong solute-membrane interactions*. Journal of Applied Polymer Science, 1980. **25**: p. 323.
102. Soltanieh, M. and W.N. Gill, *Review of reverse osmosis membranes and transport models*. Chemical Engineering Communications, 1981. **12**(4-6): p. 279-363.
103. Sherwood, T., P. Brian, and R. Fisher, *Desalination by reverse osmosis*. Industrial and Engineering Chemistry Fundamental, 1967. **6**: p. 2.
104. Jonsson, G., *Overview of theories for water and solute transport in UF/RO membranes*. Desalination, 1980. **35**(0): p. 21-38.
105. van den Berg, G.B. and C.A. Smolders, *Diffusional phenomena in membrane separation processes*. Journal of Membrane Science, 1992. **73**(2-3): p. 103-118.
106. Kedem, O. and A. Katchalsky, *Thermodynamic analysis of the permeability of biological membranes to non-electrolytes*. Biochimica et Biophysica Acta, 1958. **27**: p. 229-246.
107. Mane, P.P., et al., *Modeling Boron Rejection in Pilot- and Full-Scale Reverse Osmosis Desalination Processes*. Journal of Membrane Science, 2009. **338**: p. 119-127.
108. Fernanda Chillón Arias, M., et al., *Kinetic behaviour of sodium and boron in brackish water membranes*. Journal of Membrane Science, 2011. **368**(1-2): p. 86-94.

109. Spiegler, K.S. and O. Kedem, *Thermodynamics of hyperfiltration (reverse osmosis): criteria for efficient membranes*. Desalination, 1966. **1**(4): p. 311-326.
110. Taniguchi, M. and S. Kimura, *Estimation of transport parameters of RO membranes for seawater desalination*. Aiche Journal, 2000. **46**(10): p. 1967-1973.
111. Murthy, Z.V.P. and S.K. Gupta, *Estimation of mass transfer coefficient using a combined nonlinear membrane transport and film theory model*. Desalination, 1997. **109**(1): p. 39-49.
112. Urama, R.I. and B.J. Mariñas, *Mechanistic interpretation of solute permeation through a fully aromatic polyamide reverse osmosis membrane*. Journal of Membrane Science, 1997. **123**(2): p. 267-280.
113. Murthy, Z.V.P. and S.K. Gupta, *Sodium cyanide separation and parameter estimation for reverse osmosis thin film composite polyamide membrane*. Journal of Membrane Science, 1999. **154**(1): p. 89-103.
114. Lee, S., G. Amy, and J. Cho, *Applicability of Sherwood correlations for natural organic matter (NOM) transport in nanofiltration (NF) membranes*. Journal of Membrane Science, 2004. **240**: p. 49-65.
115. Park, P.-K., et al., *Full-scale simulation of seawater reverse osmosis desalination processes for boron removal: Effect of membrane fouling*. Water Research, 2012. **46**(12): p. 3796-3804.
116. Winnograd, Y., A. Solan, and M. Toren, *Mass-transfer in narrow channels in presence of turbulence promoters*. Desalination, 1973. **13**(2): p. 171-186.
117. Benboudinar, M., W.T. Hanbury, and S. Avlonitis, *Numerical-simulation and optimization of spiral-wound modules*. Desalination, 1992. **86**(3): p. 273-290.
118. Okada, T. and T. Matsuura, *A new transport model for pervaporation*. Journal of Membrane Science, 1991. **59**(2): p. 133-150.
119. Matsuura, T. and S. Sourirajan, *Reverse osmosis transport through capillary pores under the influence of surface forces*. Industrial & Engineering Chemistry, Process Design and Development, 1981. **20**(2): p. 273-282.
120. Jain, S. and S.K. Gupta, *Analysis of modified surface force pore flow model with concentration polarization and comparison with Spiegler-Kedem model in reverse osmosis systems*. Journal of Membrane Science, 2004. **232**(1-2): p. 45-61.
121. Mehdizadeh, H. and J.M. Dickson, *Theoretical modification of the surface force-pore flow model for reverse osmosis transport*. Journal of Membrane Science, 1989. **42**(1-2): p. 119-145.
122. Sourirajan, S., *Reverse Osmosis*. 1970, New York: Academic Press.
123. Kezia, K., et al., *Convective transport of boron through a brackish water reverse osmosis membrane*. Journal of Membrane Science, 2013. **445**(0): p. 160-169.

124. Bhattacharyya, D. and M. Williams, eds. *Theory - Reverse Osmosis*. Membrane Handbook, ed. W. Ho and K. Sirkar. 1992, Van Nostrand Reinhold: New York. 269-280.
125. Bhattacharyya, D. and C. Cheng, eds. *Separation of metal chelates by charged composite membranes*. Recent development in separation science, ed. N. Li. Vol. 9. 1986, CRC Press: Florida.
126. Dresner, L. and J.S. Johnson, *Some remarks on the integration of extended Nernst-Planck equation in the hyperfiltration of multicomponent solutions*. Desalination, 1972. **95**: p. 27-46.
127. Wang, X.L., et al., *The electrostatic and steric-hindrance model for the transport of charged solutes through nanofiltration membranes*. Journal of Membrane Science, 1997. **135**(1): p. 19-32.
128. Nir, O. and O. Lahav, *Coupling mass transport and chemical equilibrium models for improving the prediction of SWRO permeate boron concentrations*. Desalination, 2013. **310**(0): p. 87-92.
129. Knoell, T., *Chlorine's impact on the performance and properties of polyamide membranes*. Ultrapure Water, 2006. **23**(3): p. 24-31.
130. Gabelich, C.J., et al., *Enhanced oxidation of polyamide membranes using monochloramine and ferrous iron*. Journal of Membrane Science, 2005. **258**(1-2): p. 64-70.
131. da Silva, M.K., I.C. Tessaro, and K. Wada, *Investigation of oxidative degradation of polyamide reverse osmosis membranes by monochloramine solutions*. Journal of Membrane Science, 2006. **282**(1-2): p. 375-382.
132. Li, X., et al., *Chemical cleaning of PS ultrafilters fouled by the fermentation broth of glutamic acid*. Separation and Purification Technology, 2005. **42**(2): p. 181-187.
133. Liikanen, R., J. Yli-Kuivila, and R. Laukkanen, *Efficiency of various chemical cleanings for nanofiltration membrane fouled by conventionally-treated surface water*. Journal of Membrane Science, 2002. **195**(2): p. 265-276.
134. Madaeni, S.S., T. Mohamamdi, and M. Kazemi Moghadam, *Chemical cleaning of reverse osmosis membranes*. Desalination, 2001. **134**(1-3): p. 77-82.
135. Van der Bruggen, B., et al., *Direct nanofiltration of surface water using capillary membranes: comparison with flat sheet membranes*. Separation and Purification Technology, 2003. **31**(2): p. 193-201.
136. Kimura, K., et al., *Irreversible membrane fouling during ultrafiltration of surface water*. Water Research, 2004. **38**(14-15): p. 3431-3441.
137. Dow-FilmTec, *Cleaning Procedures for DOW FILMTECT FT30 Elements*. 2011.
138. Hydranautics, *Foulants and Cleaning Procedures for composite polyamide RO Membrane Elements*. 2011.

139. Al-Amoudi, A., *Effect of chemical cleaning agents on virgin nanofiltration membrane as characterized by positron annihilation spectroscopy*. Separation and Purification Technology, 2013. **110**: p. 51-56.
140. Simon, A., W.E. Price, and L.D. Nghiem, *Effects of chemical cleaning on the nanofiltration of pharmaceutically active compounds (PhACs)*. Separation and Purification Technology, 2012. **88**(0): p. 208-215.
141. Madaeni, S.S. and S. Samieirad, *Chemical cleaning of reverse osmosis membrane fouled by wastewater*. Desalination, 2010. **257**(1-3): p. 80-86.
142. Al-Amoudi, A., et al., *Cleaning results of new and fouled nanofiltration membrane characterized by zeta potential and permeability*. Separation and Purification Technology, 2007. **54**(2): p. 234-240.
143. Fujioka, T., et al., *N-nitrosamine rejection by reverse osmosis: Effects of membrane exposure to chemical cleaning reagents*. Desalination, 2013. **343**(16): p. 60-66.
144. Tian, J.y., et al., *Consecutive chemical cleaning of fouled PVC membrane using NaOH and ethanol during ultrafiltration of river water*. Water Research, 2010. **44**(1): p. 59-68.
145. Simon, A., W.E. Price, and L.D. Nghiem, *Influence of formulated chemical cleaning reagents on the surface properties and separation efficiency of nanofiltration membranes*. Journal of Membrane Science, 2013. **432**(0): p. 73-82.
146. Simon, A., et al., *Effects of caustic cleaning on pore size of nanofiltration membranes and their rejection of trace organic chemicals*. Journal of Membrane Science, 2013. **447**(0): p. 153-162.
147. Jons, S., et al., *Treatment of composite polyamide membranes to improve performance*, W.I.P. Organisation, Editor. 1999: USA.
148. Soice, N.P., et al., *Studies of oxidative degradation in polyamide RO membrane barrier layers using pendant drop mechanical analysis*. Journal of Membrane Science, 2004. **243**(1-2): p. 345-355.
149. Kwon, Y.-N. and J.O. Leckie, *Hypochlorite degradation of crosslinked polyamide membranes: I. Changes in chemical/morphological properties*. Journal of Membrane Science, 2006. **283**(1-2): p. 21-26.
150. Glater, J. and M.R. Zachariah. *Mechanistic study of halogen interaction with polyamide reverse osmosis membranes*. 1985.
151. Kawaguchi, T. and H. Tamura, *Chlorine-resistant membrane for reverse osmosis. I. Correlation between chemical structures and chlorine resistance of polyamides*. Journal of Applied Polymer Science, 1984. **29**(11): p. 3359-3367.
152. Kang, G.-D., et al., *Study on hypochlorite degradation of aromatic polyamide reverse osmosis membrane*. Journal of Membrane Science, 2007. **300**(1-2): p. 165-171.

153. Glater, J., S.-k. Hong, and M. Elimelech, *The search for a chlorine-resistant reverse osmosis membrane*. *Desalination*, 1994. **95**(3): p. 325-345.
154. Antony, A., et al., *Assessing the oxidative degradation of polyamide reverse osmosis membrane—Accelerated ageing with hypochlorite exposure*. *Journal of Membrane Science*, 2010. **347**(1-2): p. 159-164.
155. Kwon, Y.-N. and J.O. Leckie, *Hypochlorite degradation of crosslinked polyamide membranes: II. Changes in hydrogen bonding behavior and performance*. *Journal of Membrane Science*, 2006. **282**(1-2): p. 456-464.
156. Kwon, Y.-N., C.Y. Tang, and J.O. Leckie, *Change of chemical composition and hydrogen bonding behavior due to chlorination of crosslinked polyamide membranes*. *Journal of Applied Polymer Science*, 2008. **108**(4): p. 2061-2066.
157. Soice, N.P., et al., *Oxidative degradation of polyamide reverse osmosis membranes: Studies of molecular model compounds and selected membranes*. *Journal of Applied Polymer Science*, 2003. **90**(5): p. 1173-1184.
158. Koo, J.-Y., R.J. Petersen, and J.E. Cadotte. *ESCA Characterization of chlorine-damaged polyamide reverse osmosis membrane*. 1986.
159. Avlonitis, S., W.T. Hanbury, and T. Hodgkiess, *Chlorine degradation of aromatic polyamides*. *Desalination*, 1992. **85**(3): p. 321-334.
160. Schliebs, M., *Mothballs at the ready for \$1.8bn desal plant*, in *The Australian* March 27, 2013.
161. Holloway, M.D., C. Nwaoha, and O.A. Onyewuenyi, eds. *Process Plant Equipment Operation, Reliability, and Control*. 2012, Wiley: Hoboken, N.J.
162. Hydranautics, *Biocides for Disinfection and Storage of Hydranautics Membrane Elements*. 2013.
163. Dow-FilmTec, *Preservation of RO and NF systems*. 2009.
164. Toray, *Storage and Preservation*. 2004.
165. Vrijenhoek, E.M., S. Hong, and M. Elimelech, *Influence of membrane surface properties on initial rate of colloidal fouling of reverse osmosis and nanofiltration membranes*. *Journal of Membrane Science*, 2001. **188**(1): p. 115-128.
166. Song, W., et al., *Nanofiltration of natural organic matter with H₂O₂/UV pretreatment: fouling mitigation and membrane surface characterization*. *Journal of Membrane Science*, 2004. **241**(1): p. 143-160.
167. Kim, J.Y., H.K. Lee, and S.C. Kim, *Surface structure and phase separation mechanism of polysulfone membranes by atomic force microscopy*. *Journal of Membrane Science*, 1999. **163**(2): p. 159-166.
168. Schossig-Tiedemann, M. and D. Paul, *Improved preparation of membrane surfaces for field-emission scanning electron microscopy*. *Journal of Membrane Science*, 2001. **187**(1-2): p. 85-91.

169. Torras, C. and R. Garcia-Valls, *Quantification of membrane morphology by interpretation of scanning electron microscopy images*. Journal of Membrane Science, 2004. **233**(1-2): p. 119-127.
170. Elimelech, M., W.H. Chen, and J.J. Waypa, *Measuring the zeta (electrokinetic) potential of reverse osmosis membranes by a streaming potential analyzer*. Desalination, 1994. **95**(3): p. 269-286.
171. Kontturi, K. and M. Vuoristo, *Adsorption of globular proteins on polymeric microfiltration membranes*. Desalination, 1996. **104**(1-2): p. 99-105.
172. Deshmukh, S.S. and A.E. Childress, *Zeta potential of commercial RO membranes: influence of source water type and chemistry*. Desalination, 2001. **140**(1): p. 87-95.
173. Mänttari, M., A. Pihlajamäki, and M. Nyström, *Effect of pH on hydrophilicity and charge and their effect on the filtration efficiency of NF membranes at different pH*. Journal of Membrane Science, 2006. **280**(1-2): p. 311-320.
174. Li, Q., Z. Xu, and I. Pinnau, *Fouling of reverse osmosis membranes by biopolymers in wastewater secondary effluent: Role of membrane surface properties and initial permeate flux*. Journal of Membrane Science, 2007. **290**(1-2): p. 173-181.
175. Geens, J., B. Van der Bruggen, and C. Vandecasteele, *Characterisation of the solvent stability of polymeric nanofiltration membranes by measurement of contact angles and swelling*. Chemical Engineering Science, 2004. **59**(5): p. 1161-1164.
176. Tang, C.Y., Y.-N. Kwon, and J.O. Leckie, *Effect of membrane chemistry and coating layer on physiochemical properties of thin film composite polyamide RO and NF membranes: II. Membrane physiochemical properties and their dependence on polyamide and coating layers*. Desalination, 2009. **242**(1-3): p. 168-182.
177. Lee, W., et al., *Evaluation of surface properties of reverse osmosis membranes on the initial biofouling stages under no filtration condition*. Journal of Membrane Science, 2010. **351**(1-2): p. 112-122.
178. Li, Q., et al., *Understanding the dependence of contact angles of commercially RO membranes on external conditions and surface features*. Desalination, 2013. **309**: p. 38-45.
179. Hurwitz, G., G.R. Guillen, and E.M.V. Hoek, *Probing polyamide membrane surface charge, zeta potential, wettability, and hydrophilicity with contact angle measurements*. Journal of Membrane Science, 2010. **349**(1-2): p. 349-357.
180. Arkhangelsky, E., D. Kuzmenko, and V. Gitis, *Impact of chemical cleaning on properties and functioning of polyethersulfone membranes*. Journal of Membrane Science, 2007. **305**(1-2): p. 176-184.
181. Walzak, M.J., R. Davidson, and M. Biesinger, *The Use of XPS, FTIR, SEM/EDX, Contact Angle, and AFM in the Characterization of Coatings*. Journal of Materials Engineering and Performance, 1998. **7**(3): p. 317-323.

182. Tang, C.Y., Y.-N. Kwon, and J.O. Leckie, *Effect of membrane chemistry and coating layer on physiochemical properties of thin film composite polyamide RO and NF membranes: I. FTIR and XPS characterization of polyamide and coating layer chemistry*. *Desalination*, 2009. **242**(1–3): p. 149-167.
183. Sedlak, D.L., et al., *Sources and fate of nitrosodimethylamine and its precursors in municipal wastewater treatment plants*. *Water Environment Research*, 2005. **77**(1): p. 32-39.
184. US-EPA. *N-Nitrosodimethylamine (CASRN 62-75-9)*. 2008 25/09/2008]; Available from: <http://www.epa.gov/ncea/iris/subst/0045.htm>.
185. WHO, *N-Nitrosodimethylamine in drinking-water*. 2006, World Health Organization: Geneva. p. 36.
186. Fujioka, T., et al., *N-nitrosamine removal by reverse osmosis for indirect potable water reuse - A critical review based on observations from laboratory-, pilot- and full-scale studies*. *Separation and Purification Technology*, 2012. **98**: p. 503-515.
187. Fujioka, T., et al., *Effects of feed solution characteristics on the rejection of N-nitrosamines by reverse osmosis membranes*. *Journal of Membrane Science*, 2012. **409-410**: p. 66-74.
188. Jacob, C., *Seawater desalination: Boron removal by ion exchange technology*. *Desalination*, 2007. **205**(1-3): p. 47-52.
189. Nadav, N., *Boron removal from seawater reverse osmosis permeate utilizing selective ion exchange resin*. *Desalination*, 1999. **124**(1-3): p. 131-135.
190. Simonnot, M.-O., et al., *Boron removal from drinking water with a boron selective resin: is the treatment really selective?* *Water Research*, 2000. **34**(1): p. 109-116.
191. Bachelier, N., et al., *Facilitated transport of boric acid by 1,3-diols through supported liquid membranes*. *Journal of Membrane Science*, 1996. **119**(2): p. 285-294.
192. Geffen, N., et al., *Boron removal from water by complexation to polyol compounds*. *Journal of Membrane Science*, 2006. **286**(1-2): p. 45-51.
193. Dydo, P., I. Nemš, and M. Turek, *Boron removal and its concentration by reverse osmosis in the presence of polyol compounds*. *Separation and Purification Technology*, 2012. **89**(0): p. 171-180.
194. Hydranautics, *Foulants and cleaning procedures for composite polyamide RO membrane elements (ESPA, ESNA, CPA, LFC, NANO and SWC)*. *TSB107.21*. 2011.
195. Nghiem, L.D., A.I. Schäfer, and M. Elimelech, *Removal of natural hormones by nanofiltration membranes: measurement, modeling and mechanisms*. *Environmental Science and Technology*, 2004. **38**(6): p. 1888-1896.
196. Anoyal, S.J., *Complexing of polyols with cations*. *Tetrahedron*, 1974. **30**(12): p. 1695-1702.

197. Childress, A.E. and M. Elimelech, *Effect of solution chemistry on the surface charge of polymeric reverse osmosis and nanofiltration membranes*. Journal of Membrane Science, 1996. **119**(2): p. 253-268.
198. Schaep, J., et al., *Modelling the retention of ionic components for different nanofiltration membranes*. Separation and Purification Technology, 2001. **22-23**: p. 169-179.
199. Hoang, T., G. Stevens, and S. Kentish, *The effect of feed pH on the performance of a reverse osmosis membrane*. Desalination, 2010. **261**(1-2): p. 99-103.
200. Teixeira, M.R., M.J. Rosa, and M. Nyström, *The role of membrane charge on nanofiltration performance*. Journal of Membrane Science, 2005. **265**(1-2): p. 160-166.
201. Weis, A., M.R. Bird, and M. Nyström, *The chemical cleaning of polymeric UF membranes fouled with spent sulphite liquor over multiple operational cycles*. Journal of Membrane Science, 2003. **216**(1-2): p. 67-79.
202. Ang, W.S., S. Lee, and M. Elimelech, *Chemical and physical aspects of cleaning of organic-fouled reverse osmosis membranes*. Journal of Membrane Science, 2006. **272**(1-2): p. 198-210.
203. Kim, C.K., et al., *The changes of membrane performance with polyamide molecular structure in the reverse osmosis process*. Journal of Membrane Science, 2000. **165**(2): p. 189-199.
204. Akin, O. and F. Temelli, *Probing the hydrophobicity of commercial reverse osmosis membranes produced by interfacial polymerization using contact angle, XPS, FTIR, FE-SEM and AFM*. Desalination, 2011. **278**(1-3): p. 387-396.
205. Al-Amoudi, A., et al., *Cleaning results of new and fouled nanofiltration membrane characterized by contact angle, updated DSPM, flux and salts rejection*. Applied Surface Science, 2008. **254**(13): p. 3983-3992.
206. Bernstein, R., S. Belfer, and V. Freger, *Toward improved boron removal in RO by membrane modification: Feasibility and challenges*. Environmental Science and Technology, 2011. **45**(8): p. 3613-3620.
207. Li, Q. and M. Elimelech, *Organic fouling and chemical cleaning of nanofiltration membranes: Measurements and mechanisms*. Environmental Science and Technology, 2004. **38**(17): p. 4683-4693.
208. Ben Amar, N., et al., *Effect of temperature on the rejection of neutral and charged solutes by Desal 5 DK nanofiltration membrane*. Desalination, 2009. **246**(1-3): p. 294-303.
209. Majamaa, K., et al., *Preservation of reverse osmosis membranes with non oxidizing biocides - Comparison with SMBS*. Water Science & Technology: Water Supply, 2011. **11**(3): p. 342-351.
210. Fujioka, T., et al., *N-nitrosamine rejection by nanofiltration and reverse osmosis membranes: The importance of membrane characteristics*. Desalination, 2013. **316**: p. 67-75.

211. Do, V.T., et al., *Effects of chlorine exposure conditions on physiochemical properties and performance of a polyamide membrane - mechanisms and implications*. Environmental Science and Technology, 2012. **46**(24): p. 13184-13192.
212. Simon, A., et al., *Effects of membrane degradation on the removal of pharmaceutically active compounds (PhACs) by NF/RO filtration processes*. Journal of Membrane Science, 2009. **340**(1-2): p. 16-25.
213. Schnitzer, C. and S. Ripperger, *Influence of surface roughness on streaming potential method*. Chemical Engineering and Technology, 2008. **31**(11): p. 1696-1700.
214. Pavia, D.L., et al., *Introduction to Spectroscopy* 2009, Belmont, CA: Brook/Cole, Cengage Learning.
215. Porubská, M., et al., *FTIR spectroscopy study of polyamide-6 irradiated by electron and proton beams*. Polymer Degradation and Stability, 2012. **97**(4): p. 523-531.
216. Tu, K.L., et al., *Boron as a surrogate for N-nitrosodimethylamine rejection by reverse osmosis membranes in potable water reuse applications*. Environmental Science & Technology, 2013. **47**(12): p. 6425-6430.
217. Das, D.K. and O.K. Medhi, *Effect of surfactant and pH on the redox potential of microperoxidase 11 in aqueous micellar solutions*. Journal of the Chemical Society - Dalton Transactions, 1998(10): p. 1693-1698.
218. Mayhew, S.G., *The effects of pH and semiquinone formation on the oxidation-reduction potentials of flavin mononucleotide. A reappraisal*. European Journal of Biochemistry, 1999. **265**(2): p. 698-702.
219. Farhat, A., F. Ahmad, and H. Arafat, *Analytical techniques for boron quantification supporting desalination processes: A review*. Desalination, 2013. **310**: p. 9-17.
220. *Sievers UPW boron analyzer, Fact Sheet*, in *Water & Process Technologies - Analytical Instruments* 2008, GE Analytical Instrument: Boulder, CO.
221. Fujioka, T., et al., *Effects of membrane fouling on N-nitrosamine rejection by nanofiltration and reverse osmosis membranes*. Journal of Membrane Science, 2013. **427**(0): p. 311-319.
222. McDonald, J.A., et al., *Analysis of N-nitrosamines in water by isotope dilution gas chromatography–electron ionisation tandem mass spectrometry*. Talanta, 2012. **99**(0): p. 146-154.
223. Bellona, C., et al., *Factors affecting the rejection of organic solutes during NF/RO treatment - A literature review*. Water Research, 2004. **38**(12): p. 2795-2809.
224. Van Der Bruggen, B., et al., *Influence of molecular size, polarity and charge on the retention of organic molecules by nanofiltration*. Journal of Membrane Science, 1999. **156**(1): p. 29-41.

225. Bartels, C., et al., *The effect of feed ionic strength on salt passage through reverse osmosis membranes*. *Desalination*, 2005. **184**(1-3): p. 185-195.
226. Steinle-Darling, E., et al., *Evaluating the impacts of membrane type, coating, fouling, chemical properties and water chemistry on reverse osmosis rejection of seven nitrosoalkylamines, including NDMA*. *Water Research*, 2007. **41**(17): p. 3959-3967.
227. Miyashita, Y., et al., *Removal of N-Nitrosamines and their precursors by nanofiltration and reverse osmosis membranes*. *Journal of Environmental Engineering*, 2009. **135**(9): p. 788-795.
228. Hoek, E.M.V. and M. Elimelech, *Cake-enhanced concentration polarization: A new fouling mechanism for salt-rejecting membranes*. *Environmental Science and Technology*, 2003. **37**(24): p. 5581-5588.

THESIS-RELATED PUBLICATIONS

Journal articles:

Tu, K.L., A.R. Chivas, and L.D. Nghiem, Effects of chemical preservation on flux and solute rejection by reverse osmosis membranes. *Journal of Membrane Science*, 2014. 472: 202-209.

Tu, K.L., T. Fujioka, S.J. Khan, Y. Poussade, A. Roux, J.E. Drewes, A.R. Chivas, and L.D. Nghiem, Boron as a surrogate for N-nitrosodimethylamine rejection by reverse osmosis membranes in potable water reuse applications. *Environmental Science & Technology*, 2013. 47: 6425-6430.

Tu, K.L., A.R. Chivas, and L.D. Nghiem, Enhanced boron rejection by NF/RO membranes by complexation with polyols: Measurement and mechanisms. *Desalination*, 2013. 310: 115–121.

Tu, K.L., A.R. Chivas, and L.D. Nghiem, Effects of chemical cleaning on separation efficiency of a reverse osmosis membrane. *Membrane Water Treatment*. Accepted manuscript.

Conference and workshop presentations:

Tu, K.L., A.R. Chivas, and L.D. Nghiem, Boron removal by reverse osmosis membranes: effects of membrane preservation. *Challenges for Portable Water Reuse Workshop* (Oral Presentation). Jan 2014, University of Wollongong, NSW, Australia.

Tu, K.L., A.R. Chivas, and L.D. Nghiem, Boron rejection by reverse osmosis membranes: effects of operating conditions and membrane preservation. *IMSTEC 2013* (Oral Presentation). December 2013, University of Melbourne, Victoria, Australia.

Tu, K.L., A.R. Chivas, and L.D. Nghiem, Enhanced boron rejection by NF/RO membranes by complexation with polyols. *Membrane Society of Australasia 3rd Early Career Researchers Symposium* (Oral Presentation). December 2012, University of Queensland, QLD, Australia.

APPENDIX

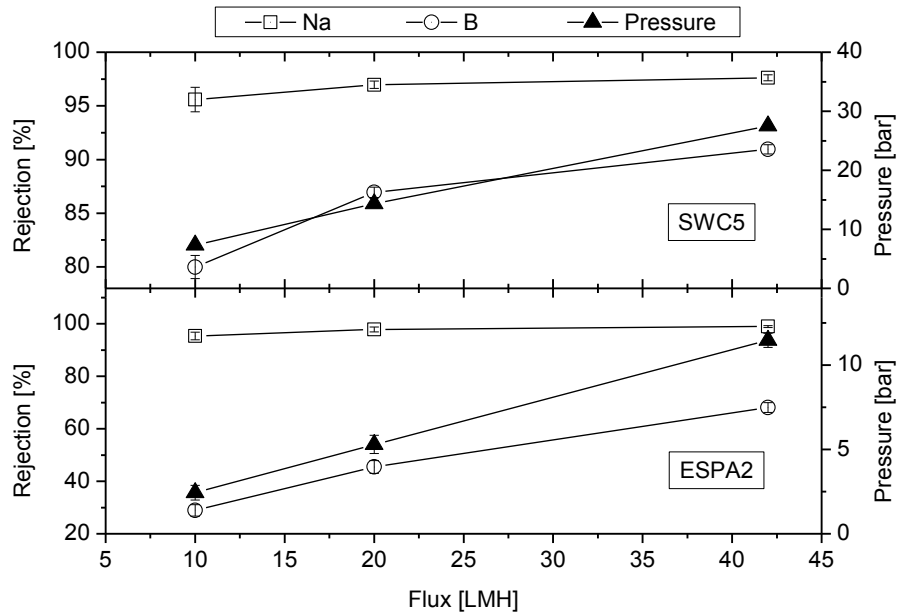


Figure A1: Standard deviation of the rejections and permeability of the ESPA2 and SWC5 membranes as results of three sequences of membrane re-assembling to the filtration cell. The testing conditions are: pH 8, temperature 20 °C, cross-flow velocity 42 cm.s⁻¹. Feedwater contains 0.43 mM (BOH)₃, 10 mM NaCl, 1 mM NaHCO₃, and 1mM CaCl₂.

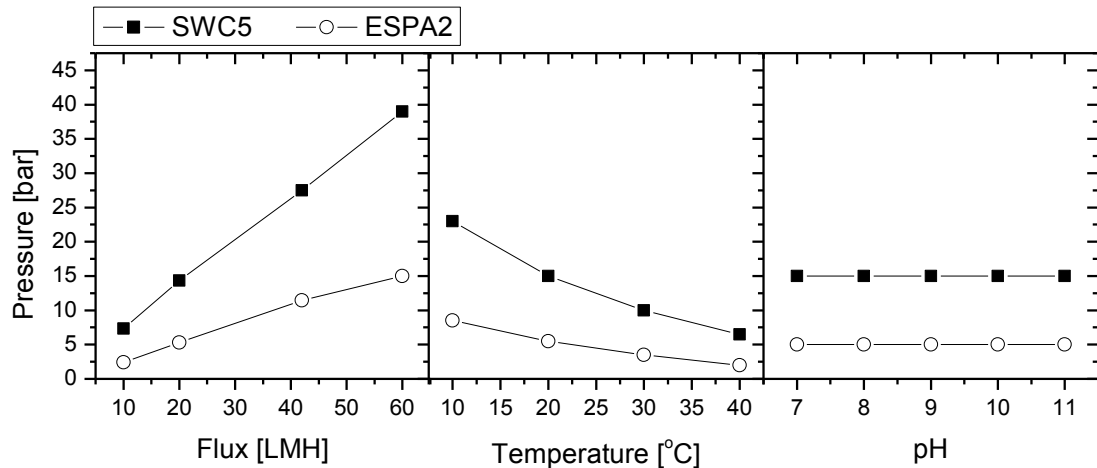


Figure A2: Applied pressure as a function of various operating fluxes, temperatures and feedwater pH values. The SWC5 and ESPA2 membranes were used. Unless otherwise stated, the testing conditions are: pH 8, temperature 20 °C, permeate flux 20 LMH, cross-flow velocity 42 cm.s⁻¹. Feedwater contains 0.43 mM (BOH)₃, 10 mM NaCl, 1 mM NaHCO₃, and 1mM CaCl₂.